DISSERTATION

submitted to the

Combined Faculty of Natural Sciences and Mathematics of the Ruperto
Carola University Heidelberg, Germany

for the degree of
Doctor of Natural Sciences

Presented by
Manu Jain Goyal (M.Sc, Biotechnology)
born in Kota, India
Oral examination: 03.07.2019

Paralog specific role of COPI pathway in P19 neuronal differentiation

Referees: Prof. Dr. Felix Wieland

Dr. Julien Béthune

This work has been carried out at the Biochemistry Center of the University of Heidelberg from January 2015 to January 2019 under the supervision of Dr. Julien Béthune.

Acknowledgement

Abstract

COPI vesicles mediate retrograde Golgi to ER transport and intra-Golgi transport within the secretory pathway. COPI vesicles are Golgi derived vesicles, which are coated with heptameric complex known as coatomer. Coatomer is made up of seven subunits α,β, β', δ, γ, ζ and ε-COP. COPI coatomer is recruited to the Golgi membrane with the help of small GTPases Arf to stimulate the vesicle formation and capture cargo proteins to deliver them to the targeted membrane.

In mammals the γ-COP subunit has two paralogs. Whereas in the related COPII system, paralogs of coat subunits were shown to expand the cargo repertoire of COPII vesicles, no paralog specific function had been described to date for COPI paralog subunits. In this work we have set out to investigate such specific functions.

Guided by RNAseq data in differentiating mouse embryonic stem cells (mES) showed that Copg1 is upregulated during neuronal differentiation. We generated Copg1 and Copg2 KO P19 pluripotent cells and studied if they could differentiate. Strikingly Copg1 KO cells fail to form tight embryonic bodies (EBs) and to form long neurites though they could differentiate into neurons.

This work shows for the first time strong evidence for paralog-specific function of the COPI pathway in mammalian cells.

Zusammenfassung

COPI-Vesikel sind verantwortlich für den retrograden Golgi -ER Transport und intra-Golgi Transporte, welche Bestandteile des Sekretionsweges sind. COPI-Vesikel sind vom Golgi stammende Vesikel, welche mit einem heptameren Komplex beschichtet sind, dem sogenannten Coatomer. Das Coatomer besteht aus sieben Untereinheiten: α, β, β', δ, γ, ζ und ε -COP. Mit der Hilfe von der kleinen GTPase Arf wird das COPI Coatomer zur Golgi-Membran rekrutiert. Dadurch kommt es zur Stimmulierung der Vesikelformation und der Rekutierung weiterer Cargo Proteine, um sie an ihre Zielmembran zu transportieren.

Bei Säugetieren existieren zwei Paraloge der γ-COP Untereinheit. Während im verwandten COPII-System Paraloge von Manteluntereinheiten das Frachtrepertoire der COPII-Vesikel erweitern konnten, wurden bislang keine paralog-spezifische Funktionen für COPI-Paralogunterinheiten beschrieben. In der folgenden Arbeit haben wir uns mit der Erforschungsolcher möglichen spezifischen Funktionen beschäftigt.

Basierend auf RNAseq-Daten, dievon sich differenzierenden mouse embryonic stem cells (mES) gesammelt wurden, konnte man einen Zusammenhang zwischen der neuronalen Differenzierung und der Copg1 Hochregulierung beobachten. Der Ansatz bestand im Folgenden darin Copg1 und Copg2 KO P19 pluripotente Zelllinien zu generieren, und deren Kapazität zur Zelldifferenzierung zu untersuchen. Auffallend war vor allem, dass Copg1 KO-Zellen nicht mehr in der Lage waren kompakte embryonale Körperchen (EBs) und Neuriten zu bilden, obwohl sie sich zu Neuronen differenzieren konnten.

In dieser Arbeit wurden zum ersten Mal aussagekräftige Hinweise auf eine paralogspezifische Funktion des COPI-Weges in Säugetierzellen gezeigt.

Table of Contents

List of Figures

List of Tables

1. Introduction

Nearly all proteins made by a cell need to be localized at define places to fulfill their functions. Specific localization can be achieved either by localized translation or protein transport. About a third of eukaryotic proteins rely on the secretory pathway to reach their final localizations. These proteins are made at the endoplasmic reticulum (ER) and then travel within small-coated vesicles from one organelle to the next.

1.1. The secretory pathway

The secretory pathway is composed of the rough endoplasmic reticulum (rough ER), ER exit sites (ERESs) the ER-to-Golgi intermediate compartment (ERGIC), the Golgi complex and post-Golgi carriers en route to their final destination. Each organelle in the secretory pathway has a precise structure, organization and function in order to provide appropriate protein folding and post-translation modifications (Mellman and Warren 2000; Spang 2009). Synthesis of proteins, intracellular transport and storage was first discovered in the pancreas cells of guinea pig during the study of digestive enzyme pathway (Caro and Palade 1964). Secretory proteins are synthesized on the polysomes attached to the rough Endoplasmic Reticulum (ER) membrane. The ER plays an important role in maintaining the quality control, for example disulfide bridge formation or N-glycosylation (Ellgaard and Ruddock 2005).

The ER is the entry site to the secretory or endomembrane system therefore around 30% of eukaryotic proteins should be targeted and translocated to ER (reviewed in (Aviram and Schuldiner 2017). Translocation of proteins can be done post-translationally or co-translationally (Cross et al. 2009; Rapoport 2007). In the co-translational pathway, proteins start the journey through the secretory pathway through their signal sequence-dependent delivery to the ER (Blobel and Dobberstein 1975). ER targeting signals are hydrophobic and an interaction through this N-terminal sequence with the signal recognition particle (SRP) guard this hydrophobic signal from premature folding of the polypeptide. Further, the ribosome-bound nascent chain is targeted to ER membrane through the interaction with the SRP receptor (Blobel and Dobberstein 1975; Berndt et al. 2009; Gilmore, Blobel, and Walter 1982; Mary et al. 2010; Walter and Blobel 1980).

Co-translational translocation is facilitated by the multi-subunit complex translocon that is situated in the ER membrane. Sec61 which is a conserved protein-conducting channel provides the core of the translocon complex. It binds to translating ribosomes to provide co-translational route for the delivery of proteins into and across the membrane (reviewed in (Pfeffer et al. 2015).

Tail anchored (TA) proteins are another group of membrane proteins which are post-translationally inserted in the ER membrane. Their hydrophobic transmembrane (TM) region helps them to get delivered to the ER and anchor them within the membrane (Osborne, Rapoport, and van den Berg 2005; Kutay, Hartmann, and Rapoport 1993). Biogenesis of TA proteins is an ATP dependent process and it requires the interaction with TRC40, which is a cytoplasmic transmembrane domain (TMD) recognition complex of 40kDa, also knowm as Asna1 (conserved homologues in yeast termed as Get3) (Favaloro et al. 2008; Stefanovic and Hegde 2007; Schuldiner et al. 2008). Carboxy terminal signal sequence of TA proteins help in its integration in the membrane post-translationally. In this case incorporation of N-glycosylation helps in correct integration of TA proteins (Borgese, Brambillasca, and Colombo 2007; Rabu and High 2007; Kutay et al. 1995). In case of co-translation signal sequence is present at the N-terminal of nascent chain (Walter and Blobel 1980).
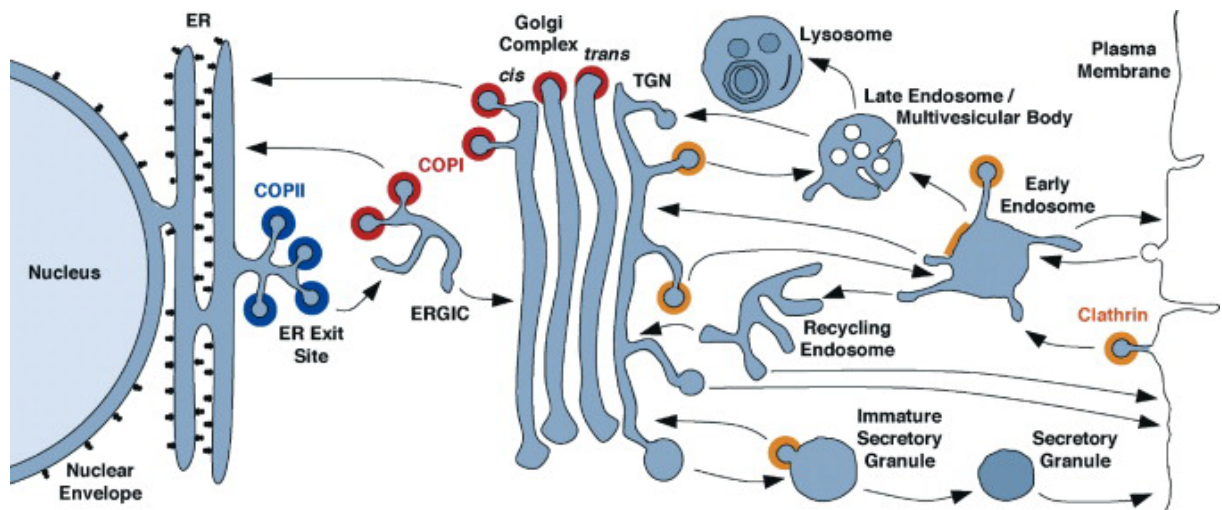
Figure 1: Schematic presentation of the secretory pathway.

The main cell organelles and different transport ways of the secretory, lysosomal and endosomal pathway are depicted. Secretory pathway vesicles COPII (blue), COPI (red) and clathrin (yellow) are presented by color labels. Reprinted from Cell, (Bonifacino and Glick 2004), Copyright (2004), with permission from Elsevier, License number: 4518820947623

Interestingly not all the secretory proteins are dependent on the SRP or Get/TRC40 pathways for the translocation. This could be due to physical restrictions or if hydrophobic ER targeting sequence fail to engage SRP. In the SRP-independent (SND) pathway for example Calmodulin might play role in promoting the substrates (Ast and Schuldiner 2013). After the translation process, secreted and lysosomal proteins are translocated in the ER lumen whereas membrane proteins are directly inserted in the ER membrane (Braakman and Bulleid 2011). Post-translational modifications for example N-glycosylation (Kornfeld and Kornfeld 1985) and disulfide bridge formation (Ellgaard and Ruddock 2005) take place in the ER lumen to provide correct folding of the protein. In the ER two systems have been described that regulate the quality control for misfolding or aggregation of proteins. One is the unfolded-protein response (UPR) in which upregulation of chaperone synthesis promotes correct folding of proteins and the second is ER-associated degradation (ERAD) in which misfolded proteins are translocated back to cytoplasm and get degraded via the ubiquitin proteasomal degradation pathway (Ellgaard and Helenius 2003; Friedlander et al. 2000).

Once proteins are correctly folded and modified they are assembled at ER exit sites and encapsulated in COPII vesicles (Klumperman 2000; Pfeffer and Rothman 1987). Two distinct models have been suggested to explain this process. The cargo capture model states that recognition of proteins via cargo receptors that interact with COPII proteins leads to their concentration in ERES and COPII vesicles. In the bulk flow model secretory proteins are carried without receptor by passive incorporation of bulk membrane and fluid. By contrast, partially folded and assembled proteins are selectively hold back in the ER (Thor et al. 2009; Wieland et al. 1987). Experimental evidence exists for both models and thus both transport mechanisms probably co-exist in cells (Béthune and Wieland 2018). ER exit sites are comprised of either composite network of tubules and vesicles or distinct buds, which are lacking ribosomes known as transition sites (Bannykh and Balch 1997; Hara-Kuge et al. 1994; Orci et al. 1991). These budding sites are coated with COPII and transform into COPII coated vesicles (Klumperman 2000). COPII vesicles transport proteins from the ER to the Golgi via the ER-Golgi intermediate compartment (ERGIC), that is described by its marker proteins the GTPase Rab2 and the intracellular lectin ERGIC53 (Hauri et al. 2000). ERGIC is also referred as vesicular-tubular clusters (VTCs), is found between the

ER and the Golgi and works as a junction for both COPI and COPII mediated transport, because marker proteins of both coated vesicles can be found in this compartment (Bannykh and Balch 1997). COPI coated vesicles are involved in the retrograde transport of proteins from the Golgi to the ER and in intra Golgi transport as well (Letourneur et al. 1994; Orci, Glick, and Rothman 1986; Serafini et al. 1991).

The Golgi is the center of the secretory pathway. The Golgi was first discovered in the nerve cells of spinal ganglia and named Golgi after Camillo Golgi (Golgi 1989). The Golgi apparatus is made of a stack of elongated membrane structure known as cisternae. Protein starts travelling from cis side of the cisternae (early Golgi) that faces the ER, then pass through the middle cisternae and finally are exported to the cell surface or the endo-lysosomal system (trans Golgi network or late Golgi) (Rothman and Wieland 1996). Each of these compartments contains a different set of glycosyltransferases as well as other enzymes, which further process glycoproteins (Pfeffer 2010). Different models have been described in the literature to explain how protein transport takes place through the Golgi complex. According to the anterograde vesicular trafficking model, the Golgi is referred as a section that possesses stable stacks in harmony with their enzymes so that cargo can be delivered through vesicular transport. By contrast, cisternal maturation model explains movement and hence maturation of the enzymes describing cis-medial-trans Golgi stacks, whereas cargo stays in one compartment. Recent models been proposed are the stable compartment of cisternal progenitors and the rapid-partitioning model. First model describes movement of cargo from ER to Golgi through vesicles and Rab dependent transformation elucidating fusion and segregation of Golgi domains. Second explains bidirectional movement of proteins via lipid sorting driving force (see reviews (Glick and Luini 2011; Jackson 2009; Pelham and Rothman 2000; Pfeffer 2010). The Golgi has two major functions that are transport of secreted proteins out of the cell and to other organelles for example to the plasma membrane or lysosomes, and the glycosylation of secreted serum proteins and plasma membrane glycoproteins. Many secreted proteins are glycoproteins (Fleischer 1983). Glycoproteins undergo several modifications during the glycosylation process before they get transferred to the final destination (Kornfeld and Kornfeld 1985). Glycosylation, a very common post-translational modification of proteins and lipids, terminates at the Golgi apparatus. Addition of sugar chain to proteins is a complex multi-

step process that requires multiple enzymes. Many of those are localized at the Golgi and exhibit a concentration gradient across the Golgi stack that is thought to ensure correct glycan chains are added to secretory proteins (Stanley 2011). In eukaryotic cells multiple endocytosis, exocytosis and membrane recycling pathways are established, which play crucial role to maintain the balance with in the cell (Farquhar 1983). During exocytosis secretory granules are discharged to the cell surface which is coupled to endocytosis in which receptor proteins are recycled back to the cell or cell uptake the material and nutrients from outside to maintain organelle quality and signaling. Clathrin coated vesicles (CCVs) have been suggested to play role during the transport along these routes (Palade 1975; Farquhar 1983; Langemeyer, Frohlich, and Ungermann 2018; Karatekin and Rothman 2018).

1.2. Vesicular Transport

In eukaryotes, protein trafficking is generally important to maintain homeostasis, and more specifically to bring newly synthesized proteins to their site of function. Virtually all newly synthesized transmembrane and secretory proteins destined to the secretory and endolysosomal systems are first inserted in the endoplasmic reticulum (ER) and then transported from the ER to the Golgi apparatus before they are delivered to their final destinations. In eukaryotic cells transport of transmembrane and secreted proteins is mainly mediated by coated vesicles (Bonifacino and Glick 2004). Three types of coated vesicles have been studied (i) Clathrin coated vesicles, (ii) COPI vesicles, (iii) COPII vesicles. Clathrin coated vesicles transport secretory proteins in the late secretory pathway and the endocytic pathway (Robinson 2004). COPII vesicles export proteins from the endoplasmic reticulum (ER) to the Golgi apparatus, termed as anterograde pathway (Hughes and Stephens 2008). COPI vesicles mediate transport routes from the Golgi apparatus to the ER, termed as retrograde pathway, and between Golgi cisternae (Bethune et al. 2006).

1.2.1.   Clathrin Coated Vesicles

Clathrin coated vesicles were first discovered while studying yolk protein absorption in developing mosquito oocyte. They were observed as coated vesicles and on their convex cytoplasmic side they have bristle coat of $20\mu m$ (Roth and Porter 1964). These coats were found to have a lattice shape structure in the cytoplasm and were named as clathrin. Initial

purifications from the pig brains revealed a single protein of 180Kda on SDS-PAGE. Amino sugars were absent on clathrin suggesting it cytoplasmic protein (Pearse 1976). From crosslinking experiment, it was found that clathrin contains three heavy chains and three light chains. Each heavy chain is tightly bound to one light chain, like this they make pair of trimers (Kirchhausen and Harrison 1981; Ungewickell and Branton 1981). Under suitable conditions polymerization of these trimers leads to formation of pentagons and hexagons coated vesicles (Crowther and Pearse 1981). A clathrin assembly protein of 50-KDa (AP50) was described to initiate assembly of clathrin coat (Keen, Chestnut, and Beck 1987). Nowadays, in higher eukaryotes, four different AP complexes have been identified and play important role in coat formation. AP1 (Keen, Chestnut, and Beck 1987)and AP4 (Dell'Angelica, Mullins, and Bonifacino 1999) play role in transporting cargos between the TGN and endosomes (Owen, Collins, and Evans 2004) whereas AP3 (Dell'Angelica et al. 1997) transports cargo from early endosomes to late endosomes or lysosomes-like organelles (Owen, Collins, and Evans 2004). AP2 coated vesicles(Ahle et al. 1988) are involved in endocytosis from the plasma membrane to endosomes. With the exception of AP-2, GTPase Arf1 helps in recruiting the adapter protein complexes on to membranes. Binding of discrete AP complexes to membranes also occurs by selective small sequence motifs which are found on the cytoplasmic domains of the cargo proteins and interaction to phosphatidylinositol phosphates (PIPs) in the membrane (Owen, Collins, and Evans 2004).

1.2.2. COPII coated vesicles

Once proteins have been translated and correctly folded they leave the ER through vesicles that package cargo proteins and fuse with the target membrane. ER vesicles are coated with the COPII coat which is made of three components Sar1p, Sec23/24p and Sec13/31p. Sar1p is a GTP-binding protein of 21kDa, that is recruited to the ER via its nucleotide exchange factor Sec12p and gets converted to its GTP-bound form (Barlowe and Schekman 1993; Nakano and Muramatsu 1989). Activated Sar1p further enlist the Sec23/24p complex. Sec24p helps in the uptake of specific cargos whereas Sec23 retain a Sar1-GAP activity which can stimulate GTP hydrolysis (Barlowe et al. 1994; Matsuoka et al. 1998).The Sec13p/31p heterodimer complex makes the outer cage and its binding to the inner Sec23p/Sec24p coat complex is umpired by Sec31p.

1.2.3.   COPI coated vesicles

Background

Purification of non-clathrin coated vesicles from isolated Golgi membranes was the first evidence for the transportation of cargo between Golgi cisternae and also possibly from the Golgi to the ER (Ref). These Golgi derived vesicles were first discovered in a cell free system when Golgi membranes were incubated with ATP and cytosol in presence of GTPγs. Subsequently the corresponding coat protein complex was named coatomer. It was observed together with ADP-ribosylation factor (Arf1), which is small Sar1p-related GTPase required from the cytosol for COPI vesicle assembly and budding (Orci et al. 1993). In addition to Arf1 and coatomer, budding of COPI vesicles from artificial lipid bilayers that mimic the Golgi membrane also needs cytoplasmic tails of p24 protein family (putative cargo receptors) or cargo proteins that contain a KKXX ER-retrieval signal (Bremser et al. 1999). In vitro studies showed that coatomer directly binds to dilysine motifs (Cosson and Letourneur 1994), which suggest its role in the retrograde pathway (Golgi to ER). Any mutation in the motifs leads to loss of binding to coatomer and impaired retrieval to the ER (Cosson and Letourneur 1994; Letourneur et al. 1994). Electron microscopic studies suggested bidirectional transport of COPI vesicles. Indeed, COPI vesicles were found to contain both pro insulin and VSV G proteins for anterograde pathway and KDEL receptors for retrograde pathway (Orci et al., 1997). A recent study unveiled a sorting mechanism for anterograde cargo, in which s-palmitoylation of proteins encourages assembly of membrane cargo at cisternal rim, thus enabling its efficient anterograde transport across the Golgi (Ernst et al. 2018). Another study also shows that different coiled-coil proteins from the golgin family can be used to isolate two different set of COPI vesicles. Vesicles bound to the golgin84-CASP tether lacked members of the p24 putative cargo receptors and contained glycosylation enzymes rather than anterograde cargos, suggesting a role of this tether in the retrograde pathway whereas the COPI vesicles bound to the p115 golgin tether contained p24 proteins and an anterograde cargo (Malsam et al. 2005). As mentioned above whether COPI vesicles mediate both retrograde and anterograde transport is still under debate and several intra-Golgi transport mechanisms have been proposed and may co-exist within cells.

1.3. COPI vesicle formation

1.3.1.   Coatomer

His$_6$-tagged radiolabeled coatomer was used to determine that the whole coatomer is recruited en bloc during COPI coated vesicle formation (Hara-Kuge et al. 1994). Coatomer is made up of seven subunits called heptameric complex: α-COP (140 kDa), β-COP (107 kDa), β'-COP (102 kDa), γ-COP (98 kDa), δ-COP (61 kDa), ε-COP (34 kDa) and ζ-COP (20 kDa) (Hara-Kuge et al. 1994). In vitro studies suggest that this complex can be disassembled at high salt concentration. A partial complex that contains α, β' and ε-COP interacts directly to γ and ζ-COP. This complex can bind to Golgi membrane due to interaction with KKXX motifs or alternatively binding to lipids of membrane (Lowe and Kreis 1995). Using two-hybrid system it was demonstrated that coatomer has two subcomplexes; α, β' and ε-COP subcomplex and β, γ, δ and ζ-COP subcomplex. β, γ, δ and ζ-COP subcomplex is related to AP adapter complexes (Eugster et al. 2000). In yeast, β' and γ-COP interact directly with Arf-GTP-activating protein (GAP) Glo3p (Eugster et al. 2000; Watson et al. 2004). In vivo analysis of α-COP showed that WD40 domain of N-terminal is non-essential for yeast cell viability but it is important for KKXX regulated trafficking also the last 170 amino acids are required for the integration of ε-COP into coatomer and also to maintain its levels (Eugster et al. 2004). EM studies unveiled that β' and α-COP do not make a cage-like structure around the β, γ, δ and ζ-COP subcomplex as previously proposed. In fact, coatomer bound to membranes cannot be divided into two subcomplexes instead the α, β', ε-COP and β, γ, δ, ζ-COP modules are interwined and, in contrast to the COPII and clathrin coats, no "outer" and "inner" layer coat can be defined (Dodonova et al. 2015). In higher eukaryotes γ-COP comes as two paralogs γ1-COP and γ2-COP, it applies to ζ-COP as well (ζ1 and ζ2-COP) (Blagitko et al. 1999; Futatsumori et al. 2000). γ-COP paralogs share 80% identity and ζ-COP shares 75% identity of amino acids. Immunofluorescence analysis reveals that β-COP is co-localized together with γ2 and ζ2-COP at cis side of the Golgi (Futatsumori et al. 2000). Only one isoform is present at a time in the coatomer complex, proposing four possible combinations of isotypes of coatomer in mammals γ1ζ1, γ1ζ2, γ2ζ2 and γ2ζ1. The first three forms of coatomer are present in a ratio of 2:1:2 respectively in the liver cytosol (Wegmann et al. 2004).

Immunogold labeling of Golgi stacks using anti- γ1-COP and anti- γ2-COP antibodies showed that γ1-COP was preferentially localized to the early Golgi and a pre-Golgi compartment and the majority of γ2-COP-containing isoforms of the complex was localized to the trans side of the Golgi (Moelleken et al. 2007).

1.3.2.　Arf1

Arf1 was first purified from rabbit liver membranes as a necessary factor for cholera toxin dependent ADP ribosylation of GTP binding regulatory component of ($G_{s\alpha}$) adenylate cyclase (Kahn and Gilman 1984). Arf1is a ubiquitous and highly conserved GTP binding protein of 21kDa. From the immunofluorescence and electron microscopy analysis it was observed in the mammalian cells that Arf is localized to the cis side of the Golgi in the cytosol. Altogether these studies suggested that Arf1 plays an important role in the secretory pathway (Stearns et al. 1990). The Arf family has 6 different mammalian Arf proteins, which can be divided into three classes based on amino acid sequences and protein sizes. Arfs 1-3 come into class I and have 180 amino acids but different sequence close to the C-terminal. Arf 4 and 5 belong to class II and have 180 amino acids and also differ in the sequence near the C-terminal. Class III Arf 6 has 175 amino acids and its sequence is the most different from Arfs 1-5 (Tsuchiya et al. 1991). Arf proteins are small GTPase and localized to the membrane containing myristoylated amphiphatic N-terminal helix, important for membrane binding. All the Arfs are localized to Golgi membrane except Arf6, which is localized to plasma membrane (PM) and Arf2 does not exist in the humans (summarized in (Donaldson and Jackson 2011). Activated form of Arf supervise the recruitment of AP1 and coatomer to the membrane (Stamnes and Rothman 1993; Austin, Hinners, and Tooze 2000). Arf activation occurs when GDP is exchanged to GTP which leads to the structural changes in the N-terminal and integrates myristoylated α helix into the membrane (Kahn, Goddard, and Newkirk 1988; Kahn et al. 1992).

1.3.3. Biogenesis of COPI vesicle

Initiation of COPI coat assembly occurs with the binding of Arf1 to the Golgi membrane. C terminal of Arf1 was recognized to interact with the diphenylalanine or diphenyllysine motifs of Golgi native transmembrane proteins of the p24 family in its GDP bound form (Contreras, Ortiz-Zapater, and Aniento 2004; Gommel et al. 2001; Majoul et al. 2001). In addition to p24 proteins ER-Golgi SNARE called membrin is also involved to recruit Arf1 to the Golgi membrane (Honda et al. 2005). After effective binding of Arf1 near to membrane exchanging of GDP to GTP occurs, which is an activation step, leads to the conformational changes in Arf1 structure. Gbf1 (Golgi BFA resistant factor) which is known as guanine nucleotide exchange factor localized to Golgi cisternae, is depicted to be in charge of this exchange (Claude et al. 1999; Garcia-Mata et al. 2003; Niu et al. 2005). This conformational change exposes the myristoylated amphiphatic N-terminal helix (this leads to firm anchorage to the membrane) and binding sites for coatomer. This exposure causes introduction of new hydrophobic face and consequently interaction with phospholipids of membrane (Antonny et al. 1997; Franco et al. 1996). Myristoylation elevates helical content of N-terminus, hence enhancing the membrane binding affinity. Myristoylated helix is proposed to extend within the lipid headgroups of the membrane (Harroun et al. 2005) more precisely the myristoyl residue interacts with the helix by folding back at the N-terminus (Liu, Kahn, and Prestegard 2010). Once Arf1 is tied to the membrane it separates from p24 proteins and the enlistment of the coat proteins begins (Sun et al. 2007). Unlike COPII and Clathrin coated vesicle COPI coatomer is recruited as an intact unit (Hara-Kuge et al. 1994). In addition to Arf1 coatomer interacts with p24 proteins as well as ER retrieval proteins via different domains. For instance, Arf1 binds with trunk domain β and γ-COP (Sun et al. 2007; Zhao et al. 1997; Zhao et al. 1999) also with ε and δ-COP (Eugster et al. 2000; Sun et al. 2007). Cryo-EM structure of COPI coatomer also supports the binding of ARF through its multiple interfaces and proposed binding of two Arf1 molecules per coatomer heptamer (Dodonova et al. 2015).
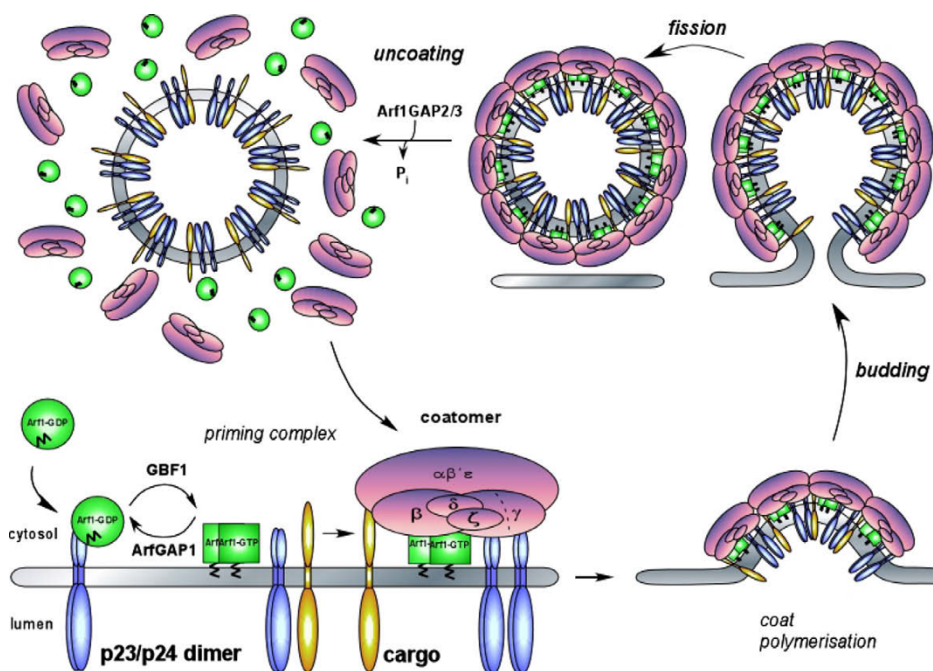
Figure 2: Schematic presentation of COPI vesicle biogenesis.
Mechanism of COPI vesicle budding and uncoating. Adapted from FEBS letters, (Beck et al. 2009), Copyright (2009), with permission from John Wiley and Sons, License number 4518830985902

Coatomer is proposed to bind with cytoplasmic domains of p24 proteins and ER native proteins (Harter and Wieland 1998; Majoul et al. 2001). Cytoplasmic domains of p24 proteins bear dilysine diphenylalanine motifs shown to interact with appendage and trunk domain of γ-COP (Bethune et al. 2006). This contact conducts a geometry change to a "*hyper-open*" form, polymerization of coatomer complexes and promotes membrane curvature (Reinhard et al. 1999; Langer et al. 2008; Dodonova et al. 2015). Besides that, WD40 domain of α and β'-COP helps coatomer in binding with KKXX or KXKXXX motifs of ER resident proteins ensuring packaging if cargo and cargo receptors in COPI vesicles (Eugster et al. 2000, 2004; Bremser et al. 1999). In the further steps during COPI coated vesicle formation budding of membrane and release of vesicle occurs. Interaction of Arf dimers with multiple coatomers in negatively curved regions (edge of the growing coat) through an inappropriate orientation of amphipathic helix leads to the deformation of the membrane (Beck et al. 2011). Arf1-GTP forms dimers which is a crucial step for membrane curvature during the vesicle formation (Beck et al. 2008). Membrane budding takes place

provided membrane curvature by coatomer whereas scission of vesicles is governed by dimerization of small GTPases ARF1 not ARF GTP hydrolysis (Adolf et al. 2013; Beck et al. 2011). After budding and before the transfer of proteins to the target membrane an important process is the uncoating of vesicles which is initialized by ARF-mediated GTP hydrolysis. This event is stimulated by enzymes called ARF-GTPase activating proteins (ARF-GAPs) (Cukierman et al. 1995; Reinhard et al. 2003; Tanigawa et al. 1993) that are directly recruited by coatomer. The final and important step of COPI vesicle formation is to deliver the protein to the target membrane which is promoted by SNARE proteins situated on acceptor and donor membranes and that promote membrane fusion (McNew et al. 2000).

Twenty years ago, genome wide analysis found paralogs of γ and ζ-COP coatomer subunits. The original γ and ζ-COP sequences were referred to as γ1 and ζ1-COP and the novel isoforms were named γ2 and ζ2-COP. γ2-COP was observed as an imprinted gene in human chromosome 7q32 overlapping with the MEST (Mesoderm Specific Transcript) gene. Both γ-COP paralogs show 80% identity in their amino acid sequence (Blagitko et al. 1999; Futatsumori et al. 2000). γ-COP is made of an N-terminal trunk domain and C-terminal appendage domain (Schledzewski, Brinkmann, and Mendel 1999; Eugster et al. 2000; Hoffman et al. 2003; Watson et al. 2004). The trunk domains shows 81% and the appendage domain shows 75% identity in mouse (Moelleken et al. 2007). The ζ2-COP paralog mainly differs from ζ1-COP by a 30 amino acids extension at its N-terminus (Futatsumori et al. 2000). In contrast with COPII sec24 paralogs that show binding of different cargos, COPI subunit paralogs have not been assigned specific functions to date (Adolf et al. 2019).

1.4. Potential role of COPI vesicles in cell polarization

Establishment and maintenance of cellular polarity is an essential process that sustains cell fate determination and differentiation, which is essential for the development of a multicellular organism or tissue. Neurons are probably the most complex cells and the epitome of cellular polarization with a long axon extending from the cell soma and an elaborate dendritic network. Neuronal polarization occurs shortly after mitosis and involves a coordinated cytoskeleton and endomembrane rearrangement allowing axon growth.

Several lines of evidence suggest that vesicular transport plays a role in axonal growth and neuronal polarization. From a previous study it is known that short treatment with Brefeldin

A, a drug that inhibits the formation of Golgi-derived transport vesicles, inhibits axonal growth of existing axons, and prevents the formation of axons from unpolarized cells (Jareb and Banker 1997) which suggests the importance of COPI vesicles during neuronal differentiation. In addition, centrosome-mediated positioning of the Golgi apparatus determines where the forming axon forms, and is necessary for axonal growth. Centrosomes, the Golgi apparatus and endosomes were found clustered together next to the place where the neurite formation starts, which is opposite to the plane of last mitotic division, indicating plane of mitotic division defines the neuronal polarization. If centrosome positioning plays important role during cell polarization, microtubule polymerization and membrane trafficking should be polarized in the direction of growth (de Anda et al. 2005). Finally, knock down of α-COP resulted in significant reduction of both dendritic and axonal growth in primary cortical neurons (Custer et al. 2013; Peter et al. 2011; Li et al. 2015). The role of COPI vesicles in the transport of proteins and lipids between the Golgi apparatus and the ER has been well described. Yet, they have been much less studied in polarized cells such as neurons. Interestingly, α-COP was observed in the neurites and growth cones in primary neurons and was transported towards the axonal growth cone upon activation by BDNF, suggesting COPI vesicles not only mediate short-range transport between Golgi and ER, but also long-range transport along the axon (Peter et al. 2011). However, their precise role in this context is currently unknown. Until now, though slightly distinct subcellular localization could be observed but no functional difference could be found between coatomer complexes containing γ1- or γ2-COP. Before starting this project, examination of publicly available whole transcriptome-profiling data indicates that γ1- and γ2-COP are differentially expressed during mouse embryonic stem cells differentiation into neurons (Tippmann et al. 2012). Altogether this suggest that COPI vesicle may play an important role during neuronal differentiation with potential paralog-specific functions in this context.

1.5. Aim of the study

The goal of this thesis is to study potential paralogs specific roles of the COPI pathway during neuronal differentiation. Recent evidence suggests that Golgi-derived vesicles play a critical role in axonal growth and polarization of neuronal cells. The precise role and function of COPI vesicles in the highly polarized neuronal cells has however, to date, remains unexplored. Recent data indicates that, in neurons, COPI vesicles travel long distances within the axon and regulate neurite outgrowth. This suggests that COPI vesicles play a yet overlooked important role in neuronal differentiation. Until now, though slightly distinct subcellular localization could be observed (Moelleken et al. 2007), no functional difference could be found between coatomer complexes containing γ1- or γ2-COP. Above studies suggests that potential functional differences between the γ1-COP and γ2-COP containing coatomers may be found in neuronal cells. This work aims to analyze the contribution and significance of COPI mediated trafficking in neuronal differentiation by addressing the following questions:

- Does the COPI pathway play a role in neuronal differentiation/establishment of cellular polarity?
- Do γ1 and γ2-COP containing coatomer have different functions in this process?

For specifications gene is referred as Copg1 and Copg2 and for protein γ1-COP and γ2-COP has used.

2.   Results

2.1. Down-regulation of Copg2 protein ratio and mRNA levels

Since whole transcriptomics analysis of the neuronal cells differentiated from mouse embryonic stem cells had indicated that Copg1 is upregulated upon neuronal differentiation, suggesting that Copg1 might play important role during neuronal differentiation (figure 3) (Tippmann et al. 2012). Based on that protein and mRNA expression of gamma-COP paralogs were investigated in P19 WT cells during neuronal differentiation.
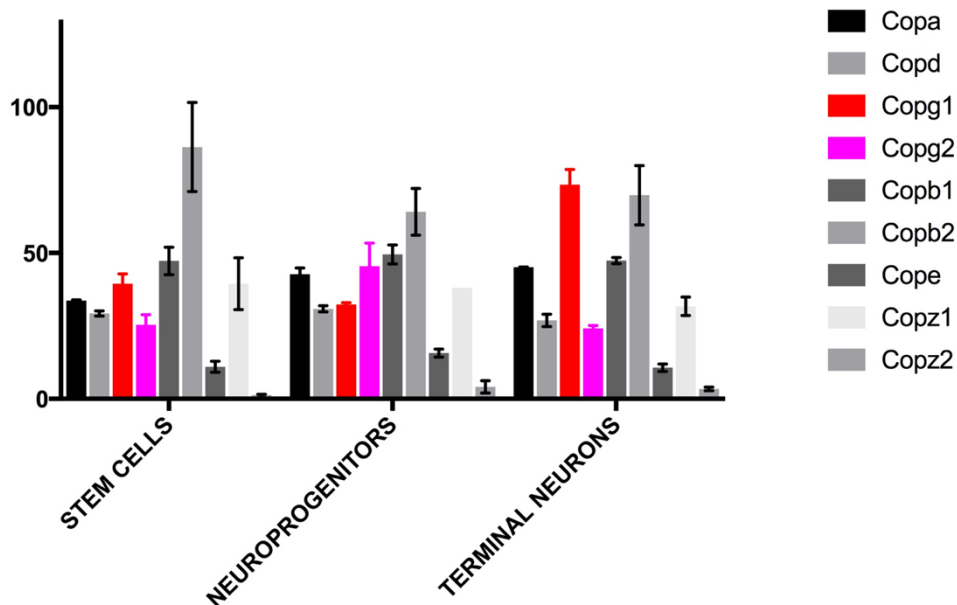
Figure 3: Transcriptomics profiling of mouse embryonic stem cells.

RNAseq expression profiling performed on mES and their derived neuroprogenitors (NP) and terminal neurons (TN). Figure was generated by Julien Béthune using raw data from (Tippmann et al. 2012)

To study the role of gamma-COPI in neuronal differentiation, P19 cells were used as a model cell line. These are mouse pluripotent cells of cancerous origin that can be differentiated into neurons and glial cells in presence of retinoic acid (RA) (Jones-Villeneuve et al. 1982). An established classical method for efficient neurogenesis of P19 has been used to differentiate the cells into neurons (figure 4). To differentiate P19 cells into neurons, cells were first cultured in non-adherent condition in presence of $0.1\mu M$ RA in 10cm bacterial plates for 4 days during which cells aggregate to form embryoid bodies

(EB). After 4 days these aggregates were collected and dissociated, plated and after two days of plating treated with 10um Cytosine-1-β-D-arabinofuranoside (AraC). The nucleoside analog AraC inhibits DNA replication and leads to DNA fragmentation, and thus acts as a poison for dividing cells. Hence AraC treatment promotes the enrichment of post-mitotic neurons. Every second-day samples were collected to isolate protein and RNA.
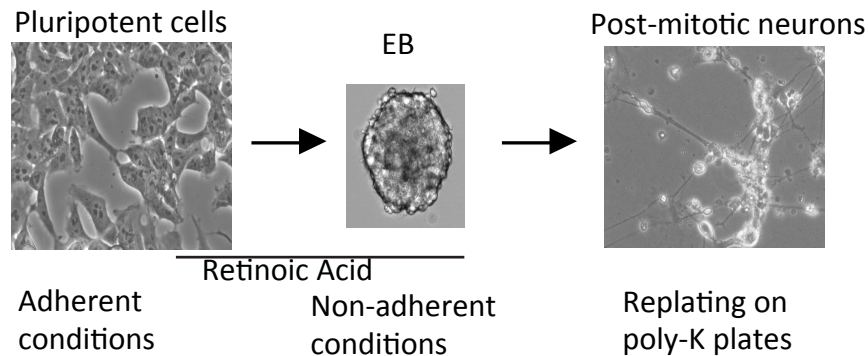
Figure 4: Schematic representation of classical two step P19 neuronal differentiation method using Retinoic Acid.

Protein expression of gamma-COP paralogs was analyzed using specific antibodies against each paralog. γ2-COP protein expression was downregulated while γ1-COP protein was upregulated at day 8 post-differentiation (figure 5a & 5c). β–tubulin III (also known as TujI) was used a neuronal-specific marker, and Oct-4 was used as a pluripotency marker. Quantification of mRNA levels of the two paralogs revealed that the expression of Copg2 was decreased but Copg1 was highly expressed during neuronal differentiation at day 8 post-differentiation (figure 5b & 5d). All the other subunits were found to behave in a similar manner to Copg1. Ratios of protein and mRNA expression of these two paralogs were measured separately which also show increase in protein and mRNA levels of Copg1.The difference in Copg1 and Copg2 regulation during neuronal differentiation suggests non-overlapping functions.
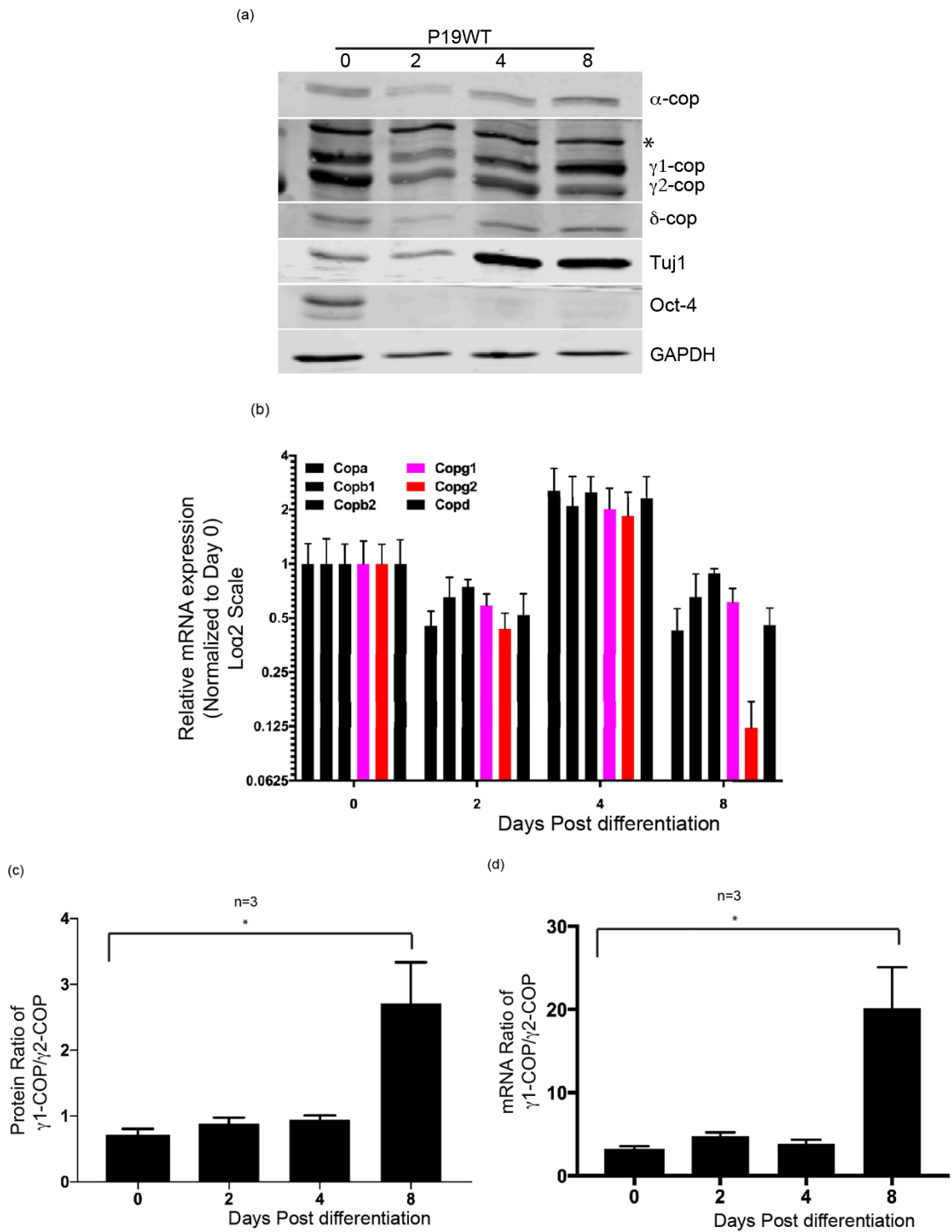
Figure 5: Differential expression of Copg1 and Copg2 paralogs during P19 neuronal differentiation.

(a-b) Show protein and mRNA expression of different COPI subunits during P19 WT neuronal differentiation. (*) shows non-specific signal. (c-d) Represent ratio of protein and mRNA of Copg1 and

Copg2 paralogs. Two-tailed unpaired t-test was performed for statically significant analysis (* p-value is <0.05).

2.2. Disruption of γ1- and γ2-COP subunits in P19 cells

To determine whether Copg1 and Copg2 are functionally redundant, loss-of-function models for both these genes were generated using state of the art cas9-mediated genome editing techniques. Single guide RNAs (sgRNAs) targeting the open reading frames of either Copg1 or Copg2 were designed using online design tools (for Copg1 MIT CRISPR tool was used (Ran et al. 2013), Copg2 CHOP-CHOP was used (Labun et al. 2016) and eSpCas9 Copg1 E-CRISP was used (Heigwer, Kerr, and Boutros 2014)) to minimize potential off-targets **(**figure 6a &b).
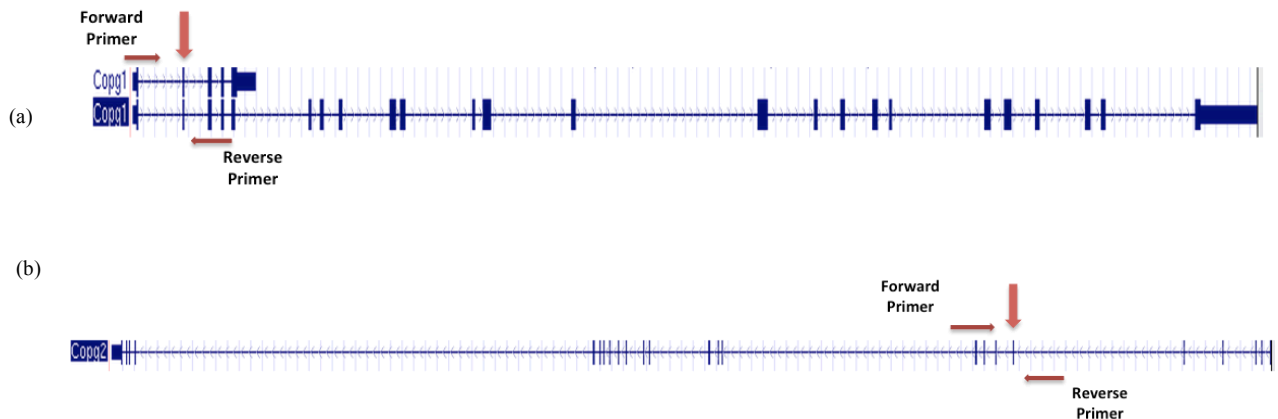
Figure 6: Schematic representation of the genomic locus of Copg1 and Copg2 paralogs.

(a-b) show schematic representation of whole locus of Copg1 and Copg2 genes respectively. Light red vertical arrow shows the exon number where sgRNA is targeted. Dark red arrows show PCR primers for T7 endonuclease assay around the cut site.

These sgRNAs were then cloned downstream of the U6 promoter into the PX458 plasmid (which also contains a Cas9 and GFP expression cassette). These plasmids, containing the individual sgRNAs, were then transfected into P19 cells to test their cutting efficiencies using a T7 endonuclease test. When the sgRNA-Cas9 complex is recruited to the genomic DNA (gDNA), it induces a double-stranded break (DSB) at that site. The resulting DSB can

then be repaired by either the error-prone non-homologous end-joining (NHEJ), or the error-free homologous recombination (HR) pathway.
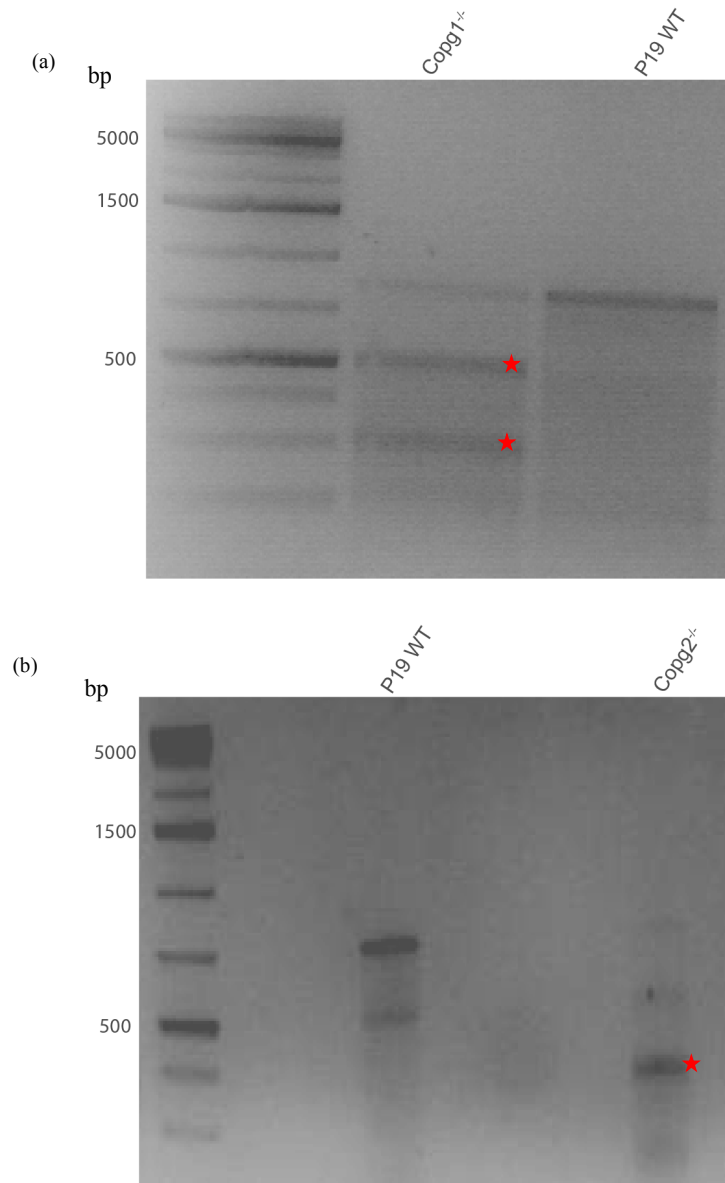
Figure 7: sgRNA cutting efficiency test.

(a & b) T7 endonuclease assay to test the efficiency of sgRNA to create double-stranded break in the gDNA. Red stars indicate expected band size after digestion. For Copg1 product length is 800 and expected bands are 299 and 501bp. For Copg2 product length is 711 and expected bands are 378 and 333 bp.

The NHEJ pathway is predominantly used by the cells and results in insertions or deletions (indels) of few base pairs at the cut site. The T7 endonuclease test exploits this property to determine the cutting efficiency of the Cas9-sgRNA complex. Genomic DNA from the transfected cells was isolated and the region around the cut site was PCR-amplified. The PCR product was denatured and reannealed by ramping down the temperature from 95° to 25°c at 1 degree per second. Since the transfected cells contained a pool of several mutants (due to Cas9 induced indels), the resulting PCR product also contained these mutations. Upon denaturation and reannealing, several DNA strands re-anneal with the wrong cognate anti-strand resulting in a heteroduplex formation (with a bulge at the sgRNA binding site). These heteroduplexes were digested with the T7 endonuclease I enzyme which recognizes and cleaves the bulge into two DNA fragments that can be seen on a 2% agarose gel (Ran et al. 2013). In case of Copg1, the sgRNA targeting exon2 whereas in case of Copg2, at the sgRNA targeting exon6, were the most efficient ones (figure 7a & 7b). Once it was confirmed that these sgRNAs were efficient in generating indels at the desired loci, they were transfected into P19 cells and 72 hours post-transfection, GFP-positive single cells were sorted into 96 well plates and allowed to grow for 2 weeks. The clones thus obtained were screened for Copg1 and Copg2 protein expression using specific antibodies against these paralogs. In case of Copg1 two clones survived after FACS sorting and two of them showed complete deletion of protein (figure 8)
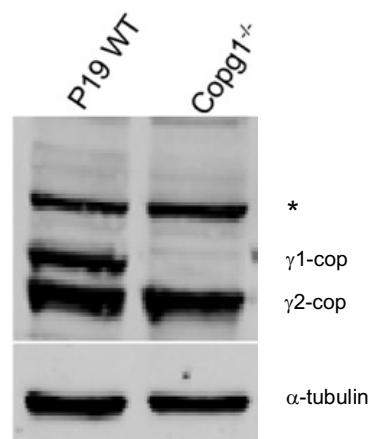
Figure 8: Analysis of P19WT and Copg1 KO cells.

Western blotting from clone 1 to see γ1-COP protein knockout. Star shows non-specific band. Expected molecular weight for γ1-COP is 99.5 kDa and for γ2-COP is 97.5 kDa and α-tubulin is 55 kDa, protein loading control.

(western blotting in the figure from clone 1) whereas for Copg2 out of several clones five clones were screened by western blotting and three clones showed complete knock out of Copg2 protein (figure 10a).
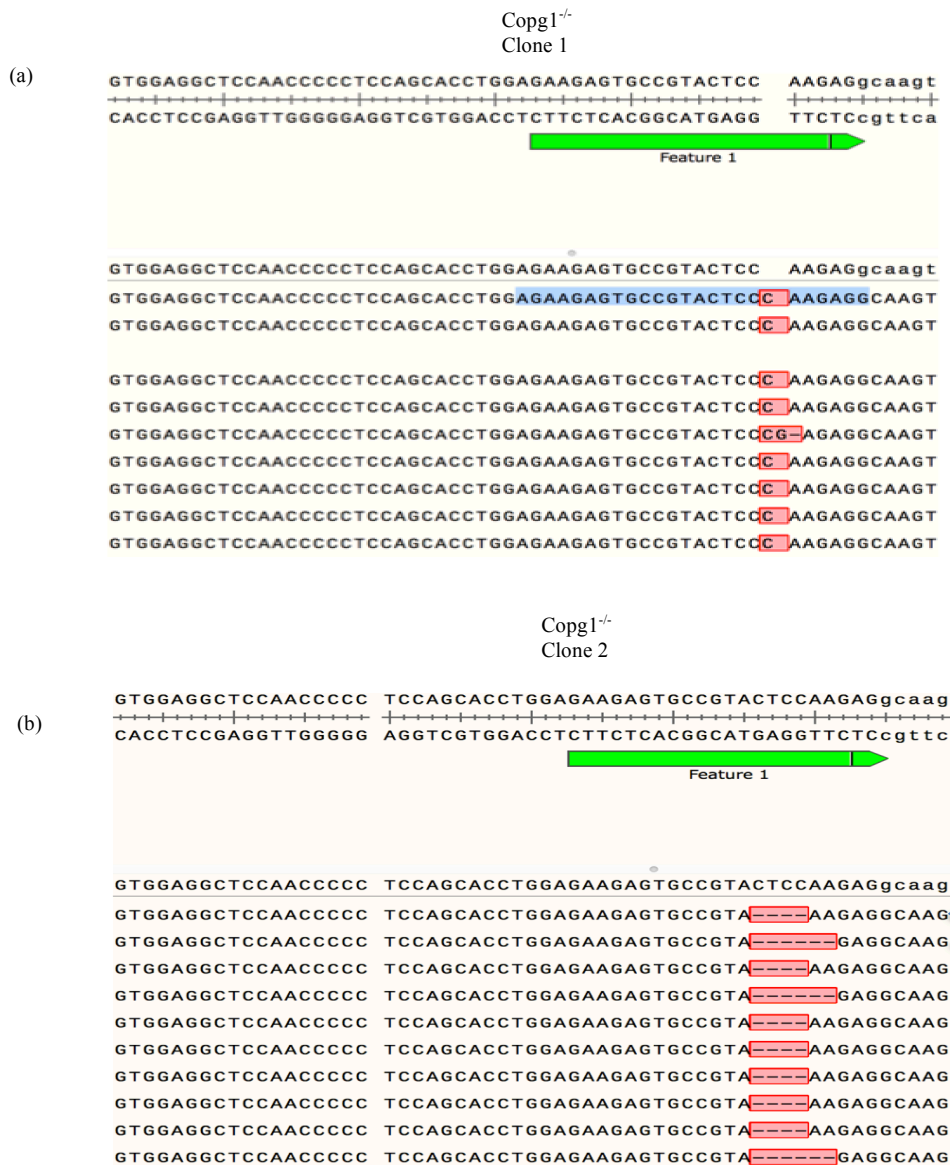
Figure 9: Sequence characterization of the γ1−COP KO clones.

(a-b) Represent frameshift mutations in the g.DNA of Copg1 KO clone 1(insertion) & 2 (deletion). Green arrows show potential sgRNAs against the targeting sequence. Red marking shows the mutations in the g.DNA sequence.

To further validate the knockout at the genomic level, gDNA from these clones were sequenced. Sanger sequencing of the Copg1(both clones) and Copg2 (clone c15) knockout clones revealed that each of them had frameshift mutations which results in premature translation termination (figure 9a-b & 10b).
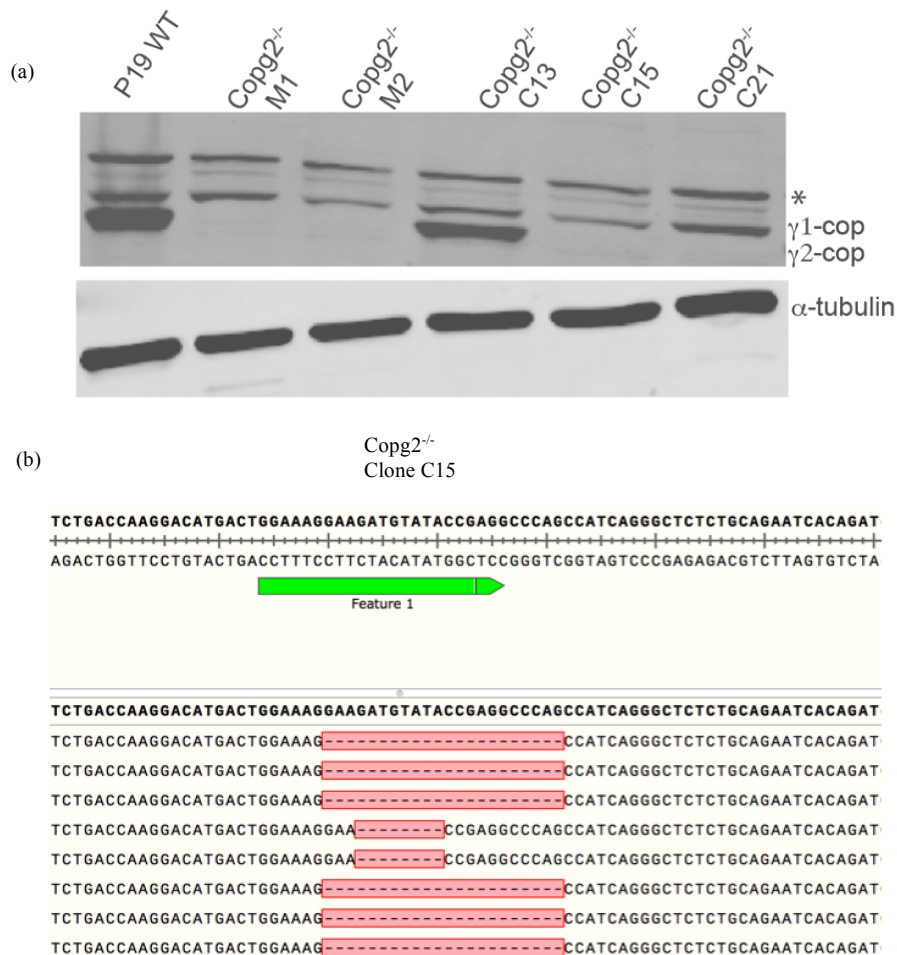
Figure 10: Analysis of the Copg2 KO clones.

(a) Western blotting of Copg2 knockout clones to check the deletion of γ2-COP protein using mixture of γ1 & γ2 COP specific antibodies. Star shows non-specific band. Expected molecular weight for γ1-COP is 99.5 kDa and for γ2-COP is 97.5 kDa and α-tubulin is 55 kDa, protein loading control. (b) Represent frameshift mutations in the g.DNA of Copg2 KO clone C15 (deletion). Green arrows show potential sgRNAs against the targeting sequence.

For the Copg1 gene an additional knockout cell line was generated using the eSpCas9(1.1) variant. In this variant, three-point mutations in the Cas9 sequence reduce off target cleavage without affecting on-target cleavage efficiency(Slaymaker et al. 2016). Out of three clones made with the eSpCas9(1.1) protein, one clone showed complete deletion of γ1-COP protein (figure 11). eSpCas9(1.1) Copg1 knockout clone was used for embryonic body formation experiments to exclude clonal variation. For further experiments this clone was not used since the rescue cell lines were generated in Copg1 KO clone1.
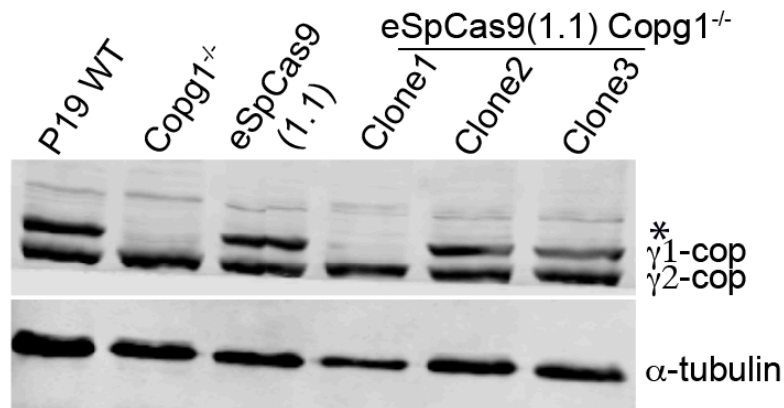
Figure 11: Analysis of the Copg1 KO clones generated using eSpCas9(1.1).

Western blotting of Copg1 knockout clones to check the deletion of γ1-COP protein using mixture of γ1 & γ2 COP specific antibodies. * represents non-specific band. Copg1 KO clone from normal CRISPR-Cas9 system was used as a positive control and eSpCas9(1.1) (empty plasmid) was used as a transfection control. Expected molecular weight for γ1-COP is 99.5 kDa and for γ2-COP is 97.5 kDa and α-tubulin is 55 kDa, protein loading control.

2.3. Generation of rescue cells

Furthermore, to validate any phenotype resulting in absence of both Copg1 and Copg2 gene, rescue cell lines were firstly generated by using PiggyBac (PB) plasmids. Copg1KO cells were rescued with full length Copg1 gene (PB-Copg1) and Copg2 KO cells were rescued with full length Copg2 gene (PB-Copg2) using PB system. In the PB system, the transgene is inserted between two inverted terminal repeat sequences (ITRs) that are recognized by the PB transpose and thus enables its random integration preferentially at TTAA

chromosomal sites of the target genome (Cary et al. 1989; Fraser et al. 1995). Pool of cells were selected with hygromycin since the integration plasmid had hygromycin selection cassette. In the rescued cell line, western blot analysis revealed that constitutive overexpression of one paralogue suppresses the expression of other paralogue (figure 12, 3rd and 6th lane from left). The rescue plasmid drive expression of γ1-COP or γ2-COP with a strong CAG promoter. In addition, the rescue cassette may integrate multiple times into the genome. This probably leads to a considerable overexpression of the exogenous myc-tagged γ-COP paralog that will then efficiently compete out the endogenous paralog for access to coatomer. As individual COP subunits are normally not observed outside of the assembled complex (Wegmann et al. 2004) and γ-COP was found to be insoluble as a recombinant protein (Wegmann et al. 2004), it is highly probable that non-assemble γ-COP is rapidly degraded. Altogether, overexpression of γ1-COP leads to the disappearance of γ2-COP and vice versa. To solve this issue, a bacterial artificial chromosome for DNA integration (Bacmid) system was used. It allows integration of an extra chromosomal copy of a gene with its own promoter into the genome, leading to physiological expression and regulation (Pennock, Shoemaker, and Miller 1984). Using this system rescue cells for Copg1 gene was generated, where the whole locus of Copg1 (with all the exons and introns) subunit, tagged with GFP at the C-terminus, was exogenously reintroduced (figure 12, 4th lane from left). Using Bacmid system protein expression of both paralogs was observed like the endogenous one and did not suppress the expression of other paralog.
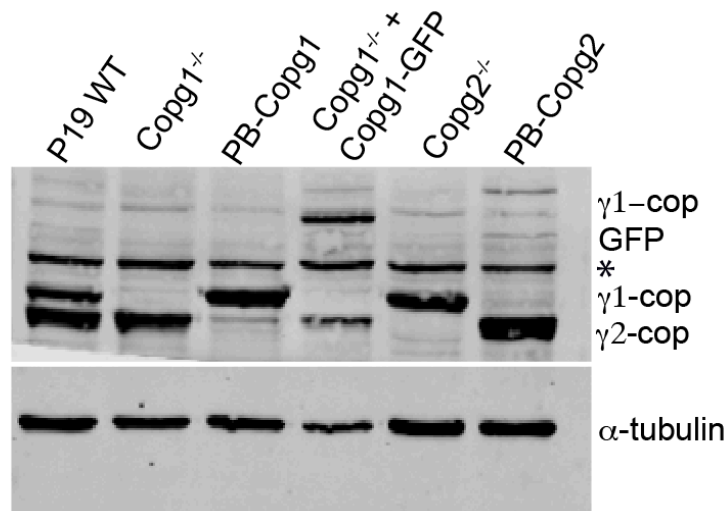
Figure 12: Copg1 rescue using piggybac and bacmid system.

Western blotting of rescue cells to see the expression of γ1 & γ2 COP protein using specific (mixed) antibodies. Star shows non-specific band. Expected molecular weight for γ1-COP is 99.5 kDa and for γ2-COP is 97.5 kDa, Copg1-GFP is 135kDa and α-tubulin is 55 kDa, protein loading control.

In the GFP-tagged γ1-COP expressing BAC-rescued cells to verify if this protein can integrate into the complex which is important for the function of the gene. From the immunoprecipitation it was observed that γ1-COP-GFP can be immunoprecipitated together with the α-COP and β'-COP subunits (figure 13a). To verify the functionality of GFP-tagged γ1-COP, Copg2 was disrupted in the BAC-rescued Copg1 knockout cell line. Since all COP subunits, except e-COP, are essential (Watson et al. 2004)**,** obtaining cells that solely express γ1-COP-GFP is a read-out for functionality. I was successful in obtaining such a cell line (figure 13b) indicating that the GFP tag does not interfere with the functionality of the gene, which also supports the data from the pulldown of coatomer.
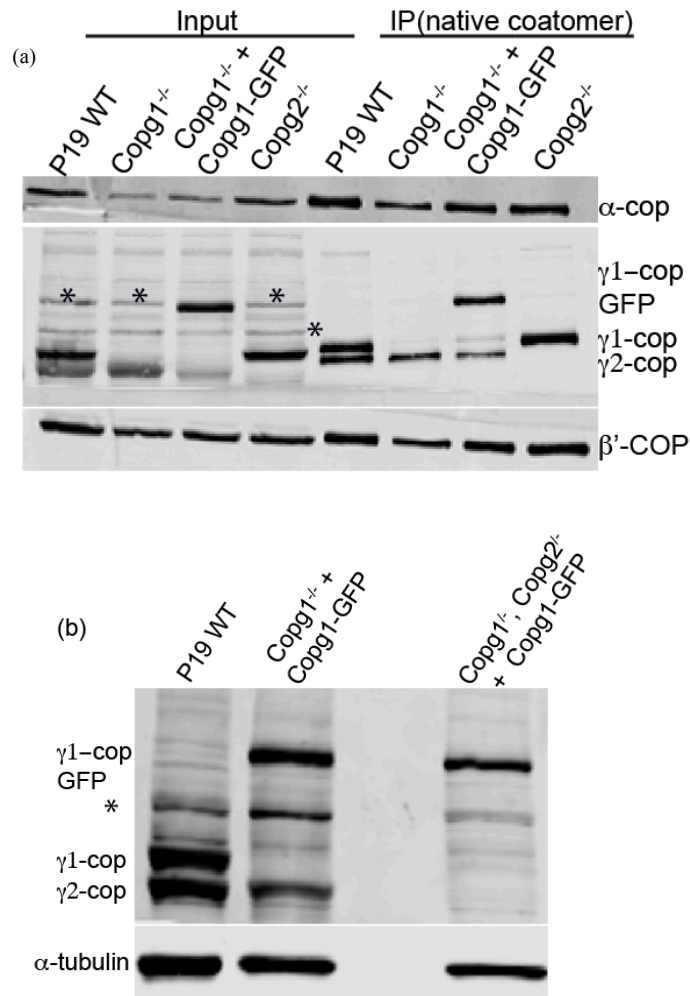
Figure 13: Functionality test for the Bacmid Copg1 rescue cells.

(a) Immunoprecipitation of different COPI subunits using CM1 antibody and blotted against specific antibodies. 2% of input was used for western blotting. (b) Western blotting of γ1-COP-GFP protein. Star shows non-specific band.

Rescue cells generated by using Bacmid system have been used for all the experiments to show recovery of the phenotype so that gene regulation can be maintained like the endogenous. For embryonic body formation and neurite formation experiments rescue cells made by using PiggyBac system have also been used.

2.4. Coatomer complex formation is not affected upon knockout

Coatomer is a very stable heptameric complex. To determine that the existing phenotype is because of the gamma paralogs it is important to see whether knock out of both paralogs affecting the expression of other subunits of coatomer. Protein expression of other subunits of coatomer were analyzed using specific antibodies. In the Copg1 KO cells expression level of Copg2 is increased and in Copg2 KO cells levels of Copg1 is increased while expression of other subunits is not affected (figure 14a). This suggests that the total amount of coatomer remains unchanged in the cell. Coatomer is only functional as a fully assembled complex. To study whether coatomer subunits are correctly incorporated into complex in the absence of one γ-COP paralog, immunoprecipitation of coatomer using the CM1 antibody, an antibody that recognizes native coatomer (Wegmann et al. 2004) was performed. All the analyzed coatomer subunits were efficiently immunoprecipitated in WT, Copg1 KO and COpg2 KO cells (figure 14b). This result shows that coatomer complex formation is unaffected in absence of one or the other paralogue of γ-COP.
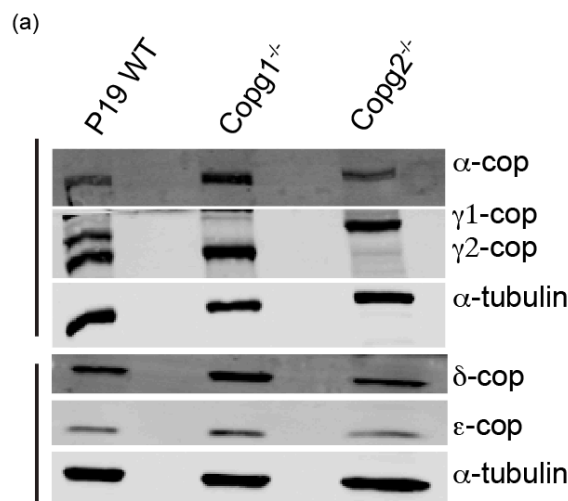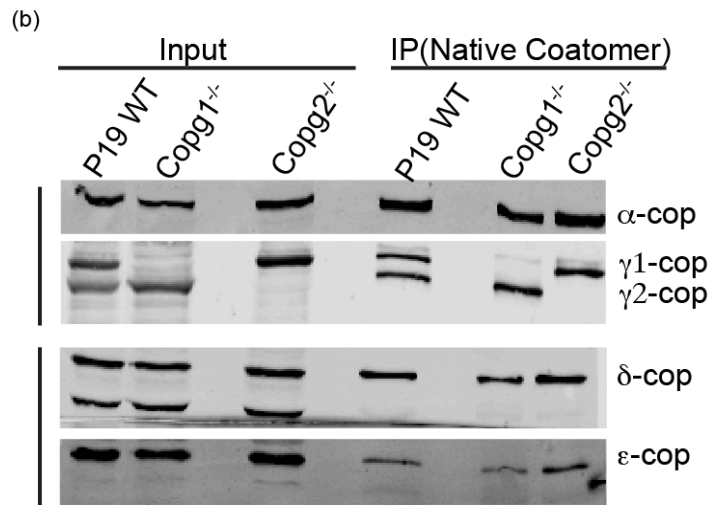
Figure 14: Analysis of coatomer subunits and complex formation.

(a) Western blotting of different COPI subunits using specific antibodies in absence of Copg1 and Copg2 genes. (b) Coatomer pulldown using CM1 (native coatomer) antibody. 2% of input was used for western blotting.

2.5. Copg1 is necessary for embryonic body formation

After generating knock out cells an important aim was to study if absence of Copg1 and Copg2 affect neurogenesis. Before starting with the neuronal differentiation pluripotency of the knockout cells was first determined. Since P19 cells are pluripotent and can be differentiated into neurons they should express pluripotent markers. Proteins levels of Nanog and Oct-4 transcription factors, which play important role during self-renewal of undifferentiated cells also known as pluripotent markers (**ref),** were analyzed by western blotting using specific antibodies. Both KO cells do express pluripotent marker (figure 15). Suggesting that pluripotency of the cells is not affected in the KO cells.

In the classical differentiation protocol, to activate signaling pathways for cell polarization, cell-cell contacts are a very important process for neural induction (Wang et al. 2006). Before the formation of neurites P19 cells are cultivated to make cell aggregates, also known as embryonic bodies, when treated with RA. Cell aggregation in presence of RA leads to the formation of mesoderm and endoderm cell types (Wang et al. 2006).
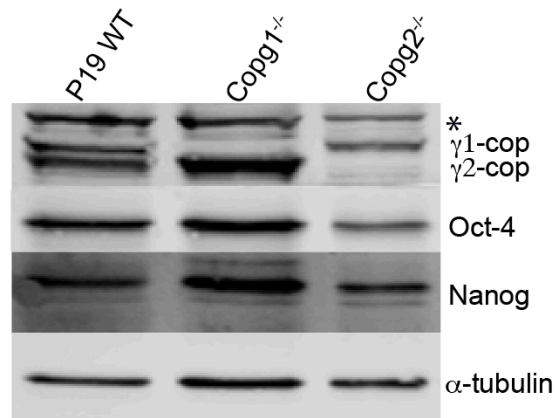
Figure 15: Analysis of pluripotency markers in Copg1 and Copg2 KO cells.

Western blotting of pluripotent markers Oct-4 and Nanog in P19WT, Copg1 and Copg2 KO cells using specific antibodies. Star shows non-specific band. Molecular weight of Oct-4 is 45kDa, Nanog is 45kDa and α-tubulin is 55 kDa, protein loading control.

To determine whether KO of γ-COP paralogs affect the embryonic body formation, the hanging drop method was used. For each hanging drop 20 μL of volume containing 200 cells were used. After two and four days of aggregation images were taken with the bright field microscope. It was observed that for the majority of P19 WT and Copg2 KO cells' embryonic bodies had tight boundaries and cells were nicely connected with each other by contrast Copg1 KO EBs lacked tight boundaries, however the cells showed aggregation but with cells loosely connected to each other (figure 16a). Partial rescue was observed in Copg1-GFP rescued cells.
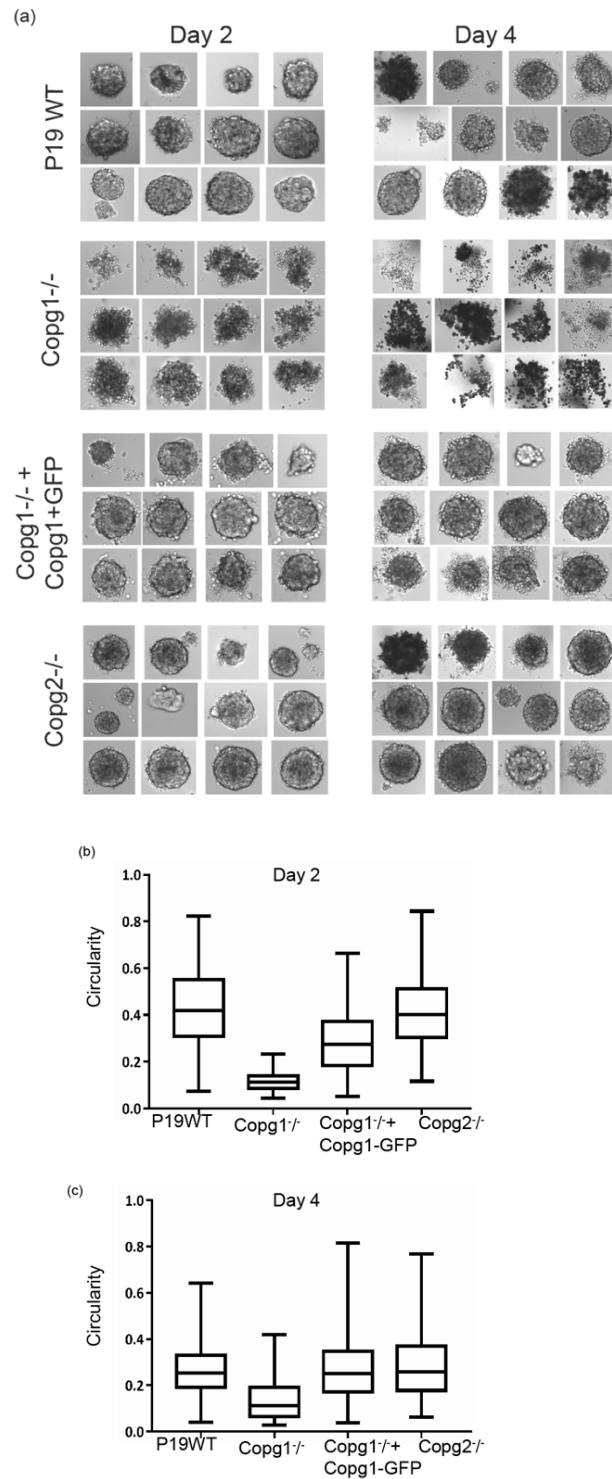
Figure 16: Hanging drop assay for Copg1 and Copg2 KO cells.

(a) Embryonic body formation at day 2 and day 4. Images were taken using 10x objective under the brightfield microscope. (b) Quantification of embryonic bodies. Circularity was measured using Fiji (imageJ). value of 1.0 indicates a perfect circle. Box plot was plotted, it indicated minimum to maximum values and line between the box shows the median value.

When embryonic bodies from eSpCas9(1.1) Copg1 were observed they also showed poor cell aggregation (figure 17a). For quantitative analysis the circularity index of embryonic bodies was measured by using ImageJ for more than 100 aggregates per condition. For the quantification, aggregates which contained more than 10 cells were taken into consideration. The circularity index gives the ratio of $4\pi*$area/perimeter^2; a value of 1.0 indicates a perfect circle. As the value approaches 0.0, it indicates an increasingly elongated shape (Values may not be valid for very small particles.) (figure 16b & 17b).
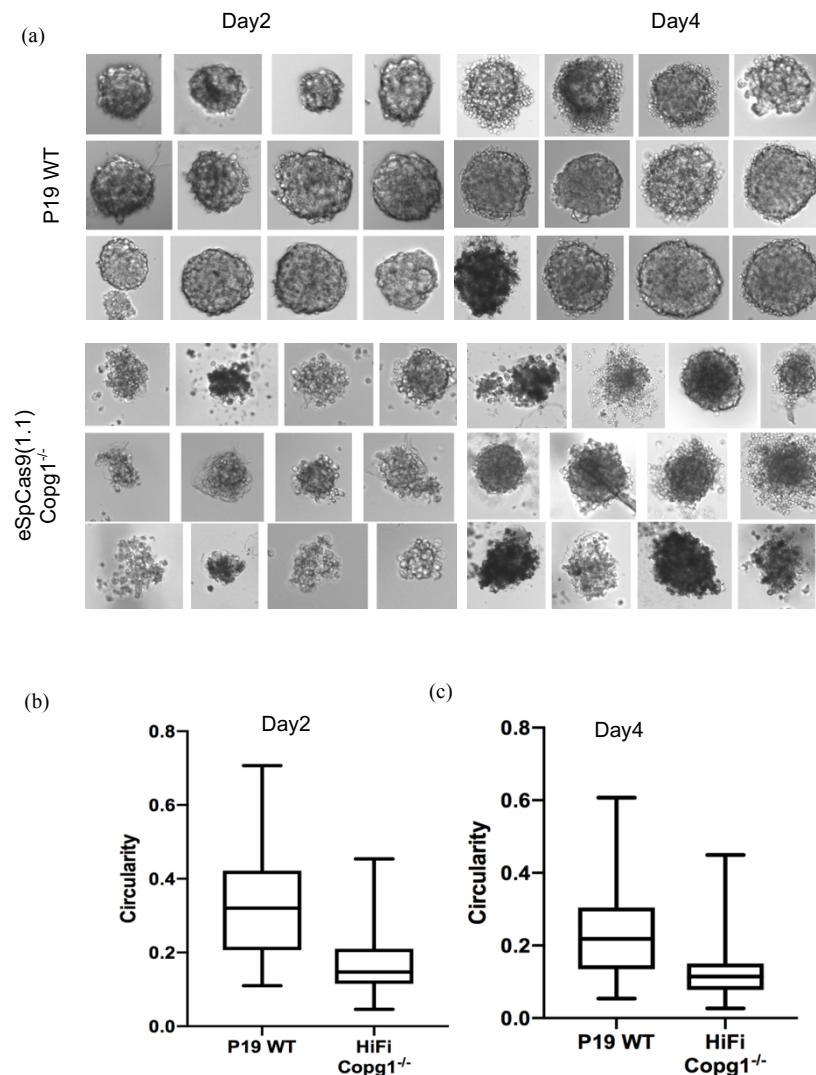
Figure 17: Hanging drop assay for HiFi Copg1 KO cells.

(a) Embryonic body formation form HiFi Copg1KO at day 2 and day 4. Images were taken using 10x objective with the help of brightfield microscope. (b) Quantification of embryonic bodies. Circularity was measured using Fiji (imageJ). value of 1.0 indicates a perfect circle. Box plot was plotted, it indicates minimum to maximum values and line between the box shows the median value.

2.6. Copg1 is necessary for neurite formation

In presence of RA cell aggregates lead to neurite formation, derived from neuroectoderm when dissociated and re-plated in adherent conditions (McBurney 1993). To analyse neurite formation, cells (10^6 total per dish) were first cultured on non-adherent bacterial dishes to make EB, which is the classical protocol, in presence of RA for 4 days. As expected from the hanging drops experiments, Copg1 KO cells show less and smaller cell aggregates with more single cells present in the background of the dish (figure 18).
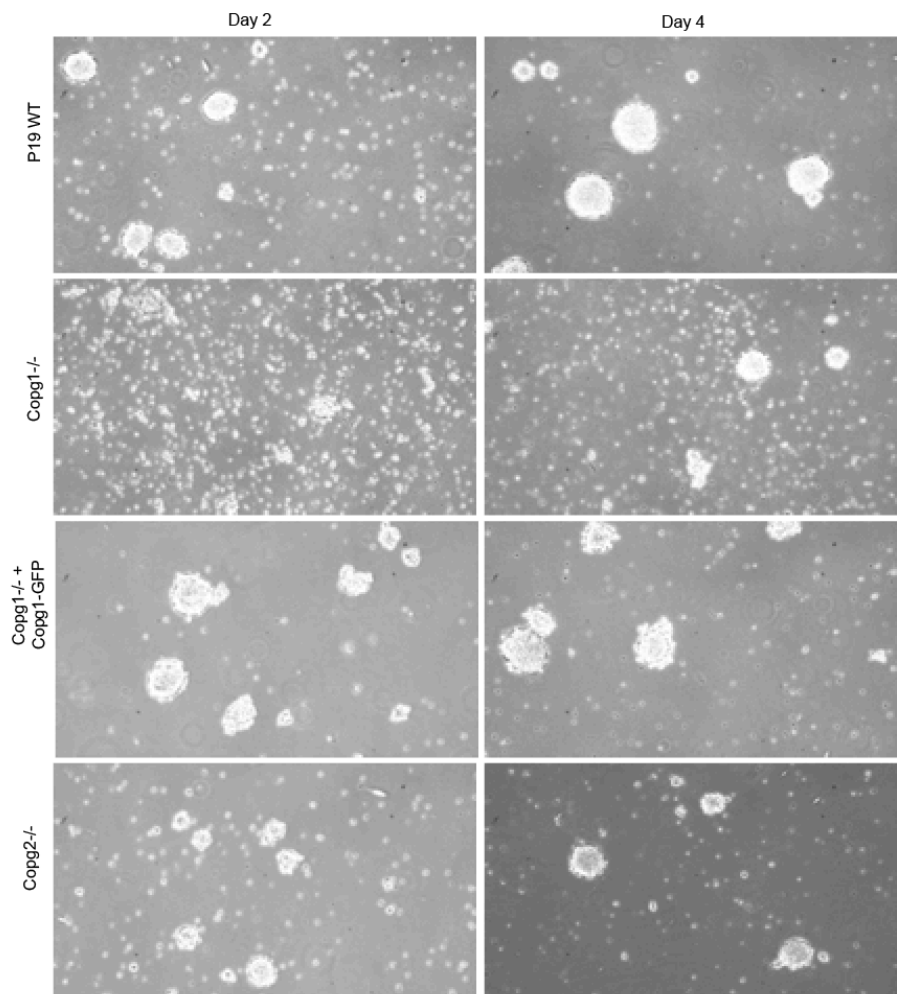
Figure 18: Cell aggregation assay in non-adherent condition.

Cell aggregation at Day2 and Day4 in presence of 0.1um RA in non-adherent condition in 10cm bacterial dish. Images were taken with 10x objective under the brightfield microscope.

After 4 days of aggregation cells were dissociated and 50,000 cells per well were plated onto poly-L-lysine coated 8-well ibidi slides. After 2 days of plating 10 µM Cytosine-1-β-D-arabinofuranoside (AraC) treatment was given so that dividing cells can be poisoned to enrich for non-dividing neuronal cells. After 8 days of differentiation protocol cells were fixed with 4% PFA and stained to detect neurite formation by immunofluorescence microscopy. To detect neurites the neuronal specific marker Tubulin ß III was detected with the specific antibody TujI was used (figure 19a).

(a)
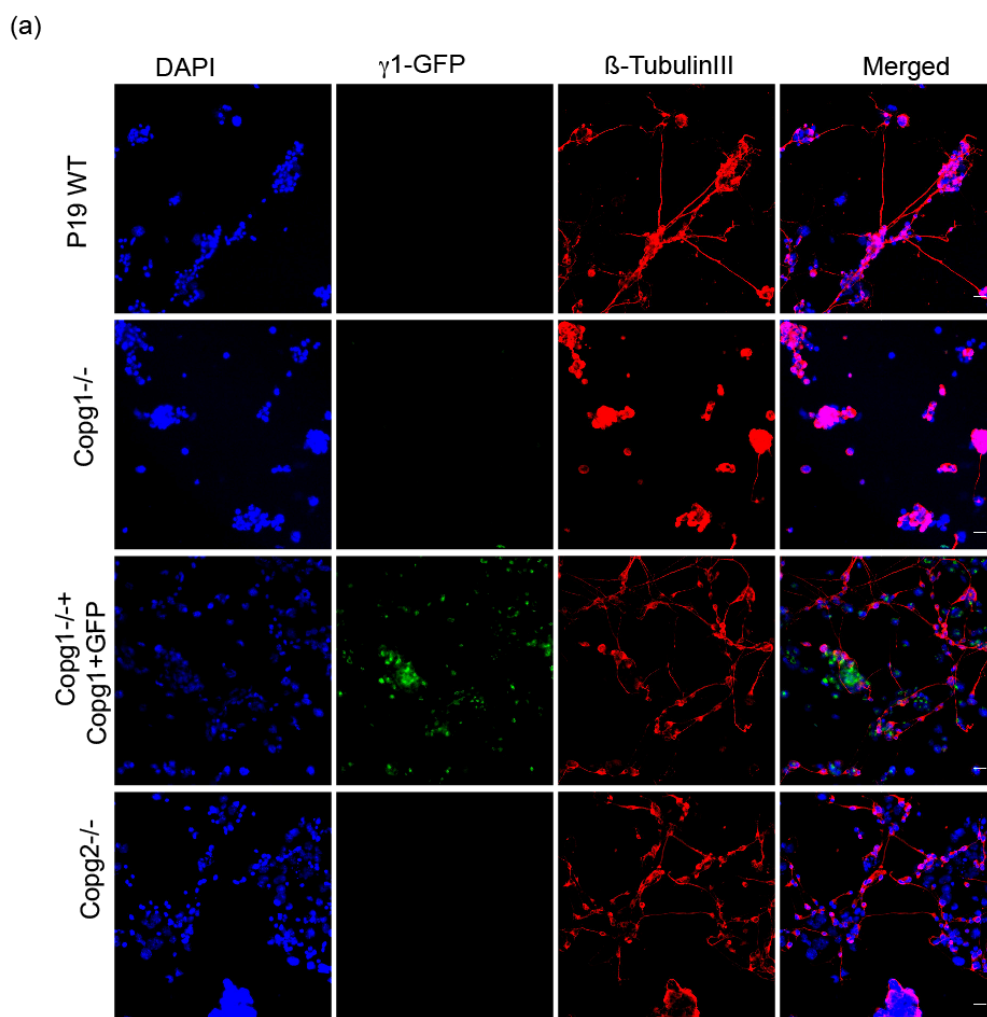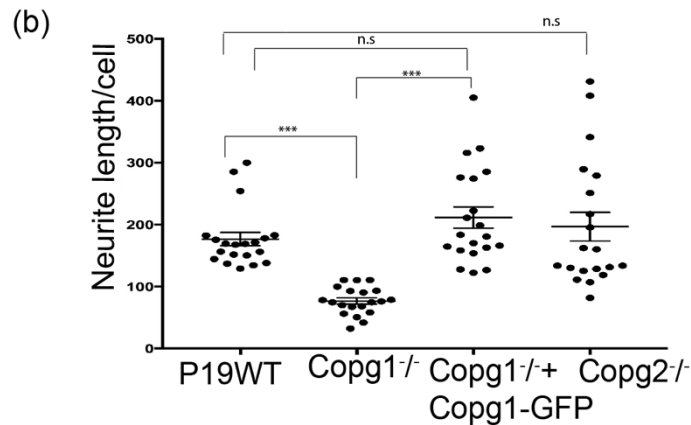
Figure 19: Immunofluorescence microscopy for neuronal differentiation using classical method.

(a) Neuronal differentiation using classical protocol and immunostaining with β-tubulinIII (Cy5, red channel) to detect neurites. DAPI (405nm, blue channel) is used to stain DNA and γ1-COP-GFP protein is observed in GFP channel (488nm, green channel). Brightness intensity is same for all the images blue (600-800), green (700-1100) and red channel (600-700). Scale bar is 30um. (b) Quantification of neurite length using neurite quant software. Two-tailed unpaired t-test was performed for the statically significant analysis (*** p-value is <0.0001). Here n=20 since 20 random pictures were taken for the analysis.

From the immunofluorescence microscopy it was observed that Copg1 KO cells do not show a comparable neurite outgrowth pattern to the P19 WT cells. They have either none or very short neurites (figure 19a). However, Copg1 KO cells do show staining against ß-tubulin III antibody, which was also observed by western blot analysis (figure 20a), which means they have the ability to differentiate into neurons but they are incapable of producing neurites. This phenotype was rescued in Copg1-GFP rescued cells. By contrast Copg2 KO cells show similar neurite outgrowth compared to the P19 WT cells (figure 19a & b). In the initial analysis of P19 WT cells during neuronal differentiation, I observed that γ2-COP protein is less expressed at late differentiation stages (figure 5a). I thus sought to check if there are sufficient amounts of coatomer present during all neuronal differentiation stages upon Copg1 KO. Protein expression for γ1 and γ2-COP was observed comparable to P19WT cells. Two other coatomer subunits α−COP and δ−COP were observed to be expressed at comparable levels in P19 WT and Copg1 KO cells during neuronal

differentiation. Oct-4 and Tubulin ß III used as pluripotency and neuronal markers respectively, were also comparable in WT and Copg1 KO cells (figure 20a & 20b)
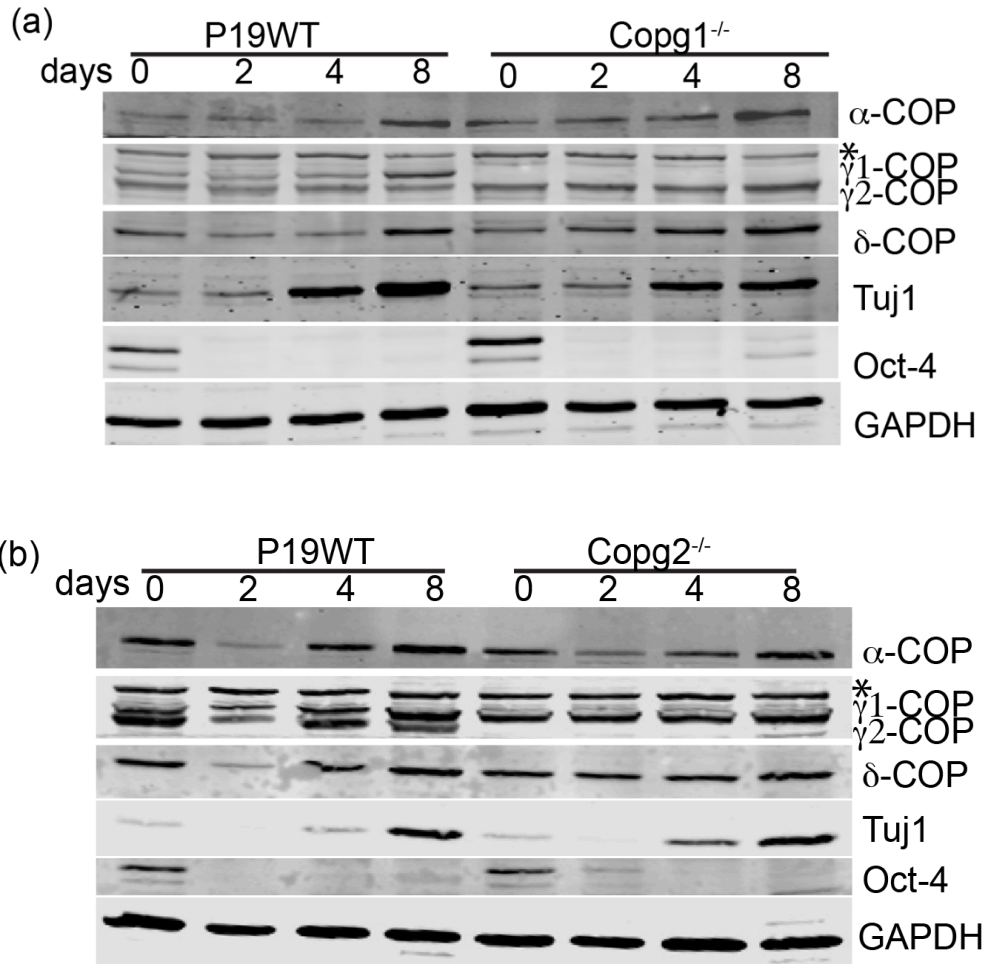
Figure 20: Analysis of different coatomer subunit during classical neuronal differentiation.

Western blotting of different COPI subunits, neuronal and pluripotent marker during neuronal differentiation of P19WT, Copg1 and Copg2 KO cells using specific antibodies. Star shows non-specific band. Molecular weight of α-COP 135 kDa, δ-COP 60 kDa, Tuj1 55kDa, Oct-4 45 kDa and GAPDH is 35 kDa, used for protein loading control. Western blotting was done by Karla Lopez.

Interestingly when the PB rescue cells for Copg1 and Copg2 genes were treated with 0.1µM of RA to induce EB formation on non-adherent bacterial dishes, Copg1 rescue cells showed fewer single cells in the background and improved cell aggregation compared to Copg1 KO

cells whereas EBs from Copg2 rescue cells were similar to those of Copg2 KO cells. EB morphology was quantified as described above with the circularity index (figure 21a & 21b).

(a)
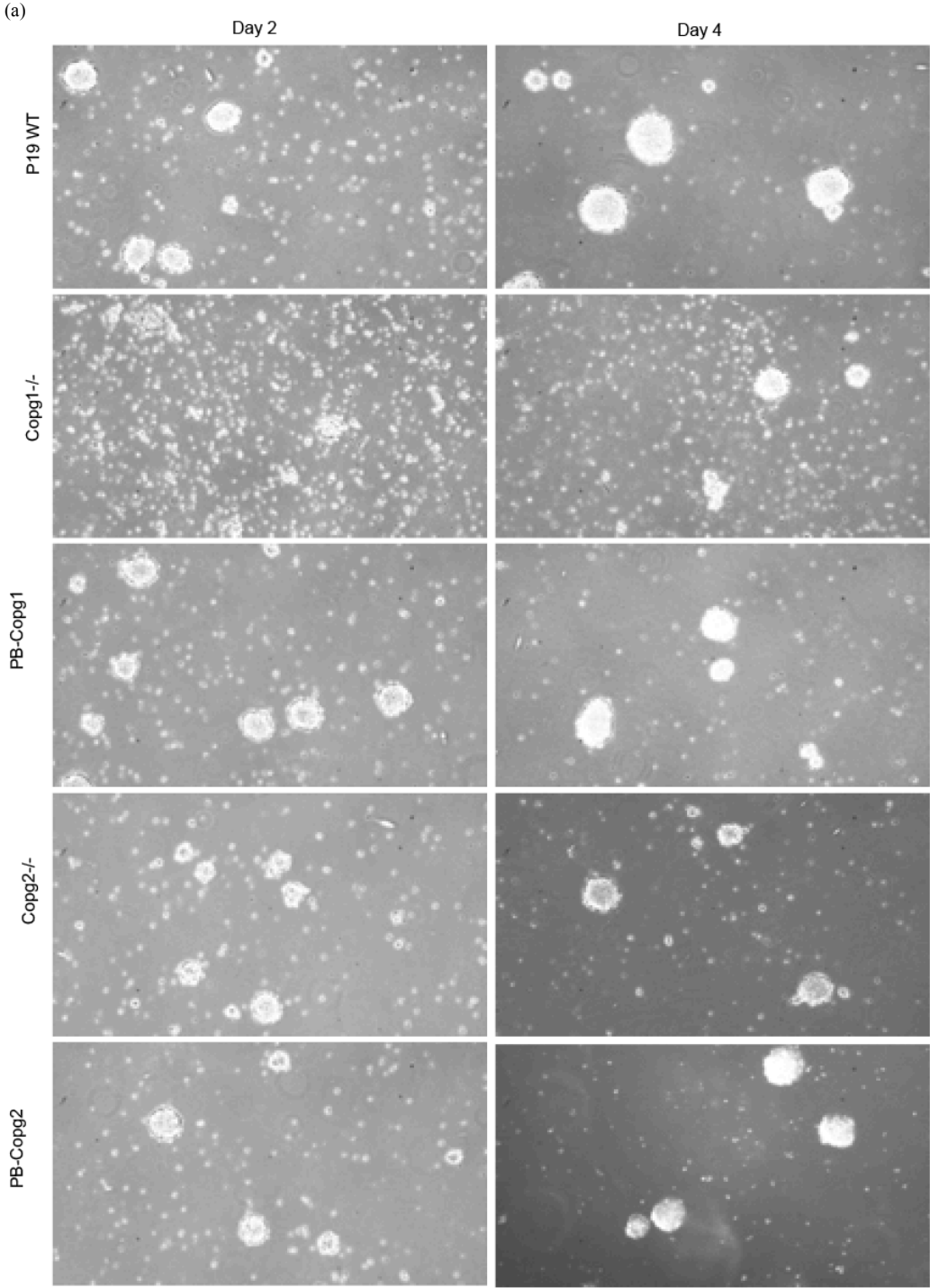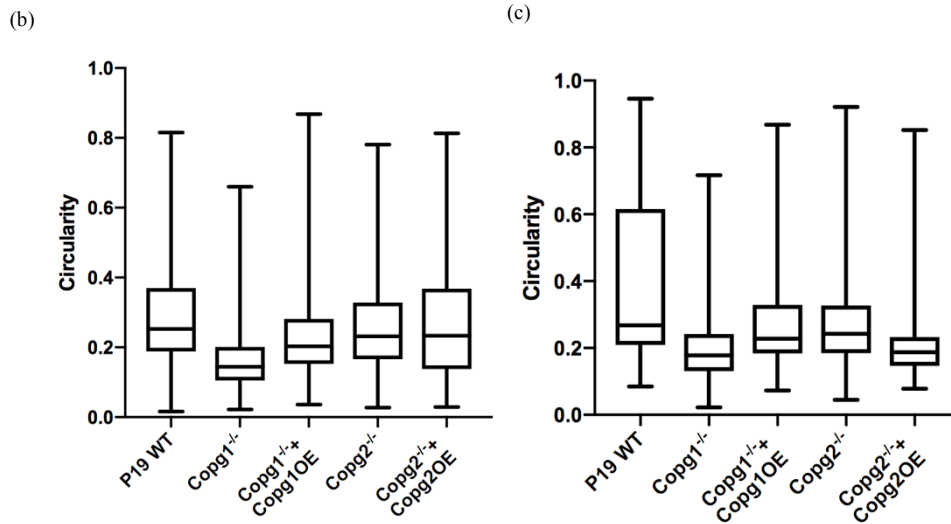
Figure 21: Cell aggregation assay for PB rescue cells.

(a) Cell aggregation at Day2 and Day4 in presence of 0.1um RA in non-adherent condition in 10cm bacterial dish. Images were taken with 10x objective under the brightfield microscope. (b&c) Quantification of embryonic bodies. Circularity was measured using Fiji (imageJ). value of 1.0 indicates a perfect circle. Box plot was plotted, it indicates minimum to maximum values and line between the box shows the median value.

When these aggregates were plated on poly-L-lysine coated plates and treated with 10μM of AraC, PB-Copg1 rescue cells showed improved neurite growth after 8 days of differentiation compared to Copg1 KO cells. While PB-Copg2 rescue cells showed reduced neurite outgrowth compared to Copg2 KO cells (figure 22a). Neurite lengths were measured using the same software Neurite Quant like previous data (figure 22b). Suggesting that increasing in protein levels of γ2-COP would show reverse phenotype supporting γ1-COP specific phenotype. As shown above, with the strong constitutive overexpression of γ1-COP as the expense of γ2-COP, PB-Copg1 rescue cells resemble Copg2 KO cells. Conversely, for the same reason, PB-Copg2 rescue cells are a mimic of Copg1 KO cells. Altogether, these results unravel an important function of γ1-COP during neurite formation and also suggest that increased expression of γ2-COP cannot overcome the phenotype of Copg1 KO cells.

(a)

| | DAPI | ß-TubulinIII | Merged |

P19 WT

Copg1-/-

PB-Copg1

Copg2-/-

PB-Copg2
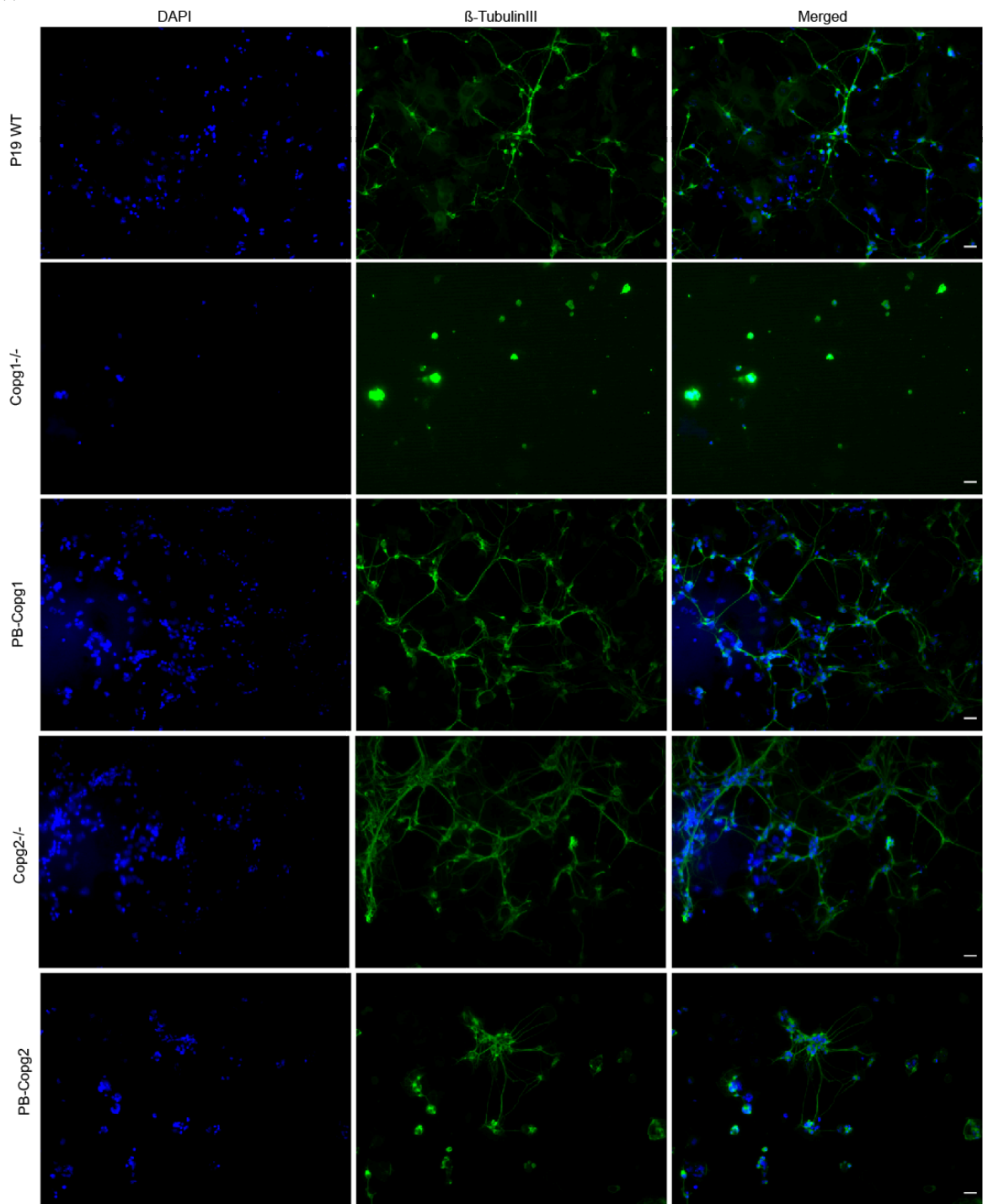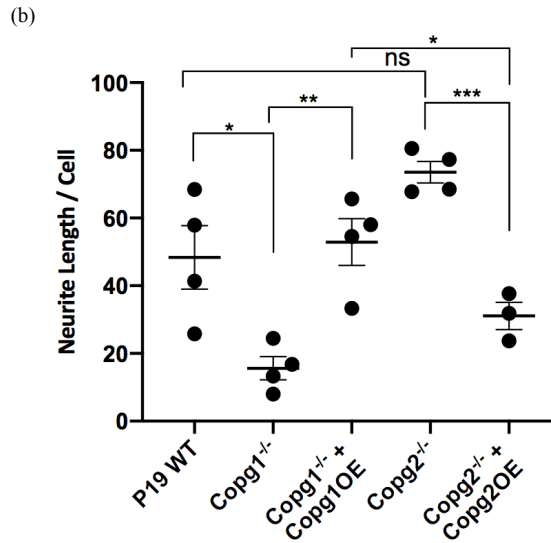
Figure 22: Immunofluorescence microscopy for neuronal differentiation in PB rescue cells using classical method.

(a) Neuronal differentiation using classical protocol method and immunostaining of the neurites using antibody against Tubulin ß III (TujI) (488nm, green channel) DAPI (405nm, blue channel) is used to stain DNA. Brightness intensity is same for all the images blue channel (54-129), green channel (0-184). Scale bar is 0.3um. (b) Quantification of neurite length using neurite quant software. Two-tailed unpaired t-test was performed for the statically significant analysis (p-value * <0.05, ** < 0.01, * <0.0001). Each dot indicates around 100 cells in total 500 cells were used for the analysis. Here n=5 since 5 random pictures were taken.**

2.7. Copg1 Knock out shows changes in Golgi morphology

It is very well established that COPI-coated vesicles are Golgi-derived vesicles and one of the important transport pathways in eukaryotic cells. It was thus important to analyze if the knockout of γ-COP paralogs affects morphology that organelle because this can affect the secretion or localization of proteins inside the cell. To analyze Golgi morphology, electron microscopic (EM) analysis was performed in the P19 WT monolayer cells together with Copg1/Copg2 KO and Copg1-GFP rescue cells (figure 23a). 30 cells per sample and around 60-70 Golgi stacks were used for the analysis.

From the quantification it was observed that:

1) More Golgi stacks per cell in Copg1 and Copg2 KO cells, not significant when compared WT vs. rescue.

2) Smaller Golgi area in Copg1 and Copg2 KO cells, not significant when compared WT vs. rescue.

3) More vesicles around Golgi stacks in Copg1 KO, suggests stronger fragmentation in these cells.

4) Smallest ellipse similar in all conditions: no dispersion of Golgi stacks throughout the cells. Both γ1 and γ2-COP are necessary for a correct Golgi morphology. Fragmented Golgi is usually coupled to transport defects and may for example affect the correct localization of glycosylation enzymes (figure 23b-e).

(a)

P19WT

Copg1^{-/-}

Copg2^{-/-}
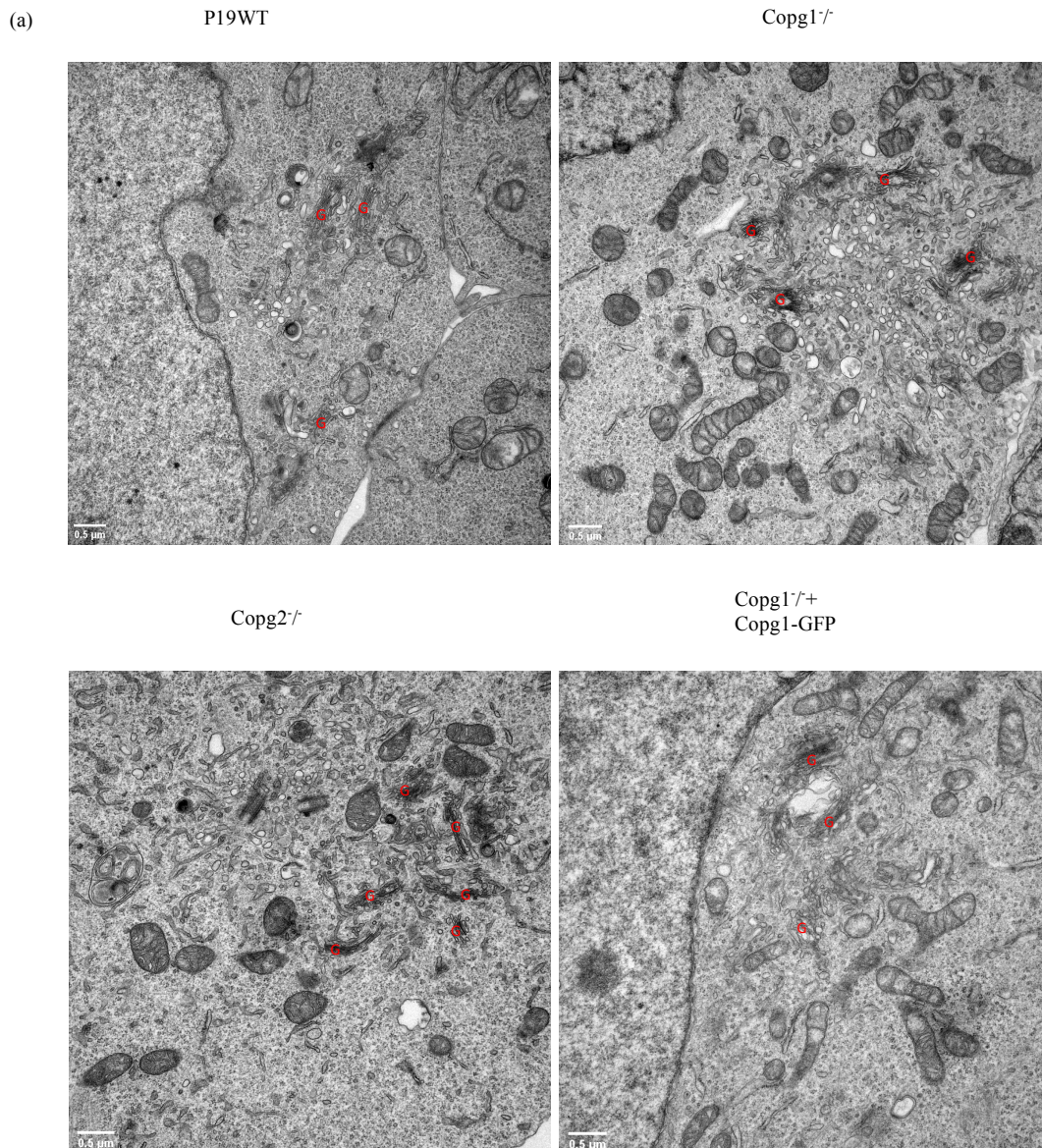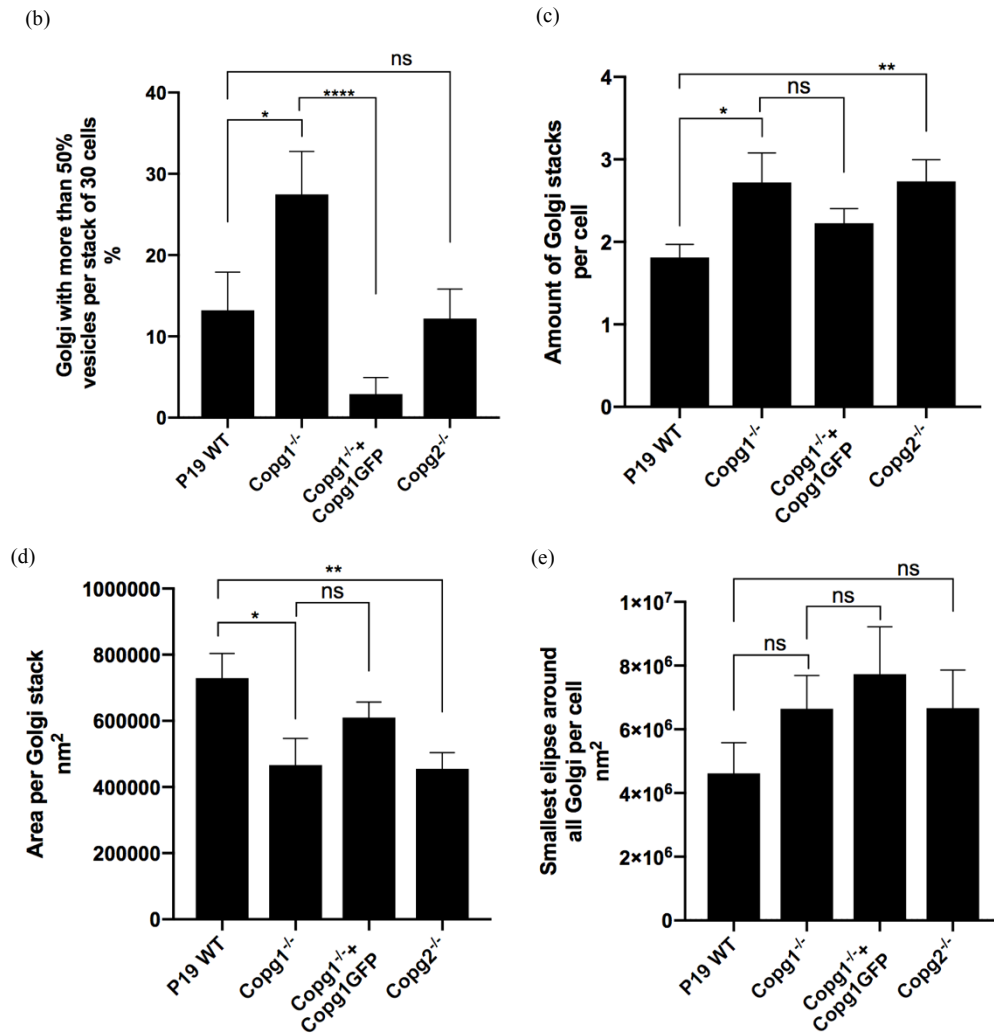
Copg1^{-/-}+
Copg1-GFP

Figure 23: Endomembrane morphology analysis.

(a) Electron microscopy of Golgi morphology in P19 WT, Copg1/Copg2 KO and Copg1 rescue cells. (b) Quantification of total amount of Golgi stacks per cell (c) Area of Golgi stacks (d) % of Golgi with more than 50% of vesicles per stack (e) Distribution of Golgi through-out the cell. Samples were fixed and embedded at the EM core facility. Further analysis imaging and quantification was done in collaboration with Judith Klumperman's group. (p-value * <0.05, ** < 0.01, * <0.0001).**

From the electron microscopic study, it was observed that Golgi is fragmented in Copg1KO cells we also wanted to see if the ER is stressed. ER stress inhibits neurite outgrowth (Kawada et al. 2014). To exclude that we checked the apoptosis in the KO cells, since ER

stress induce the apoptotic cell death, found no apoptotic bodies in the cells. In these knockout cells, cell death was also determined by using the apoptosis marker Caspase-3. As a positive control for apopotic cells, P19 WT cells were treated with 1μM of Thapsigargin for 6hrs to induce ER stress which further leads to the cell death. By contrast to the thapsigargin-treated cells, WT and KO cells did not show significant staining for Caspase-3 suggesting knockout of γ1-COP or γ2-COP does not lead to pro-apoptotic cells (figure 24).
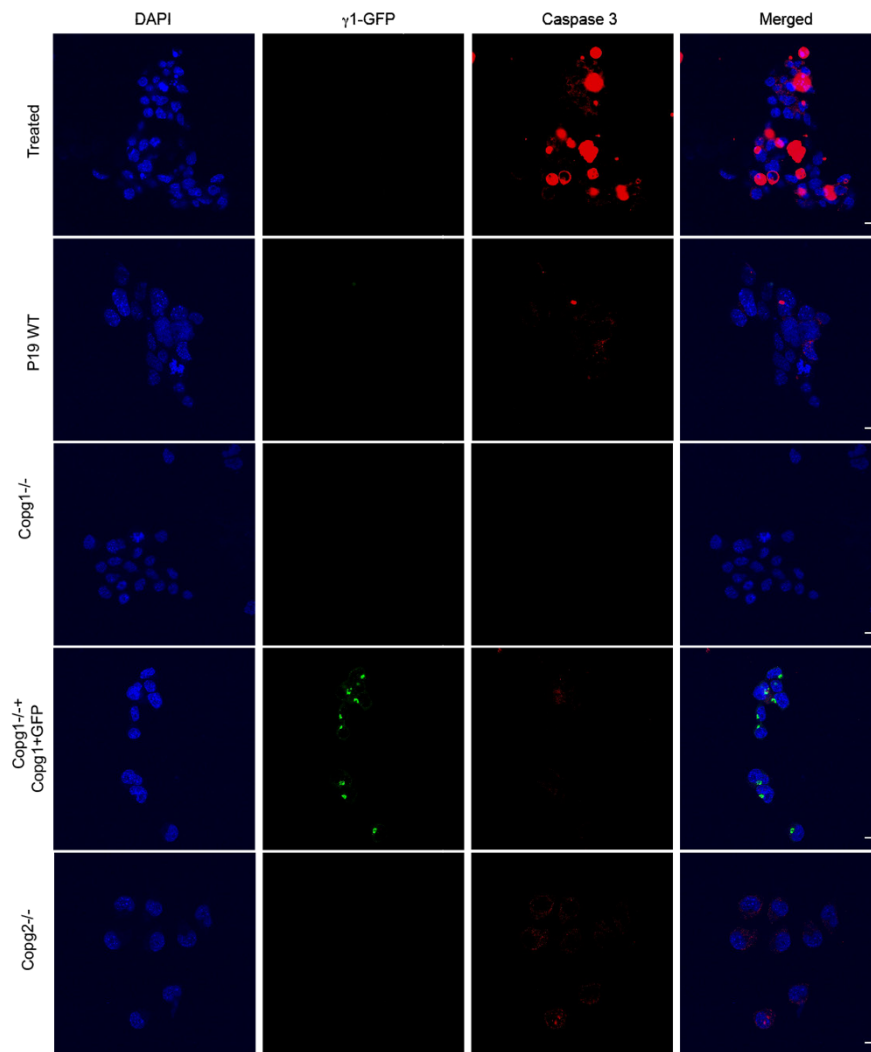
Figure 24: Immunofluorescence microscopy for apoptosis marker.

Immunostaining of cells with cleaved caspase-3 antibody. Red channel (cy5) shows fluorescence for apoptosis marker. DAPI (405nm, blue channel) is used to stain DNA and γ1-COP-GFP protein is observed in GFP channel (488nm, green channel). Brightness intensity is same for all the images blue channel (67-173), green (225-3624) and red (1425-4095). Scale bar is 10um. Immunostaining was done by Karla Lopez

2.8. Copg1 Knock out shows delay in cell cycle

Knock out clones were tested for cell growth to analyze if cell proliferation is affected upon knock out of γ-COP paralogs. Cells were incubated at 37^0C for 72hrs in an incubator fitted with a camera to allow live-cell imaging. Percentage area occupancy of the cells over time was measured and analyzed using the Inqucyte software. Both KO cells showed slower growth compared to WT cells with Copg1 KO cells showing the slowest proliferation rates. This phenotype of Copg1 KO cells was partially rescued with COPG1-GFP rescue cells (figure 25). Suggesting that both the paralogs are important for the cell proliferation.
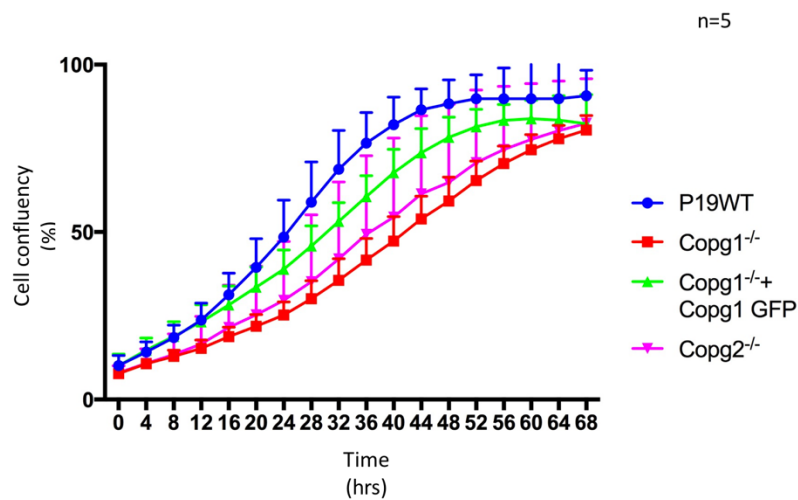
Figure 25: Analysis of cell proliferation.

Cell proliferation curve was generated using Inqucyte software. It shows percentage of the confluency of the cells per area over the 72hrs. Copg1 and Copg2 KO cells show slow growth compare to P19WT cells.

To further characterize the observed differences in proliferation rates, propidium iodide (PI) DNA staining was performed to analyze the cell cycle in WT and KO cells. PI staining is used to stain DNA to determine cell viability. It binds to double stranded DNA by intercalating between the base pairs. 100000 Cells were seeded in the 12 well plate for 24hrs. Fluorescence-activated cell sorting (FACS) was used to measure the fluorescence intensity of the dye which shows the population of cells in different phases of the cell cycle. It was found that Copg1 knock out has more cells in G1 phase and less cells in G2

phase as it shows lower intensity peak for G2 phase (figure 26b) and this phenotype was also overcome in the Copg1 rescue cells (figure 26d). Interestingly Copg2 KO cells which also showed slower growth compare to P19WT cells during cell proliferation do not show any block at a specific cell cycle stage (figure 26c), indicating an altogether slower cell cycle. This result also shows that the two γ-COP paralogs are not functionally redundant as they affect the cell cycle differently (figure 26b & 26c).
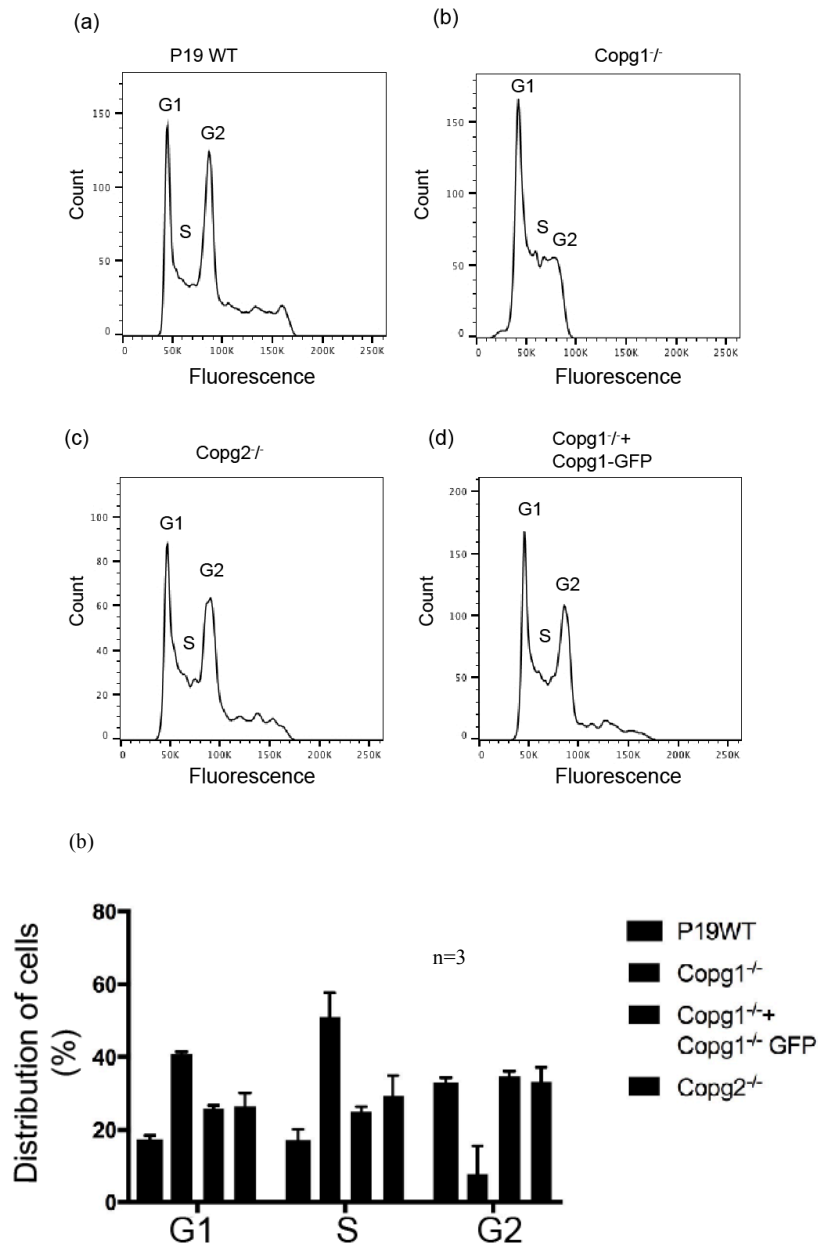
Figure 26: Cell cycle analysis.

2.9. Copg1 Knock out shows reduced neurite outgrowth using NeuroD2 differentiation method

Cell aggregation is important for the neurite outgrowth in presence of RA (Wang et al. 2006). We wanted to see if the cells are bypassed from the cell aggregation and if this effects the neurite out growth. To study the same cells were differentiated into neurons using another protocol in which cells were co-transfected with neurod2-mcherry, a basic helix-loop-helix (BHLH) transcription factor and its dimerization partner E12. After co-transfection cyclin-dependent kinase inhibitor p27^{Kip1} is elevated and cell cycle withdrawal occurs in the cell, which lead to the induction of neuronal differentiation. After 6 days only, neuronal cells are survived in the culture because media was replaced every second day with and without Glutamine along with AraC (Farah et al. 2000). With this protocol cells do not make embryonic body, after 6 days of differentiation immunostaining for neuronal specific marker TujI or Tubulin ß III was performed. Similar to the two-step differentiation protocol, Copg1 KO cells show much less neurite outgrowth compare to P19 WT cells. Rescue of neurite outgrowth was observed in Copg1-GFP cells (figure 27a). Neurite lengths were analyzed from both protocols using the Neurite Quant software, an open software for high content screening of neuronal morphogenesis (Dehmelt et al. 2011), for quantitative analysis and then plotted the number of cells in the analyzed field. (figure 27b). Each dot in the graph indicates analysis of 100-200 cells in total more than 1000 cells were used for the quantification. Quantification of neurite length tells us that even without embryonic body formation Copg1KO cells do not have neurite formation as compare to the P19WT cells.
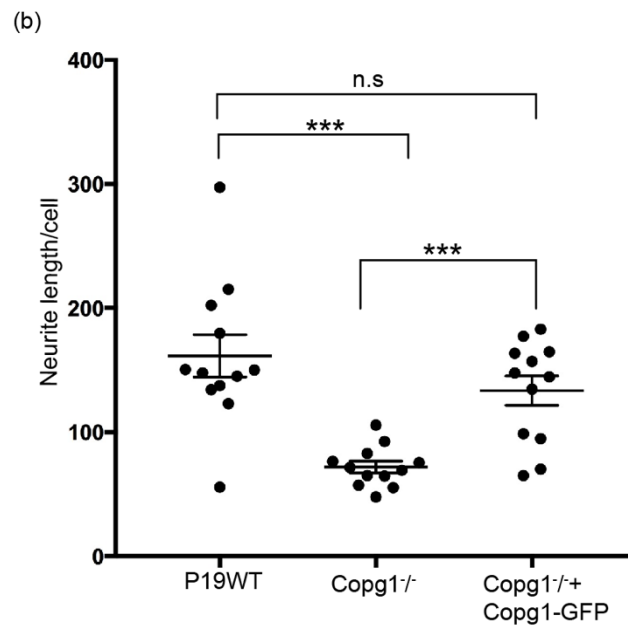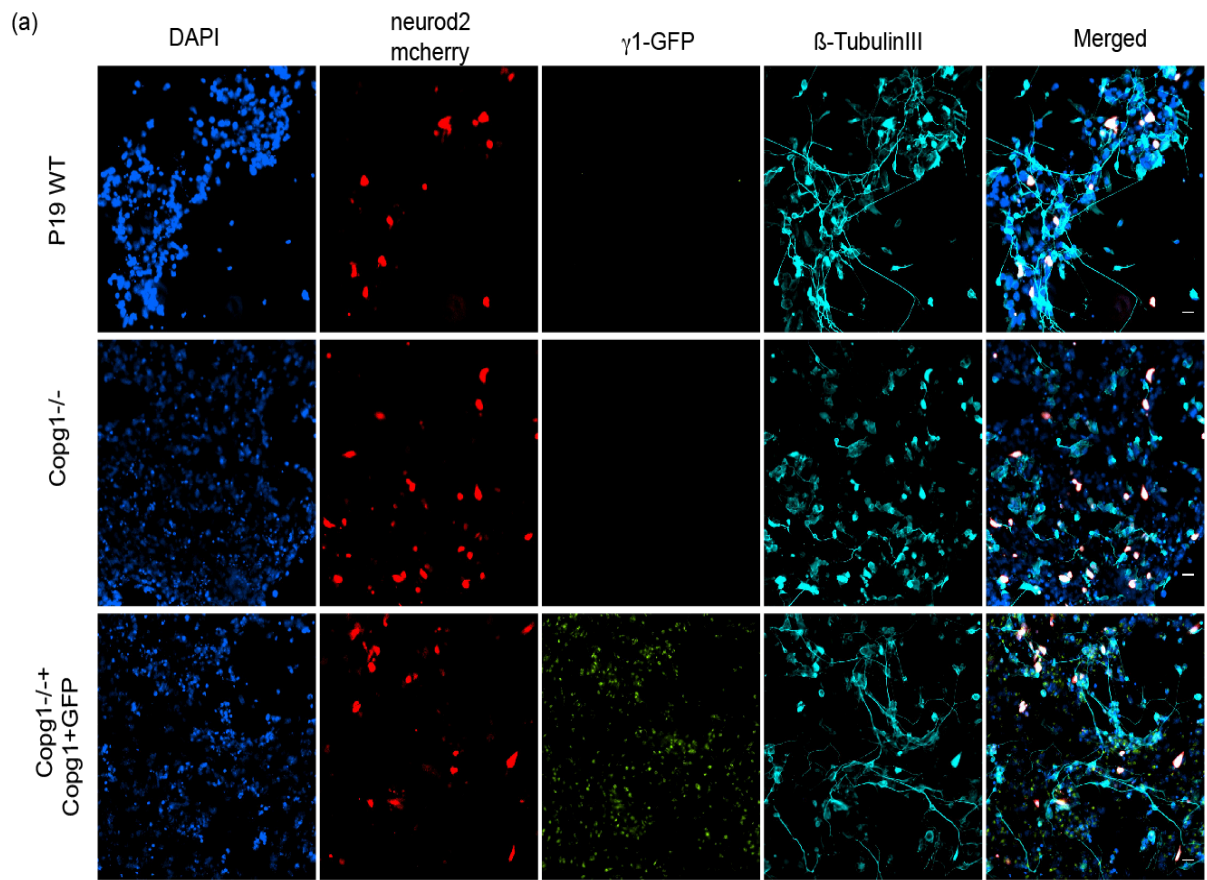
Figure 27: Immunofluorescence microscopy for neuronal differentiation using NeuroD2 method.

(a) Neuronal differentiation using neuroD2 differentiation method and immunostaining of the neurites using β-tubulinIII (FITC, Cyan color) antibody. DAPI (405nm, blue channel) is used to stain DNA and γ1-COP-GFP protein is observed in GFP channel (488nm, green channel). Brightness intensity is same for all the images blue (800-1500), red channel (600-900), green (800-1400) and cyan (600-1200). Scale bar is 30um. (b) Quantification of neurite length using neurite quant software. Two-tailed unpaired t-test was performed for the statically significant analysis (*** p-value <0.0001). Here n=12 since 12 random pictures were taken for the analysis.

3. Discussion

Two COPI subunits come as two paralogs. However, by contrast to Sec24 paralogs that have been shown to expand the cargo repertoire of COPII vesicle, no clear function has been assigned to COPI paralog subunits. In addition, though the function and mechanism of the COPI pathway is generally well defined, more cell type-specific functions are not well studied. Publicly available whole transcriptomics data pointed that both gamma-COP paralogs are expressed differentially during mouse embryonic stem cells differentiation (Tippmann et al. 2012). Using γ1- and γ2-COP KO cell lines we have uncovered a role for γ1-COP in this process by independently regulating EB formation and neurite extension. In addition, and more generally Golgi morphology analysis and proliferation assays suggest that γ1- and γ2-COP are only partially redundant but both have specific functions. Altogether this suggest that gamma-COP paralogs, which were considered to be redundant until now, also clearly have specialized non-redundant functions.

3.1. COPII paralogs

Human cells express four different paralogs of Sec24p. Increased number of COP subunits are suggested to extend cargo repertoire since every coat variant is proposed to reveal contrasting affinity for cargo transport signals (Mancias and Goldberg 2008; Wendeler, Paccaud, and Hauri 2007). Several studies have shown the functional difference between Sec24 isoforms depending on the paralog used during the coating and the transport of vesicles (Adolf et al. 2019). There are few studies which suggest that COPII pathway might have cell specific function as well. For example, colocalization of endogenous Sec13 protein with exogenously expressed Sec24-YFP protein suggests presence of ER exit sites in neuronal dendrites and also cargo carriers generated from these sites are distributed throughout the dendrites (Horton and Ehlers 2003). Additionally, precise targeting of GABA-1 transporter to axon is depend upon COPII and ARFGAP1(Reiterer et al. 2008). In recent study it was shown that Sec24c knockout in mice neural progenitors during embryogenesis causes unfolded protein response and apoptosis in postmitotic neurons (Wang et al. 2018). This study suggested that Sec24c is a crucial cargo adapter of COPII dependent transport in postmitotic neurons which has partial overlapping function with Sec24d in mammals.

3.2. COPI paralogs

COPI coated vesicles are made of seven subunits. γ-COP subunit has two paralogs in mammalian cells. These two paralogs are differentially localized in the cell at the Golgi; γ1-COP is localized more at the cis side of the Golgi and γ2-COP is more at the trans side of the Golgi (Moelleken et al. 2007). However, proteomics analysis of COPI vesicles generated with the different isoforms of γ/ζ-COP containing coat complex did not detect any paralog-specific cargo proteins, but as only cargo receptors and core machinery were detected (Adolf et al. 2019) this could be due to the limitation of the detection assay.

Our study from γ1-COP KO cells shows impaired embryonic body formation compared to WT cells. Failure in embryonic body formation can be due to loss or mislocalization of any cell surface protein. A possible way to find out the putative lost or mislocalized surface protein(s) would be to do the proteomic study of knockout cells together with WT and rescue cells. So-called organelle proteomics maps can be generated by combining a SILAC-based approach to a differential fractionation approach in which organelles can be separated partially with a minimum number of fractionation steps which will generate organelle profiles providing high-accuracy quantification of each fraction against an invariant reference to find out mislocalized proteins via mass- spectrometry (Itzhak et al. 2016). Unfortunately, in a pilot attempt at SILAC based proteomic analysis from different organelle fractions of the cells we failed to detect any specific cargo protein. This was however be due to an unexpected big variation in protein levels between KO and WT cells which greatly limited the possibility to compare different organelle maps. This variation was most probably due to clonal effects with the KO cell line being quite unique when compared to the pool of parental P19 cells. A way to circumvent this would be to use a pool of KO cell lines. Another way to find putative specific cargo proteins of the γ-COP paralogs could be to perform BioID experiments in which the Copg1 and Copg2 genes would be tagged with the BirA* enzyme to allow the labeling of potential interacting partners in living cells in a proximity-dependent manner (Roux et al. 2012). Another point of interest would be to study cell secretion in the KO cells. Since from the endomembrane morphology study it was observed that Golgi is fragmented in Copg1 KO cells, which may affect the secretion of proteins, I am at the moment performing RUSH assays to study cell secretion.

This assay is depending upon the two expressed fusion proteins. One is hook protein which is fused with streptavidin, stably expressed at donor compartment and the other one is the reporter protein which is fused with the SBP and can bind reversibly with streptavidin. When Biotin treatment is given streptavidin can outcompete with it and the reporter protein is free to release. In our case, secretory protein E-Cadherin (reporter protein) which is tagged with a fluorescent protein and in presence of Biotin it should be released to the plasma membrane which can be observed under the microscope (Boncompain et al. 2012). A last potential function of γ1-COP may be in the regulation of the glycolysation of proteins and lipids. Indeed, in a recent study it was shown that pathogenic mutation in the Scyl1-(binding partner of COPI coatomer) (Burman et al. 2008; Burman, Hamlin, and McPherson 2010)) binding protein (Scyl1BP1) GORAB causes defective protein glycosylation (Witkos et al. 2019). COPI is important for recycling of Golgi-resident protein as well as glycosylation enzymes (Fisher and Ungar 2016). Precise distribution of glycosylation enzymes within Golgi is important for the properties and function of glycoproteins and glycolipids (Fisher and Ungar 2016) and abnormalities in glycosylation can lead to cognitive diseases (Joshi et al. 2014).

In vertebrates, the plasma membrane of neurites is enriched in gangliosides, which belongs to an heterogenous family of acidic glycosphingolipids (Liour, Kapitonov, and Yu 2000)(Sandhoff and Harzer 2013). Glycosphingolipids (GSLs) are derived from glucosylceramide (transmembrane protein), important for embryonic development (Jeckel et al. 1992; Futerman and Pagano 1991). De-novo synthesis of gangliosides initiates at ER in combination with glycosyltransferase at the Golgi complex followed by delivery to the plasma membrane. These gangliosides play important role in cell-cell adhesion, neuronal differentiation, and defects in gangliosides cause neurodegeneration (Liour, Kapitonov, and Yu 2000; Daniotti and Iglesias-Bartolome 2011; Kwak et al. 2011). There is switch between ganglioside pattern during neural development, failure in the switch can lead to pathological diseases (Russo et al. 2018). Gangliosides pattern changes from GM3 and GD3 (simple pattern) to complex pattern (a and b series of gangliosides) in vertebrate brain (Yu 1994). Undifferentiated cells express GM3 and GD3 gangliosides and as cells progress towards the neurite outgrowth stage GM1, GM2, GD1a, GD1b, GT1b and GQ1b gangliosides are

upregulated (Liour, Kapitonov, and Yu 2000). Although this switch with in the gangliosides pattern is not the inducer of neuronal differentiation rather result of neuronal differentiation but important for neural development.

Since the study of endomembrane morphology reveals that γ1-COP KO cells have swollen and vesiculated Golgi cisternae, which can affect the distribution of Golgi enzymes, it would be interesting to study the ganglioside pattern of WT and Copg1 KO cells during the neuronal differentiation.

To summarize, up to now, there was no evidence which indicate paralog-specialized functions or cell-type specific functions of COPI vesicles. Altogether, with my work, this is the first time that a γ1-COP specific phenotype is described. Moreover, this phenotype is observed during neuronal differentiation, which unravels a critical contribution of the COPI pathway in this process. This study opens the question if these two gamma-COP paralogs have other cell specific functions and what is their mechanisms. At the moment we do not know why γ1-COP specific phenotype cannot be overcome by the γ2-COP in the cell. This raises further questions if these two paralogs have different cargo-binding sites which make them play independent role in different trafficking pathways. By answering such questions novel pathways may be discovered which might be important in understanding and treating pathological disorders.

4. Materials and Methods

4.1. Materials

4.1.1.   Antibodies

Table 1: Primary antibodies

Antibody	Host	Company and catalogue number	Application and dilution
anti-Nanog	rabbit	Biomol (A300397AT)	WB, 1:1000
anti-Oct-4	Rabbit	Abcam (ab18976)	WB, 1:500
anti-ß-Tubulin (TujI/TUBB3)	mouse	Biolegend (MMS435P25)	WB, 1:1000
anti-δ-COP (877)	Rabbit	Wieland group (BZH, Heidelberg)	WB, 1:1000
anti-γ1-COP	rabbit	Wieland group (BZH, Heidelberg)	WB, 1:500
anti-γ2-COP	rabbit	Wieland group (BZH, Heidelberg)	WB, 1:500
anti-α-COP (1409B)	rabbit	Wieland group (BZH, Heidelberg)	WB, 1:5000
anti-ε-COP	rabbit	Wieland group (BZH, Heidelberg)	WB, 1:2000
Cleaved Caspase-3	rabbit	Cell Signaling (9661T)	IF, 1:100
anti-CM1	rabbit	Wieland group (BZH, Heidelberg)	IP

anti-GAPDH	mouse	Proteintech (60004-1-Ig)	WB, 1:20000
anti-α–tubulin	mouse	Sigma (T5168)	WB, 1:10000
anti-α–tubulin	rabbit	Abcam (Ab18251)	WB, 1:10000

Table 2: <u>Secondary antibodies</u>

Antibody	Host	Company and catalogue number	Application and dilution
anti-mouse IgG IRDye 800CW	goat	LI-COR (926-32210)	WB, 1:10000
anti-mouse IgG Alexa Fluor 680	goat	Thermo Scientific (A21057)	WB, 1:10000
anti-rabbit IgG IRDye 800CW	goat	LI-COR (926-32211)	WB, 1:10000
anti-rabbit IgG IRDye 680CW	goat	LI-COR (926-68071)	WB, 1:10000
anti-mouse Alexa 647	donkey	Invitrogen (A28175)	IF, 1:1000
anti-rabbit Alexa 633	goat	Invitrogen (A21070)	IF, 1:1000
anti-mouse Alexa 546	goat	Invitrogen (A11030)	IF, 1:1000

4.1.2.   Eukaryotic strains

Table 3: <u>Eukaryotic strains</u>

Strain	Species	Manufacturer
P19 WT	Mouse	Sigma (95102107)
P19 Copg1$^{-/-}$	Mouse	generated in this study
P19 Copg2$^{-/-}$	Mouse	generated in this study
P19 CRISPR-Cas9 control	Mouse	generated in this study
P19 HiFi Copg1$^{-/-}$	Mouse	generated in this study
P19 HiFi CRISPR-Cas9 Conrtol	Mouse	generated in this study
P19 PiggyBac Copg1$^{-/-}$+ Copg1-OE	Mouse	generated in this study

P19 PiggyBac Copg2$^{-/-}$+ Copg2-OE	Mouse	generated in this study
P19 BACMID Copg1$^{-/-}$ + LAP-Copg1$^{-/-}$-GFP	Mouse	Dr. Michaela Müller-McNicoll (Goethe University Frankfurt)

4.1.3. Cells medium and supplements

Table 4: Composition of P19 cells medium

Component	Company and catalogue number	Concentration
Alpha-MEM	Sigma (M4526)	~88% (v/v)
Fetal Bovine Serum	BioWest (S181B)	10%(v/v)
L-Glutamine	Sigma (G7513)	2 mM (1% (v/v))
Penicillin-Streptomycin	Gibco (15140-122)	1%(v/v)

Table 5: Other supplements and antibiotics

Supplement name	Company and catalogue number	Concentration
Hygromycin B	Sigma (H0654)	150 μg/mL
Retinoic Acid	Sigma Aldrich (R-2625)	0.1 μM
AraC	Sigma (C1768)	10 μM
Thapsigargin	Caymen Chemicals (Cay10522-1)	1 μM
Neurobasal media	Thermo (21103049)	1x
B27-supplement	Life technology (12587010)	1x
Ampicillin	Sigma (A9518)	100 μg/mL
Kanamycin	Carl Roth (T832.1)	34 μg/mL

Table 6: Other buffers or solutions used in cell culture

Name	Company and catalogue number
D-PBS	Sigma (D8537)
Trypsin	Gibco (2530054)
Optimem	Gibco (31985070)
DMSO	Sigma (D2438)
Cell dissociation buffer	Gibco (13151014)
Poly-L/D-Lysine	Sigma (P0899)
DNAseI	Applichem (A3778)

4.1.4.   Prokaryotic strains

Table 7: <u>Prokaryotic strains</u>

Strain	Species	Company	Application
DH5α	*E.Coli*	Invitrogen	Cloning
BL21 star	*E.Coli*	Invitrogen	Protein expression

4.1.5.   Prokaryotes growth medium

Table 8: <u>Media for prokaryotes</u>

Medium	Ingredients	Company and catalogue number
LB (for 1 L)	10 g Bactotryptone	BD (211705)
	5 g Bactoyeast	Roth (2363.3)
	10 g NaCl	Sigma (31434)
	1mL NaOH (1M)	Bernd-Kraft (1474574)
LB Agar	350 mL LB Medium + 1.5% (w/v) Agar	Fluka (05040)
LB Plates	LB Agar + 100 µg/mL Ampicillin	Sigma (A9518)

	LB Agar + 34 µg/mL Kanamycin	Carl Roth (T832.1)
SOB	2% (w/v) Bactotryptone	BD (211705)
(pH 6.7-7)	0.5% (w/v) Bactoyeast	Roth (2363.3)
	10 mM NaCl	Sigma (31434)
	2.5mM KCl 10 mM MgCl$_2$ 10 mM MgSO$_4$	Applichem (A3582) Applichem (A3618) Millipore (1.05886)

LB, LB-Agar and SOB medium were autoclaved prior to use.

4.1.6.   Material for cloning procedures and kits

All the reagents used for cloning (restriction enzymes, ligase, polymerases, etc.) were purchased from New England Biolabs (NEB).

Table 9: <u>Kits</u>

Kit	Application	Company and catalogue number
GeneElute HP Plasmid Miniprep Kit	Plasmid purification	Sigma (NA0160)
GeneElute HP Plasmid Midiprep Kit	Plasmid purification	Sigma (33209)
Zymo Pure^{TM} MidiPrep kit Fast Gene Gel PCR Extraction kit Zymo RNA First Strand cDNA synthesis Kit QIamp DNA Mini kit	Endotoxin free plasmidpurification DNA purification and agarose gel extraction RNA extraction cDNA preparation Genomic DNA extraction	Zymo (D4200) Nippon Genetics (91302) Zymo (R2052) Roche Qiagen (51304)
TA Cloning Kit	Cloning of PCR fragments	Invitrogen (45-0046)

4.1.7. Plasmids

Table 10: <u>Plasmids used in this study:</u>

Plasmid	Description	Source
pSPCas9(BB)-2TA-GFP	Cas9-GFP	Addgene (48138)
pSPCas9(BB)-2TA-GFP COPG1 exon2 sgRNA	sgRNA targeting exon2 with Cas9	Generated during the study
pSPCas9(BB)-2TA-GFP COPG2 exon6 sgRNA	sgRNA targeting exon4 with Cas9	Generated during the study
eSpCas9(1.1)	High fidelity Cas9-GFP	Sven Diederichs' lab
eSpCas9(1.1) COPG1 exon2 sgRNA	sgRNA targeting exon2 with Cas9	Generated during the study
pCyL50-mCOPG1-Hyg	Full length Copg1	Generated during the study by Julien Bethune
pCyL50-mCOPG2-Hyg	Full length Copg2	Generated during the study by Julien Bethune
CAG-NeuroD2 ires mcherry	NeuroD2-mCherry	Generated during the study
p3xflag mE47/E12	NeuroD2 binding partner	Addgene (34585)

Maps and sequences from plasmids were generated in the Béthune's Lab, are saved in the database and can be requested if needed.

4.1.8.   Primers and oligos

All the primers/oligos were purchased in desalted and lyophilized form from IDT.

Table 11: List of primers and oligos used for molecular cloning:

Plasmid	sense oligo	antisense oligo
COPG1 sgRNA exon2	CACCGAAGAGTGCCGTACTCCAAG	AAACGCACATTTCCGGGGATTGAT
COPG2 sgRNA exon4	CACCGGAAAGGAAGATGTATACCG	AAACCGGTATACATCTTCCTTTCC

Plasmid	PCR Template	Forward oligo	Reverse oligo
COPG1 sgRNA exon2 T7-endonuclease		TCACAGTTCGGGGCTGTAAC	TCACAGTTCGGGGCTGTAAC
COPG2 sgRNA exon4 T7-endonuclease		ACCACAACACAATAACAAGGTAGCA	ACCACAACACAATAACAAGGTAGCA
mCherry Cloning primer	pJB023_pReporter-Mut-hmga2-BoxB	ATGGTGAGCAAGGGCGAGGAGGATA	TTACTTGTACAGCTCGTCCATGCCG

List of primers and oligos used in qPCR:

Gene	IDT prime Time Assay Name	Forward primer	Reverse primer
Copa	Mm.PT.58.3138 9808	CAA ACC GAT TCC GAG CAA C	ACC TAC GAC CTA TAC ACC ATC C
Copb1	Mm.PT.58.7341 394	ATA AGC AAC ATA GCC TCA GCA	CTC GCC ACA ACT CTA ACC AA
Copb2	Mm.PT.58.3249 1925	CCG AAG CTC TTG TTC CTC AA	CCA CAG ACC ATT CAG CAC A
Copg1	Mm.PT.58.5337 327	CTG ATG ATG CAG TCC ACA ATG	GTG CCA GAA GTA TCC TCG AAA G
Copg2	qMmCID00052 46	ATC CTA CCT CGT TAG CCT GTA	AAG AAG AAT GTA AAA GGT GGT GTG
Arcn1	Mm.PT.58.7859 979	CTC CAA GTT TCA AAG CCT TGC	CAG CCA TGA TCA CAG AGA CTA TC
Copz1	Mm.PT.58.9686 781	CCC TCC ATC TAC AAT TTC ATC CA	TCT GAA CTG CCT CTT CGA TTC
Copz2	Mm.PT.58.1395 1793	AAA CCA TCT GCT CCT TCA CG	GAA CCT TCT CTC TAC ACC ATC AAG
Cope	Mm.PT.58.8414 483	AGG ATC TGA ATC GTC ATG GC	GAC CAA TAC CAC TTT CCT GCT

4.1.9. Buffer for agarose gels electrophoresis

Table 12: TAE agarose electrophoresis buffer composition

Buffer	Ingredients	Company and catalogue number
TAE (Tris Acetate - EDTA)	40 mM Tris	Roth (4855.2)
(pH 8)	40 mM Acetic Acid	Sigma (33209)
	1mM EDTA pH 8	Applichem (A0878)

4.1.10. Buffers and Solutions for SDS-Page and Western Blotting

Table 13: Buffers and solutions for SDS-Page and Western Blotting

Name	Ingredients	Company and catalogue number
PBS (1X)	7.4 g NaCl	Sigma (31434)
	3.18 g $Na_2HPO_4 * 12H_2O$	VWR (28028.298)
	0.36 g $NaH_2PO_4 * 2H_2O$	Grüssing (12133)
0.1% PBST	1X PBS + 0.1% Tween 20(v/v)	Roth (9127.1)
Sample Loading Dye (5X)	5% β–Mercaptoethanol	Sigma (M6250)
	0.02% Bromophenol blue	Waldeck (4F-057)
	30% Glycerol	Sigma (G5516)
	10% SDS	Sigma (05030)
	250 mM Tris	Sigma (31434)
Running Buffer (1X)	25 mM Tris	Sigma (31434)
	192 mM Glycine	Sigma (33226)
	0.1% SDS	Sigma (05030)
Wet Blotting Buffer	25 mM Tris	Sigma (31434)
	192 mM Glycine	Sigma (33226)
	0.1% SDS	Sigma (05030)
Semi-dry Blotting Buffer	48 mM Tris	Sigma (31434)
	39 mM Glycine	Sigma (33226)
	20% Ethanol	
	0.1% SDS	Sigma (05030)

Blocking Buffer	5% Milk in PBS	Roth (T145.1)
Buffer for antibody dilutions	1-3% BSA in 0.1%PBST	Roth (8076.2)
Destaining Solution	20% Ethanol 5% Acetic Acid	Fuka (33209)
Coomassie Staining Solution	40% Ethanol 10 % Acetic Acid 0.25% Brilliant Blue R250	Fuka (33209) Applichem (A1092)

Name	Ingredients	Company and catalogue number
Coomassie Brilliant Blue G250 staining solution	5% Aluminiumsulfate 10% Ethanol 8% Phosphoric Acid 0.5% Brilliant Blue G250	Applichem (A3578) Sigma (30417) Applichem (A3480)
Destaining Brilliant Blue Solution	10% Ethanol 2% Phosphoric Acid	Sigma (30417)

4.2. Molecular Biology Methods

4.2.1. DNA constructs

NeuroD2-mCherry plasmid was generated using MscI and BsrgI restriction enzymes. PCR fragment was amplified using pReporter-Mut-hmga2-BoxB as a PCR template. mCherry fragment was ligated with the digested NeuroD2-GFP plasmid where GFP was removed using MscI and BsrgI enzymes. Ligation was performed using Quick ligase enzyme 5mins at room temperature.

For annealing of oligos the reaction was incubated at 95°C for 5 mins and then ramped down to 25° at 0.1°C per sec. Cloning of oligo within Cas9-GFP vector is a one-step cloning reaction where digestion of the GFP-Cas9 vector and ligation were performed together in one reaction. The reaction was assembled as follow:

Component	Amount (µL)
pSPCas9(BB)-2TA-GFP	100ng
Oligo duplex	1µl
Quick ligase Buffer (2X) NEB	10µl
BbsI	1
Quick ligase	1
Water	up to 20
Total	20

For the cloning of CRISPR/Cas9 plasmid, oligos containing the BbsI restriction enzyme overhangs were annealed. Oligos for sgRNA were designed using CRISPR mit /chop-chop/ E-CRISPR tools.

Component	Amount (µL)
sgRNA sense (100 µM)	1
sgRNA antisense (100 µM)	1
Quick ligation Buffer (2X) NEB	5
Water	3
Total	10

The reaction was incubated in the Thermal cycler (Analytic Jena) using the following program:

Cycle number	Condition
1-6	1st step: 37°C for 5 min, 2nd step: 16°C for 5 min

Correct sequence of all plasmids was obtained by Sanger sequencing method (Eurofins Genomic)

4.2.2. Polymerase chain reaction, restriction digestion and ligation

All PCR reactions were performed using Q5 High Fidelity DNA Polymerase (NEB) except the T7 endonuclease assay where Dream Taq DNA polymerase was used following the manufacturer's protocol in a Thermal cycler FlexCycler[2] (Analytic Jena). Annealing temperatures were calculated using the online tool NEB Tm Calculator or gradient PCR. All restriction digestions were performed using NEB restriction enzymes according to manufacturer's protocols. Ligations were performed using Quick Ligation™ Kit (NEB) according to manufacturer's instructions.

4.2.3. Bacterial transformation

50 µl of chemically competent DH5α cells were mixed with 2-3 µL of ligation reaction and incubated for 10 to 30 min on ice. Heat shock was performed for 45 sec at 42°C followed by 2 min incubation on ice. After 200 µL of LB medium was added to the cells and the incubated for 1 hour at 37°C with agitation. Transformed cells were spread on LB Agar plates containing the appropriate antibiotic and incubated ON at 37°C.

4.2.4. DNA isolation and purification

Single colonies were picked and inoculated ON in LB media along with the appropriate antibiotic at 37 °C. From bacterial cultures DNA isolation was performed using the Plasmid Mini or Midi Kit GeneElute HP (Sigma) and in case of stable cell line preparation with the endotoxin free DNA Isolation kit Zymo Pure™ Plasmid Midiprep Kit (Zymo Research). DNA clean up and gel extraction was performed using the Fast Gene Gel PCR Extraction kit (Nippon Genetics).

4.2.5. Preparation of protein lysates

Media was removed from the cells and collected by centrifuging at 1000g for 3mins. Pellet was washed once with PBS and recovered the pellet. Add 100µl of lysis buffer (according to the cell pellet). Lysed samples were kept for 10mins on ice and in every 10mins sonicated

(Bandelin SONOREX, TYP: RK31) for 30 secs (repeated 3 times). After that centrifuged for 45mins at maximum speed at in cooled centrifuge. Gently collected the supernatant and O.D was taken 595nm by using Bradford assay.

Lysis Buffer	25mM Tris HCl (pH 7.4) + 150mM NaCl + 0.05% Triton + 1mM DTT + 1xPI

4.2.6. RNA isolation

Cells pellets were lysed by adding TRI reagent, following the manufacturer's protocol. Samples were then incubated for 5 mins at RT and then equal volume of 100% Ethanol was added. RNA purification was performed using Direct-zol™ RNA Miniprep (Zymo Research) which includes a DNAse treatment step. RNA samples were eluted in RNAse free water and stored at -80°C.

4.2.7. Determination of DNA or RNA concentration

DNA and RNA concentration of samples was determined using the ND-1000 spectrophotometer from PeqLab (Erlangen, Germany) by measuring the absorbance of the sample at 260 nm. Calculation of the concentrations was done by using the corresponding software based on Lambert Beers Law.

4.2.8. cDNA preparation

cDNAs were made using the First Transcriptor first strand cDNA synthesis kit (Roche). Before preparing cDNA 1 µg of RNA was treated with DNAseI (NEB) for 10 mins at 37°C followed by an inactivation step for 15 min at 75°C. Primer annealing was done for 10 mins at 65°C using 11 or 12 µL of pre-treated RNA using either oligo(dT) or random hexamers primers by adding 2 µl dNTPs (10 mM each) and 1µL of oligos(dT) (50 µM) or 2µl of random hexamers (600 µM), in a total volume of 15 µL. Further cDNA synthesis step was performed using 4 µL of the Transcriptor reverse transcriptase reaction buffer (5X), 0.5 µL of Protector RNase inhibitor and 0.5 µL of Transcriptor RT in a final volume of 20 µL.

Final cDNA synthesis was performed for 1h at 50°C, followed by an inactivation step for 5 min at 85°C.

4.2.9.   qPCR

qPCRs were performed in a StepOne Plus Real-Time PCR system (Applied Biosciences) using 2 µL of 1/5 cDNA diluted samples in water together with 0.25 µM of each primer and Fast Start Universal SYBR Green (2X) (Roche). The heating block of the thermo-cycler was pre-heated for 2 min at 50°C followed by an initial denaturation for 5 min at 95°C. A total of 40 cycles with 15 sec at 95°C for denaturation, 15 sec at 55°C for annealing and 30 sec at 72°C for elongation were used. Each reaction was performed in technical duplicates and the relative expression levels were calculated using the formula $2^{-(\Delta Ct)}$, where ΔCt is Ct (HPRT) and Ct is the equivalent cycle number at which the chosen threshold is crossed.

4.2.10.   Protein expression in E.Coli

GST tagged plasmids pProGST-TEV-mγ1appendage and pProGST-TEV-mγ2appendage were transformed in BL21(DE3) cells. For the transformation 0.5ul of BL21 competent cells were used and incubated for 5mins on ice. Then heat shock was done at 42°C for 45 sec followed by incubation on ice for 2mins. After 80ul of LB medium was mixed in the reaction and incubated at 37°C for 15 mins and then cells were spread on LB-ampicillin plates. Further single colony from each was inoculated in 3ml of LB media containing ampicillin at 37°C ON. It is critical to use fresh plates for protein purification. Later on, 3ml culture was transferred to 1litr of medium at 37°C for each and 180rpm and measure O.D until it reaches 0.6 at 600nm wavelength. After that 0.1mM of IPTG was added to induce protein expression and incubated ON at 16°C and 180rpm. Next day cells were recovered by centrifuging at 4000g for 10mins. Pellets were resuspended in 20ml of lysis buffer (snapped freeze in liquid nitrogen until further processing. Thaw resuspended cell pellets in a water bath). Cells were lysed by multiple passages through a high pressure cell homogenizer. Lysate was then centrifuged at 30'000 x g, 4°C for 10 mins. The supernatant was then recentrifuged at 100'000 x g, 4°C for 1 hr. The second supernatant is the starting material for the purification (Take a small sample for SDS-PAGE).

Lysis Buffer	1x PBS + 1mM DTT + Protease inhibitor cocktail

4.3.Biochemical Methods

4.3.1.   Protein purification

1ml of glutathione beads (glutathione sepharose high performance, Amersham biosciences, Freiburg) were pre-equilibrated with PBS containing 1mM DTT. Cleared cell lysate was loaded on to pre-equilibrated beads for 1he at room temperature. Beads were recovered by centrifuging at 1000g for 3mins. Supernatant was kept at 4ºc until final SDS-PAGE analysis. Beads were washed 3 times with 40ml of ice cold PBS contained 1mM DTT (all the supernatants were kept at 4ºc as wash1, wash2, wash3 samples until final SDS-PAGE analysis). Beads were incubated with 1ml of elution buffer for 10mins at room temperature. Eluted material was recovered by pouring into 5ml disposable column with a frit (Bio-Rad, Munich) (this was kept as sample elution1). 1ml of elution buffer was added on top of the column and eluted material eluted (elution sample2). This was repeated one more time (elution sample3). Fractions containing recombinant protein were pooled together some sample was kept for SDS-PAGE analysis. Protein was dialysed against 2L PBS+ 10% glycerol and 1mM DTT (cold buffers were used in the cold room. Dialyses tube was used MW cut-off below 30kDa. It was done in 2 rounds 1x 1hr and 1x overnight). Next day dialysed sample was recovered and protein concentration was measured. Sample was aliquoted and snapped freeze in liquid nitrogen and stored at -80ºc.

Elution Buffer	50 mM Tris pH 8.0 + 150 mM KCl + 1 mM DTT + 20 mM Glutathione

It is critical to adjust the pH after addition of glutathione. This buffer has to be prepared fresh and cannot be conserved for more than a couple of weeks at -20°C)

4.3.2. Negative affinity purification of anti γ1 and γ2 antibodies

2.5 mg of GST-γ1-appendage and GST-γ2-appendage proteins were thawed on ice. Both proteins were centrifuged at 100'000g (45'000 rpm with a TLA-55 rotor) for 1h at 4°C in the table top ultracentrifuge (ultracentrifugation resistant 1.5 mL tubes were used). 2 x 300 µL (bedvolume) of glutathione-sepharose beads were equilibrated with PBS + 1mM DTT (by washing the beads twice with 1 mL buffer). Supernatants from the ultracentrifugation were recovered and mixed then with the pre-equilibrated beads (300 µL per supernatant), PBS was added + 1 mM DTT to both 1.5 mL tubes so that ca. 1.4 mL volume is occupied and incubated overnight at 4°C on the rotating plate.

Next day beads were washed three times with 1 mL PBS (No DTT). 7.5 mL of anti γ1-COP serum (r1.2 serum) and anti γ2-COP serum (r2.2 serum) were thawed. 750µl of 10x PBS was added to both sera. GST-γ1-appendage coupled beads were added to anti γ2-COP serum and GST-γ2-appendage coupled beads were added to γ1-COP serum. Serum and beads were incubated for 2hrs at room temperature on the rotating wheel and after transferred to two 1ml BioRad disposable columns and flow through was recovered on ice. Once the flow through is collected 1ml of PBS was added to both columns and additional elution was collected in the same tubes on ice (10µl of sample was kept for SDS-PAGE analysis). Further ammonium sulfate was added progressively to both antibody solutions (eluted material) to 40% saturation at 4^{0}c (24.3g/100ml), incubated 10 more mins in the cold room on rotating wheel. Later centrifuged at 7000g at 4^{0}c and supernatant was discarded carefully and pellets were resuspended in 5ml PBS. Antibodies were dialyzed three times (2x 1 hr and 1x overnight) against 1L PBS (use a cut-off of 14-16 kDa). Next day dialyzed material was recovered and centrifuged at 100,000g for 1hr at 4°c (10µl of sample was kept for SDS-PAGE analysis). Absorbance was measured at λ=280nm for both samples, PBS was used for blank. IgG concentration was calculated according to Beer-Lambert law (A=ε.l.c, for IgG ε= 210,000 $M^{-1}.cm^{-1}$). Supernatant was aliquoted, flashed free in liquid nitrogen and stored at -80^{0}c.

4.3.3. Agarose gel electrophoresis

DNA bands were excised by using 0.5-2% (w/v) agarose (Sigma) gel, depending on the size of the product, in TAE buffer added with 1:50000 diluted Red Safe ^{TM} stain (iNtRON Biotechnology). 6X Purple loading Dye (NEB) was used for loading the samples and 1kb plus DNA ladder GeneRuler^{TM} to identify the size of the DNA. GelDoc system (BioRad) was used to detect the DNA bands under the UV irradiation. To excise the bands during the experiments LED Iluminator (INTAS) was used to prevent UV induced DNA mutations.

4.3.4. SDS-PAGE

Sodium-dodecylsulfate polyacrylamide gel electrophoresis (SDS-PAGE) was used to separate the protein based on the size (Laemmli et al. 1970). Homemade gels were made with 4% stacking gel and 8-15% resolving gels or 4-20% gradient gels. Protean II system from BioRad was used with a constant voltage of 110V until the samples passed the stacking gel and with 160V for the separating gel. Before loading samples were mixed with 5X SDS loading dye and boiled at 95^{0}C for 5 mins. Blue star prestained protein marker plus (Nippon Genetics) was used to detect the molecular weight of the protein.

The following components were used to prepare the SDS gels:

Stacking gel	H$_2$O [mL]	Tris pH 6.8(1M) [mL]	30% Acrylide[mL]	10% SDS [µL]	10% APS [µL]	TEMED [µL]
4%	1.4	0.25	0.33	20	20	2

Separating gel	H$_2$O [mL]	Tris pH 8.8 (1M) [mL]	30% Acrylamide [mL]	10% SDS [µL]	10% APS [µL]	TEMED [µL]
8%	2.3		1.3			
10%	1.9	1.3	1.7	50	50	4
12%	1.6		2			
15%	1.1		2.5			

For making a gradient gel first pipette 2.5 mL of the lower percent solution and then 2.5 mL of the higher percent solution. Then draw up to 2 air bubble to mix and generate a gradient, repeat this step. The following components were used to prepare the SDS gradient gel:

Separating gel	H$_2$O [mL]	Tris pH 8.8 (1M) [mL]	30% Acrylamide	10% SDS [µL]	10% APS [µL]	TEMED [µL]
4%	1.79		0.4			
6%	1.59		0.6			
8%	1.39		0.8			
10%	1.19	0.75	1	30	30	2.5
12%	0.99		1.2			
15%	0.688		1.5			
20%	0.188		2			

4.3.5. Western Blot

Proteins were transferred into a PVDF membrane (Millipore) using either the Trans Blot Turbo System (semi dry transfer) (Biorad) or a Mini Trans-Blot Cell (wet transfer) (Biorad) for 1h at 100 V or ON at 80 mA in case of high molecular weight protein, according to the manufacturer's instructions. After that membranes were blocked in blocking buffer for 1 hr at RT or ON at 4°C. Then membranes were incubated with the primary antibody using the suggested concentration for 1h at RT or ON at 4°C. After three washing steps of 10 min

each with 0.1%PBST, IRDye coupled secondary antibodies were used to detect primary antibodies for 1h at RT. The membrane was then washed two times with 0.1% PBST and one time with PBS for 10 min. To detect the blots Odyssey CLx imaging system (LICOR) was used. Analysis of the blots was performed using the Image Studio Software (LICOR) following the producer instructions.

4.3.6.   Coomassie Staining

Following gel electrophoretic separation, polyacrylamide gels were stained with Coomassie Staining solution and microwave for 1min after that kept on shaker for 10mins. Gels were then rinse in water before adding the coomassie destaining solution for around 30 min, followed by several washes with water.

4.3.7.   Determination of protein concentration

Protein concentration was determined using the Bradford assay. BSA solutions with in a range of 250-3000 ng/µL were used to generate a BSA standard curve. 1ml volume of reaction mixture was prepared where Bradford solution is diluted 1:2 from Bradford Ultra Expedeon. After mixing the samples they were incubated for 5 min at RT before measuring the O.D using 6310 Spectrophotometer (Jenway) at a wavelength of 595 nm. Concentrations of the samples were determined by using the standard curve.

4.3.8.   Cytosol preparation from adherent cells

Cells were used from two full confluent 15cm dishes. Cells were washed in the dishes twice with cold PBS. Then lysis buffer was added to the first dish (second plate still in PBS) and scrap the cells. Scrapped cells were transferred to the second plate and scrapped the cells from this plate as well. Transfer scrapped cells to a 1.5 mL tube and keep on ice. Cells were lysed further using gauge needles 20 times (10 times up, 10 times down) through a 21 Gauge needle and then 20 times through a 27 Gauge needle. Centrifuge the lysed cells at 4°C, 800x g, 5 min to remove nuclei and cell debris. Take the supernatant and transfer to ultracentrifugation-resistant 1.5 mL tubes. Centrifuge at 4°C, 100'000x g, 1h. Carefully

remove the supernatant and transfer to a fresh 1.5 mL tube, keep on ice until use (always used freshly prepared cytosol for coatomer IP). Estimate protein concentration using a Bradford assay. Expect a yield of ca. 1.5 mg protein per 15 cm plate.

Lysis Buffer	25mM Tris, pH 7.4 + 150mM NaCl + 1mM EDTA + Protease inhibitor cocktail

4.3.9.   Coatomer pulldown

Freshly prepared cytosol was used corresponding to 500µg protein. Before that magnetic ProteinG beads for IP needs to be equilibrated. Per IP, use 10 µL magnetic ProteinG beads. Beads were washed twice with IP buffer. (If doing three IPs, wash 30 µL beads by mixing them with 1 mL IP buffer, then recover the beads on a magnet. After the second wash, proceed to antibody coupling). Then 100 µL CM1 supernatant per 10 µL ProteinG beads was added, filled up the tube to ca. 1.4 mL with IP buffer and incubated for 1h at RT on a rotating wheel. Then, beads were washed once with IP buffer (1mL).

If doing three IPs, add 300 µL CM1 supernatant per 30 µL ProteinG beads, fill up the tube to ca. 1.4 mL with IP buffer and incubated for 1h at RT on a rotating wheel. Then, beads were washed once with IP buffer (1mL). Finally, resuspended the beads in 150 µL IP buffer and distributed in 3 x 50µL in three fresh tubes. 500µg protein was loaded on to the beads, if needed fill up the tubes to ca. 1.4 mL with IP buffer containing protease inhibitors. Incubated for 1h at RT on a rotating wheel. Then beads were washed three times with IP buffer to remove unbound proteins. Bound proteins were eluted by incubating the beads with 20 µL 3x SDS loading buffer and incubation at 70°C for 10 min. Beads were separated from the eluted material on a magnet, and the eluted material was transferred to a fresh tube.

Lysis Buffer	25mM Tris, pH 7.4 + 150mM NaCl + 1mM EDTA + 0.025% (v/v) tween20 + Protease inhibitor cocktail

4.4. Cell Biology Methods

4.4.1.   Cell Culture

All P19 cells lines are listed in Table 4, were cultured at 37°C with 5% CO_2 in a humidified incubator. Cells were splitted in every two days in a ratio of 1:10. P19 growth medium (alpha-MEM) contained 10%FBS + 1% Pen/Streptomycin + 1% Glutamine. Contamination of mycoplasma was regularly tested using a Mycoplasma PCR detection kit (Mycoscope, Genlatis).

4.4.2.   Heat inactivation of serum

500ml bottle was thawed overnight in 4^0c fridge. Next day bottle was place in 37ºc incubator to complete the thawing, in every 10mins bottle was inverted for complete mixing. Water in the incubator was filled higher than the serum level. Once serum is completely thawed it was incubated 15mins more to equilibrate with the 37ºc bath. Temperature of the water bath was raised to 56ºc. In 30-35 mins temperature of the water bath was reached to 56ºc. In every 10mins bottle was inverted for complete mixing. After that serum was kept for 30mins and in every 10mins bottle was inverted for complete mixing. After 30mins of incubation serum was cooled down at room temperature for 30mins. Serum was aliquoted in 50ml falcon tubes under the cell culture hood and stored at -20ºc.

4.4.3.   Generation of stable cell line

P19 Copg1 and Copg2 KO cells were generated by using CRISPR-Cas9 gene editing tool. sgRNAs against Copg1 and Copg2 genes were cloned into pSPCas9(BB)-2TA-GFP vector between BbsI restriction enzyme sites. 200,000 cells/ml were seeded in 6 well plate and after 12 hrs 2.5µg of sgRNA cloned pSPCas9(BB)-2TA-GFP vector was transfected using lipofectamin3000. After 72 hrs GFP positive cells were selected and transferred into 96 well plate using FACS single cell sorting machine (ZMBH-Flow Cytometry &FACS Core Facility) detection kit (Mycoscope, Genlatis).

P19 PB-Copg1 and PB-Copg2 cells were generated by seeding Copg1Ko and Copg2 KO cells respectively, 200,000 cells/ml were in 6 well plate and after 12 hrs 2.5μg of plasmid was mixed with lipofectamin3000 reagent. 1,5 μg pBase plasmid (pJB114, coding for the PiggyBac transposase) 1,5 μg pCyl50 plasmid (coding for the gene to be inserted and the selection marker. Both plasmids were diluted in 125 μL OptiMEM. 5μl of P3000 reagent was added and gently and briefly mixed. 5 μL lipofectamine 3000 + 120 μL OptiMEM were prepared, briefly and gently mixed. Lipofectamine and DNA were mixed together and incubated for 5-10 min at room temperature. 250 μL of the transfection mix per well was added to transfect. Next day cells were transferred into two 10 cm plates: one containing about 1/3 of the transfected cells, the other about 1/5 of the transfected cells. At that point selection antibiotic was not added. Cells were incubated for 3 days to allow transposition to occur. At day 6 Medium of the transfected cells was changed to growth medium containing the selection antibiotic (Hygromycin 150μg/ml). Growth medium was replaced every 2nd - 3rd day with fresh medium containing selection antibiotic. Cells were trasferred to a new plate when they reach ca. 80% confluency. After 15-16 days all m164-GFP transfected cells were green. Transfected cells were kept on selection media for another 4-5 days, then stocks were made and then cells were characterized by doing Western blotting.

4.4.4.   FACS Sorting

After transfection media was removed and then washed with PBS. Then cells were trypsinized. Cells were resuspended in (to neutralize the trypsine) serum free media with 5% dissociation buffer and centrifuged at 500g for 5 mins at room temperature to pellet the cells. Supernatant was discarded and resuspended again in 500ul serum free media with 5% dissociation buffer. Cells were passed through a cell strainer to remove clumps. Cells were transferred on ice until cell sorting. 96 well plates were prepared prior to processing the cells by adding 200 ul media per well (contained antibiotics) and transferred it to 37ᵒc incubator until the cells are ready. After sorting cells were transferred to the 96 well plates to 37ᵒc incubator. After two weeks colonies were transferred into the 12 well plate and later on to the 6 well plate. Then clones were screened by doing western blotting.

4.4.5.   Transient transfection

Cells were seeded to 60-70% confluency one day before to transfection. After 12 hrs of seeding transfection was done using Jet-Prime reagent in a 1:2 (DNA: Reagent) ratio. Transfection was followed according to manufacturer's protocol. In 6 well plate 2.5μg of DNA was used.

In 8 well Ibidi slides reverse transfection was done. After poly-L/D-lysine coating seeding of cells (30,000-40,000 cells) and transfection (using Jet-prime reagent) were done together according to manufacturer's protocol in a ratio of 1:2 (DNA: Reagent). 250ng DNA was used in 8well Ibidi slides

4.4.6.   Poly-L/D-Lysine coating

Surface was aseptically coated with 1.0 mL/25 cm^2 (only). Rock gently to ensure even coating of the culture surface (for 6 well 360μl per well). After 5 minutes solution was removed by aspiration and thoroughly rinse surface with sterile tissue culture grade water 2 times. Allowed drying at least 2 hours before introducing cells and medium.

4.4.7.   Hanging drop assay

200 cells were seeded (cells are treated with Retinoic Acid 0.1um with 5% FBS in growth medium) per drop. One drop is equal to 20ul. 30 drops were made inside the lid of 10cm bacterial dish. Dish was filled with 10ml PBS to avoid evaporation. Lid was inverted carefully not too fast neither too slow. After two- and four-days images were taken. For taking images lid was inverted on empty dish. Images were taken using 10x objective.

4.4.8.   P19 differentiation

10^6 cells were cultured in α-MEM medium along with 5% FBS+ 1% Pen/Streptomycin + 1% Glutamine and 0.1μM RA to make cell aggregates in bacterial 10cm dish in non-adherent conditions. After two days fresh media was replaced and new 0.1μM was added. After 4 days of aggregation aggregates were centrifuged at 1000g for 5mins and then washed once with serum free media. After that aggregates were dissociated using 2ml trypsin + 50μg/ml DNAseI (prevents gel formation) and incubated for 10mins in 37ºc

incubator. Further 4ml of P19 growth media was added to stop the trypsin activity and cells were collected by centrifuging at 1000g for 5mins. Pellet was resuspended in 5ml of fresh P19 growth media and then cells were counted and 3.75cells/ml cells were plated onto poly-L/D-lysine coated 6 well plate and in case of plating on to Ibidi 8well slides cells were resuspended in 1ml of fresh media and passed through the BD strainer in order to remove the clumps. After 2 days of plating fresh media was added along with 10μM of AraC in order to kill dividing cells.

4.4.9.   Immunofluorescence

After seeding or differentiation of the cells, cells were washed carefully with warm 300 mL PBS, then incubated with warm 300 μL of PBS+4% formaldehyde at 37°C for 20 min to fix the cells. Cells were washed twice with 300 μL PBS, and then incubated with 300μL PBS+0.25% Triton X-100 at room temperature for 10 mins to permeabilize the cells. Cells were washed twice with 300 μL PBS + 2% BSA. For blocking cells were incubated with 300 μL PBS + 10% BSA for 30 min at RT. Then incubated with primary antibody diluted in PBS, 2% BSA, 150 μL per well, 1h at room temperature or overnight. After that cells were washed three times with PBS, 2% BSA. Then incubated with secondary antibody diluted 1:1000 in PBS, 2% BSA, 150 μL per well, 30 min at room temperature in the dark. Later cells were washed twice with PBS, 2% BSA. Then incubated with DAPI (diluted at 0.1μg/mL in PBS), 150 μL per well, 10 min at room temperature in the dark. Two brief and gentle washes were done with PBS, 2% BSA + one gentle wash with PBS. Ibidi mounting medium dropwise was added to cells, not directly on the cells, about 150 μL per well.

5. Bibliography

Adolf, F., M. Rhiel, B. Hessling, Q. Gao, A. Hellwig, J. Bethune, and F. T. Wieland. 2019. 'Proteomic Profiling of Mammalian COPII and COPI Vesicles', *Cell Rep*, 26: 250-65 e5.

Adolf, Frank, Alexia Herrmann, Andrea Hellwig, Rainer Beck, Britta Brügger, and Felix T. Wieland. 2013. 'Scission of COPI and COPII Vesicles Is Independent of GTP Hydrolysis', *Traffic*, 14: 922-32.

Ahle, S., A. Mann, U. Eichelsbacher, and E. Ungewickell. 1988. 'Structural relationships between clathrin assembly proteins from the Golgi and the plasma membrane', *EMBO J*, 7: 919-29.

Antonny, B., S. Beraud-Dufour, P. Chardin, and M. Chabre. 1997. 'N-terminal hydrophobic residues of the G-protein ADP-ribosylation factor-1 insert into membrane phospholipids upon GDP to GTP exchange', *Biochemistry*, 36: 4675-84.

Ast, T., and M. Schuldiner. 2013. 'All roads lead to Rome (but some may be harder to travel): SRP-independent translocation into the endoplasmic reticulum', *Crit Rev Biochem Mol Biol*, 48: 273-88.

Austin, Carol, Ina Hinners, and Sharon A. Tooze. 2000. 'Direct and GTP-dependent Interaction of ADP-ribosylation Factor 1 with Clathrin Adaptor Protein AP-1 on Immature Secretory Granules', *Journal of Biological Chemistry*, 275: 21862-69.

Aviram, N., and M. Schuldiner. 2017. 'Targeting and translocation of proteins to the endoplasmic reticulum at a glance', *J Cell Sci*, 130: 4079-85.

Bannykh, S. I., and W. E. Balch. 1997. 'Membrane dynamics at the endoplasmic reticulum-Golgi interface', *J Cell Biol*, 138: 1-4.

Barlowe, C., L. Orci, T. Yeung, M. Hosobuchi, S. Hamamoto, N. Salama, M. F. Rexach, M. Ravazzola, M. Amherdt, and R. Schekman. 1994. 'COPII: a membrane coat formed by Sec proteins that drive vesicle budding from the endoplasmic reticulum', *Cell*, 77: 895-907.

Barlowe, C., and R. Schekman. 1993. 'SEC12 encodes a guanine-nucleotide-exchange factor essential for transport vesicle budding from the ER', *Nature*, 365: 347-9.

Beck, R., S. Prinz, P. Diestelkotter-Bachert, S. Rohling, F. Adolf, K. Hoehner, S. Welsch, P. Ronchi, B. Brugger, J. A. Briggs, and F. Wieland. 2011. 'Coatomer and dimeric ADP ribosylation factor 1 promote distinct steps in membrane scission', *J Cell Biol*, 194: 765-77.

Beck, R., M. Rawet, F. T. Wieland, and D. Cassel. 2009. 'The COPI system: molecular mechanisms and function', *FEBS Lett*, 583: 2701-9.

Beck, R., Z. Sun, F. Adolf, C. Rutz, J. Bassler, K. Wild, I. Sinning, E. Hurt, B. Brugger, J. Bethune, and F. Wieland. 2008. 'Membrane curvature induced by Arf1-GTP is essential for vesicle formation', *Proc Natl Acad Sci U S A*, 105: 11731-6.

Berndt, U., S. Oellerer, Y. Zhang, A. E. Johnson, and S. Rospert. 2009. 'A signal-anchor sequence stimulates signal recognition particle binding to ribosomes from inside the exit tunnel', *Proc Natl Acad Sci U S A*, 106: 1398-403.

Bethune, J., M. Kol, J. Hoffmann, I. Reckmann, B. Brugger, and F. Wieland. 2006. 'Coatomer, the coat protein of COPI transport vesicles, discriminates endoplasmic reticulum residents from p24 proteins', *Mol Cell Biol*, 26: 8011-21.

Blagitko, N., U. Schulz, A. A. Schinzel, H. H. Ropers, and V. M. Kalscheuer. 1999. 'gamma2-COP, a novel imprinted gene on chromosome 7q32, defines a new imprinting cluster in the human genome', *Hum Mol Genet*, 8: 2387-96.

Blobel, G., and B. Dobberstein. 1975. 'Transfer of proteins across membranes. I. Presence of proteolytically processed and unprocessed nascent immunoglobulin light chains on membrane-bound ribosomes of murine myeloma', *J Cell Biol*, 67: 835-51.

Boncompain, G., S. Divoux, N. Gareil, H. de Forges, A. Lescure, L. Latreche, V. Mercanti, F. Jollivet, G. Raposo, and F. Perez. 2012. 'Synchronization of secretory protein traffic in populations of cells', *Nat Methods*, 9: 493-8.

Bonifacino, J. S., and B. S. Glick. 2004. 'The mechanisms of vesicle budding and fusion', *Cell*, 116: 153-66.

Borgese, N., S. Brambillasca, and S. Colombo. 2007. 'How tails guide tail-anchored proteins to their destinations', *Curr Opin Cell Biol*, 19: 368-75.

Braakman, I., and N. J. Bulleid. 2011. 'Protein folding and modification in the mammalian endoplasmic reticulum', *Annu Rev Biochem*, 80: 71-99.

Bremser, M., W. Nickel, M. Schweikert, M. Ravazzola, M. Amherdt, C. A. Hughes, T. H. Sollner, J. E. Rothman, and F. T. Wieland. 1999. 'Coupling of coat assembly and vesicle budding to packaging of putative cargo receptors', *Cell*, 96: 495-506.

Burman, J. L., L. Bourbonniere, J. Philie, T. Stroh, S. Y. Dejgaard, J. F. Presley, and P. S. McPherson. 2008. 'Scyl1, mutated in a recessive form of spinocerebellar neurodegeneration, regulates COPI-mediated retrograde traffic', *J Biol Chem*, 283: 22774-86.

Burman, J. L., J. N. Hamlin, and P. S. McPherson. 2010. 'Scyl1 regulates Golgi morphology', *PLoS One*, 5: e9537.

Caro, L. G., and G. E. Palade. 1964. 'Protein Synthesis, Storage, and Discharge in the Pancreatic Exocrine Cell. An Autoradiographic Study', *J Cell Biol*, 20: 473-95.

Cary, L. C., M. Goebel, B. G. Corsaro, H. G. Wang, E. Rosen, and M. J. Fraser. 1989. 'Transposon mutagenesis of baculoviruses: analysis of Trichoplusia ni transposon IFP2 insertions within the FP-locus of nuclear polyhedrosis viruses', *Virology*, 172: 156-69.

Claude, A., B. P. Zhao, C. E. Kuziemsky, S. Dahan, S. J. Berger, J. P. Yan, A. D. Armold, E. M. Sullivan, and P. Melancon. 1999. 'GBF1: A novel Golgi-associated BFA-resistant guanine nucleotide exchange factor that displays specificity for ADP-ribosylation factor 5', *J Cell Biol*, 146: 71-84.

Contreras, I., E. Ortiz-Zapater, and F. Aniento. 2004. 'Sorting signals in the cytosolic tail of membrane proteins involved in the interaction with plant ARF1 and coatomer', *Plant J*, 38: 685-98.

Cosson, P., and F. Letourneur. 1994. 'Coatomer interaction with di-lysine endoplasmic reticulum retention motifs', *Science*, 263: 1629-31.

Cross, Benedict C. S., Irmgard Sinning, Joen Luirink, and Stephen High. 2009. 'Delivering proteins for export from the cytosol', *Nature Reviews Molecular Cell Biology*, 10: 255-64.

Crowther, R. A., and B. M. Pearse. 1981. 'Assembly and packing of clathrin into coats', *J Cell Biol*, 91: 790-7.

Cukierman, E., I. Huber, M. Rotman, and D. Cassel. 1995. 'The ARF1 GTPase-activating protein: zinc finger motif and Golgi complex localization', *Science*, 270: 1999-2002.

Custer, S. K., A. G. Todd, N. N. Singh, and E. J. Androphy. 2013. 'Dilysine motifs in exon 2b of SMN protein mediate binding to the COPI vesicle protein alpha-COP and neurite outgrowth in a cell culture model of spinal muscular atrophy', *Hum Mol Genet*, 22: 4043-52.

Daniotti, J. L., and R. Iglesias-Bartolome. 2011. 'Metabolic pathways and intracellular trafficking of gangliosides', *IUBMB Life*, 63: 513-20.

de Anda, F. C., G. Pollarolo, J. S. Da Silva, P. G. Camoletto, F. Feiguin, and C. G. Dotti. 2005. 'Centrosome localization determines neuronal polarity', *Nature*, 436: 704-8.

Dehmelt, L., G. Poplawski, E. Hwang, and S. Halpain. 2011. 'NeuriteQuant: an open source toolkit for high content screens of neuronal morphogenesis', *BMC Neurosci*, 12: 100.

Dell'Angelica, E. C., C. Mullins, and J. S. Bonifacino. 1999. 'AP-4, a novel protein complex related to clathrin adaptors', *J Biol Chem*, 274: 7278-85.

Dell'Angelica, E. C., H. Ohno, C. E. Ooi, E. Rabinovich, K. W. Roche, and J. S. Bonifacino. 1997. 'AP-3: an adaptor-like protein complex with ubiquitous expression', *EMBO J*, 16: 917-28.

Dodonova, S. O., P. Diestelkoetter-Bachert, A. von Appen, W. J. Hagen, R. Beck, M. Beck, F. Wieland, and J. A. Briggs. 2015. 'VESICULAR TRANSPORT. A structure of the COPI coat and the role of coat proteins in membrane vesicle assembly', *Science*, 349: 195-8.

Donaldson, J. G., and C. L. Jackson. 2011. 'ARF family G proteins and their regulators: roles in membrane transport, development and disease', *Nat Rev Mol Cell Biol*, 12: 362-75.

Ellgaard, L., and A. Helenius. 2003. 'Quality control in the endoplasmic reticulum', *Nat Rev Mol Cell Biol*, 4: 181-91.

Ellgaard, L., and L. W. Ruddock. 2005. 'The human protein disulphide isomerase family: substrate interactions and functional properties', *EMBO Rep*, 6: 28-32.

Ernst, A. M., S. A. Syed, O. Zaki, F. Bottanelli, H. Zheng, M. Hacke, Z. Xi, F. Rivera-Molina, M. Graham, A. A. Rebane, P. Bjorkholm, D. Baddeley, D. Toomre, F. Pincet, and J. E. Rothman. 2018. 'S-Palmitoylation Sorts Membrane Cargo for Anterograde Transport in the Golgi', *Dev Cell*, 47: 479-93 e7.

Eugster, A., G. Frigerio, M. Dale, and R. Duden. 2000. 'COP I domains required for coatomer integrity, and novel interactions with ARF and ARF-GAP', *EMBO J*, 19: 3905-17.

———. 2004. 'The alpha- and beta'-COP WD40 domains mediate cargo-selective interactions with distinct di-lysine motifs', *Mol Biol Cell*, 15: 1011-23.

Farah, M. H., J. M. Olson, H. B. Sucic, R. I. Hume, S. J. Tapscott, and D. L. Turner. 2000. 'Generation of neurons by transient expression of neural bHLH proteins in mammalian cells', *Development*, 127: 693-702.

Farquhar, M. G. 1983. 'Multiple pathways of exocytosis, endocytosis, and membrane recycling: validation of a Golgi route', *Fed Proc*, 42: 2407-13.

Favaloro, V., M. Spasic, B. Schwappach, and B. Dobberstein. 2008. 'Distinct targeting pathways for the membrane insertion of tail-anchored (TA) proteins', *J Cell Sci*, 121: 1832-40.

Fisher, P., and D. Ungar. 2016. 'Bridging the Gap between Glycosylation and Vesicle Traffic', *Front Cell Dev Biol*, 4: 15.

Fleischer, B. 1983. 'Mechanism of glycosylation in the Golgi apparatus', *J Histochem Cytochem*, 31: 1033-40.

Franco, M., P. Chardin, M. Chabre, and S. Paris. 1996. 'Myristoylation-facilitated binding of the G protein ARF1GDP to membrane phospholipids is required for its activation by a soluble nucleotide exchange factor', *J Biol Chem*, 271: 1573-8.

Fraser, M. J., L. Cary, K. Boonvisudhi, and H. G. Wang. 1995. 'Assay for movement of Lepidopteran transposon IFP2 in insect cells using a baculovirus genome as a target DNA', *Virology*, 211: 397-407.

Friedlander, R., E. Jarosch, J. Urban, C. Volkwein, and T. Sommer. 2000. 'A regulatory link between ER-associated protein degradation and the unfolded-protein response', *Nat Cell Biol*, 2: 379-84.

Futatsumori, M., K. Kasai, H. Takatsu, H. W. Shin, and K. Nakayama. 2000. 'Identification and characterization of novel isoforms of COP I subunits', *J Biochem*, 128: 793-801.

Futerman, A. H., and R. E. Pagano. 1991. 'Determination of the intracellular sites and topology of glucosylceramide synthesis in rat liver', *Biochem J*, 280 (Pt 2): 295-302.

Garcia-Mata, R., T. Szul, C. Alvarez, and E. Sztul. 2003. 'ADP-ribosylation factor/COPI-dependent events at the endoplasmic reticulum-Golgi interface are regulated by the guanine nucleotide exchange factor GBF1', *Mol Biol Cell*, 14: 2250-61.

Gilmore, R., G. Blobel, and P. Walter. 1982. 'Protein translocation across the endoplasmic reticulum. I. Detection in the microsomal membrane of a receptor for the signal recognition particle', *J Cell Biol*, 95: 463-9.

Glick, B. S., and A. Luini. 2011. 'Models for Golgi Traffic: A Critical Assessment', *Cold Spring Harbor Perspectives in Biology*, 3: a005215-a15.

Golgi, C. 1989. 'On the structure of the nerve cells of the spinal ganglia. 1898', *J Microsc*, 155: 9-14.

Gommel, D. U., A. R. Memon, A. Heiss, F. Lottspeich, J. Pfannstiel, J. Lechner, C. Reinhard, J. B. Helms, W. Nickel, and F. T. Wieland. 2001. 'Recruitment to Golgi membranes of ADP-ribosylation factor 1 is mediated by the cytoplasmic domain of p23', *EMBO J*, 20: 6751-60.

Hara-Kuge, S., O. Kuge, L. Orci, M. Amherdt, M. Ravazzola, F. T. Wieland, and J. E. Rothman. 1994. 'En bloc incorporation of coatomer subunits during the assembly of COP-coated vesicles', *J Cell Biol*, 124: 883-92.

Harroun, Thad A., Jeremy P. Bradshaw, Kia Balali-Mood, and John Katsaras. 2005. 'A structural study of the myristoylated N-terminus of ARF1', *Biochimica et Biophysica Acta (BBA) - Biomembranes*, 1668: 138-44.

Harter, C., and F. T. Wieland. 1998. 'A single binding site for dilysine retrieval motifs and p23 within the gamma subunit of coatomer', *Proc Natl Acad Sci U S A*, 95: 11649-54.

Hauri, H. P., F. Kappeler, H. Andersson, and C. Appenzeller. 2000. 'ERGIC-53 and traffic in the secretory pathway', *J Cell Sci*, 113 (Pt 4): 587-96.

Heigwer, F., G. Kerr, and M. Boutros. 2014. 'E-CRISP: fast CRISPR target site identification', *Nat Methods*, 11: 122-3.

Hoffman, G. R., P. B. Rahl, R. N. Collins, and R. A. Cerione. 2003. 'Conserved structural motifs in intracellular trafficking pathways: structure of the gammaCOP appendage domain', *Mol Cell*, 12: 615-25.

Honda, Akira, Omayma S. Al-Awar, Jesse C. Hay, and Julie G. Donaldson. 2005. 'Targeting of Arf-1 to the early Golgi by membrin, an ER-Golgi SNARE', *The Journal of Cell Biology*, 168: 1039-51.

Horton, A. C., and M. D. Ehlers. 2003. 'Dual modes of endoplasmic reticulum-to-Golgi transport in dendrites revealed by live-cell imaging', *J Neurosci*, 23: 6188-99.

Hughes, H., and D. J. Stephens. 2008. 'Assembly, organization, and function of the COPII coat', *Histochem Cell Biol*, 129: 129-51.

Itzhak, D. N., S. Tyanova, J. Cox, and G. H. Borner. 2016. 'Global, quantitative and dynamic mapping of protein subcellular localization', *Elife*, 5.

Jackson, C. L. 2009. 'Mechanisms of transport through the Golgi complex', *Journal of Cell Science*, 122: 443-52.

Jareb, M., and G. Banker. 1997. 'Inhibition of axonal growth by brefeldin A in hippocampal neurons in culture', *J Neurosci*, 17: 8955-63.

Jeckel, D., A. Karrenbauer, K. N. Burger, G. van Meer, and F. Wieland. 1992. 'Glucosylceramide is synthesized at the cytosolic surface of various Golgi subfractions', *J Cell Biol*, 117: 259-67.

Jones-Villeneuve, E. M., M. W. McBurney, K. A. Rogers, and V. I. Kalnins. 1982. 'Retinoic acid induces embryonal carcinoma cells to differentiate into neurons and glial cells', *J Cell Biol*, 94: 253-62.

Joshi, G., Y. Chi, Z. Huang, and Y. Wang. 2014. 'Abeta-induced Golgi fragmentation in Alzheimer's disease enhances Abeta production', *Proc Natl Acad Sci U S A*, 111: E1230-9.

Kahn, R. A., and A. G. Gilman. 1984. 'Purification of a protein cofactor required for ADP-ribosylation of the stimulatory regulatory component of adenylate cyclase by cholera toxin', *J Biol Chem*, 259: 6228-34.

Kahn, R. A., C. Goddard, and M. Newkirk. 1988. 'Chemical and immunological characterization of the 21-kDa ADP-ribosylation factor of adenylate cyclase', *J Biol Chem*, 263: 8282-7.

Kahn, R. A., P. Randazzo, T. Serafini, O. Weiss, C. Rulka, J. Clark, M. Amherdt, P. Roller, L. Orci, and J. E. Rothman. 1992. 'The amino terminus of ADP-ribosylation factor (ARF) is a critical determinant of ARF activities and is a potent and specific inhibitor of protein transport', *J Biol Chem*, 267: 13039-46.

Karatekin, E., and J. E. Rothman. 2018. 'FEBS Letters Special Issue on Exocytosis and Endocytosis', *FEBS Lett*, 592: 3477-79.

Kawada, K., T. Iekumo, R. Saito, M. Kaneko, S. Mimori, Y. Nomura, and Y. Okuma. 2014. 'Aberrant neuronal differentiation and inhibition of dendrite outgrowth resulting from endoplasmic reticulum stress', *J Neurosci Res*, 92: 1122-33.

Keen, J. H., M. H. Chestnut, and K. A. Beck. 1987. 'The clathrin coat assembly polypeptide complex. Autophosphorylation and assembly activities', *J Biol Chem*, 262: 3864-71.

Kirchhausen, T., and S. C. Harrison. 1981. 'Protein organization in clathrin trimers', *Cell*, 23: 755-61.

Klumperman, J. 2000. 'Transport between ER and Golgi', *Curr Opin Cell Biol*, 12: 445-9.

Kornfeld, R., and S. Kornfeld. 1985. 'Assembly of asparagine-linked oligosaccharides', *Annu Rev Biochem*, 54: 631-64.

Kutay, U., G. Ahnert-Hilger, E. Hartmann, B. Wiedenmann, and T. A. Rapoport. 1995. 'Transport route for synaptobrevin via a novel pathway of insertion into the endoplasmic reticulum membrane', *EMBO J*, 14: 217-23.

Kutay, U., E. Hartmann, and T. A. Rapoport. 1993. 'A class of membrane proteins with a C-terminal anchor', *Trends Cell Biol*, 3: 72-5.

Kwak, D. H., B. B. Seo, K. T. Chang, and Y. K. Choo. 2011. 'Roles of gangliosides in mouse embryogenesis and embryonic stem cell differentiation', *Exp Mol Med*, 43: 379-88.

Labun, K., T. G. Montague, J. A. Gagnon, S. B. Thyme, and E. Valen. 2016. 'CHOPCHOP v2: a web tool for the next generation of CRISPR genome engineering', *Nucleic Acids Res*, 44: W272-6.

Laemmli, U. K., E. Molbert, M. Showe, and E. Kellenberger. 1970. 'Form-determining function of the genes required for the assembly of the head of bacteriophage T4', *J Mol Biol*, 49: 99-113.

Langemeyer, L., F. Frohlich, and C. Ungermann. 2018. 'Rab GTPase Function in Endosome and Lysosome Biogenesis', *Trends Cell Biol*, 28: 957-70.

Langer, J. D., C. M. Roth, J. Bethune, E. H. Stoops, B. Brugger, D. P. Herten, and F. T. Wieland. 2008. 'A conformational change in the alpha-subunit of coatomer induced by ligand binding to gamma-COP revealed by single-pair FRET', *Traffic*, 9: 597-607.

Letourneur, F., E. C. Gaynor, S. Hennecke, C. Demolliere, R. Duden, S. D. Emr, H. Riezman, and P. Cosson. 1994. 'Coatomer is essential for retrieval of dilysine-tagged proteins to the endoplasmic reticulum', *Cell*, 79: 1199-207.

Li, H., S. K. Custer, T. Gilson, T. Hao le, C. E. Beattie, and E. J. Androphy. 2015. 'alpha-COP binding to the survival motor neuron protein SMN is required for neuronal process outgrowth', *Hum Mol Genet*, 24: 7295-307.

Liour, S. S., D. Kapitonov, and R. K. Yu. 2000. 'Expression of gangliosides in neuronal development of P19 embryonal carcinoma stem cells', *J Neurosci Res*, 62: 363-73.

Liu, Y., R. A. Kahn, and J. H. Prestegard. 2010. 'Dynamic structure of membrane-anchored Arf*GTP', *Nat Struct Mol Biol*, 17: 876-81.

Lowe, M., and T. E. Kreis. 1995. 'In vitro assembly and disassembly of coatomer', *J Biol Chem*, 270: 31364-71.

Majoul, I., M. Straub, S. W. Hell, R. Duden, and H. D. Soling. 2001. 'KDEL-cargo regulates interactions between proteins involved in COPI vesicle traffic: measurements in living cells using FRET', *Dev Cell*, 1: 139-53.

Malsam, J., A. Satoh, L. Pelletier, and G. Warren. 2005. 'Golgin tethers define subpopulations of COPI vesicles', *Science*, 307: 1095-8.

Mancias, J. D., and J. Goldberg. 2008. 'Structural basis of cargo membrane protein discrimination by the human COPII coat machinery', *EMBO J*, 27: 2918-28.

Mary, C., A. Scherrer, L. Huck, A. K. Lakkaraju, Y. Thomas, A. E. Johnson, and K. Strub. 2010. 'Residues in SRP9/14 essential for elongation arrest activity of the signal recognition particle define a positively charged functional domain on one side of the protein', *RNA*, 16: 969-79.

Matsuoka, K., L. Orci, M. Amherdt, S. Y. Bednarek, S. Hamamoto, R. Schekman, and T. Yeung. 1998. 'COPII-coated vesicle formation reconstituted with purified coat proteins and chemically defined liposomes', *Cell*, 93: 263-75.

McBurney, M. W. 1993. 'P19 embryonal carcinoma cells', *Int J Dev Biol*, 37: 135-40.

McNew, J. A., T. Weber, F. Parlati, R. J. Johnston, T. J. Melia, T. H. Sollner, and J. E. Rothman. 2000. 'Close is not enough: SNARE-dependent membrane fusion requires an active mechanism that transduces force to membrane anchors', *J Cell Biol*, 150: 105-17.

Mellman, I., and G. Warren. 2000. 'The road taken: past and future foundations of membrane traffic', *Cell*, 100: 99-112.

Moelleken, J., J. Malsam, M. J. Betts, A. Movafeghi, I. Reckmann, I. Meissner, A. Hellwig, R. B. Russell, T. Sollner, B. Brugger, and F. T. Wieland. 2007. 'Differential localization of coatomer complex isoforms within the Golgi apparatus', *Proceedings of the National Academy of Sciences*, 104: 4425-30.

Nakano, A., and M. Muramatsu. 1989. 'A novel GTP-binding protein, Sar1p, is involved in transport from the endoplasmic reticulum to the Golgi apparatus', *J Cell Biol*, 109: 2677-91.

Niu, T. K., A. C. Pfeifer, J. Lippincott-Schwartz, and C. L. Jackson. 2005. 'Dynamics of GBF1, a Brefeldin A-sensitive Arf1 exchange factor at the Golgi', *Mol Biol Cell*, 16: 1213-22.

Orci, L., D. J. Palmer, M. Ravazzola, A. Perrelet, M. Amherdt, and J. E. Rothman. 1993. 'Budding from Golgi membranes requires the coatomer complex of non-clathrin coat proteins', *Nature*, 362: 648-52.

Orci, L., M. Ravazzola, P. Meda, C. Holcomb, H. P. Moore, L. Hicke, and R. Schekman. 1991. 'Mammalian Sec23p homologue is restricted to the endoplasmic reticulum transitional cytoplasm', *Proc Natl Acad Sci U S A*, 88: 8611-5.

Orci, Lelio, Benjamin S. Glick, and James E. Rothman. 1986. 'A new type of coated vesicular carrier that appears not to contain clathrin: Its possible role in protein transport within the Golgi stack', *Cell*, 46: 171-84.

Osborne, A. R., T. A. Rapoport, and B. van den Berg. 2005. 'Protein translocation by the Sec61/SecY channel', *Annu Rev Cell Dev Biol*, 21: 529-50.

Owen, D. J., B. M. Collins, and P. R. Evans. 2004. 'Adaptors for clathrin coats: structure and function', *Annu Rev Cell Dev Biol*, 20: 153-91.

Palade, G. 1975. 'Intracellular aspects of the process of protein synthesis', *Science*, 189: 347-58.

Pearse, B. M. 1976. 'Clathrin: a unique protein associated with intracellular transfer of membrane by coated vesicles', *Proc Natl Acad Sci U S A*, 73: 1255-9.

Pelham, H. R., and J. E. Rothman. 2000. 'The debate about transport in the Golgi--two sides of the same coin?', *Cell*, 102: 713-9.

Pennock, G. D., C. Shoemaker, and L. K. Miller. 1984. 'Strong and regulated expression of Escherichia coli beta-galactosidase in insect cells with a baculovirus vector', *Mol Cell Biol*, 4: 399-406.

Peter, C. J., M. Evans, V. Thayanithy, N. Taniguchi-Ishigaki, I. Bach, A. Kolpak, G. J. Bassell, W. Rossoll, C. L. Lorson, Z. Z. Bao, and E. J. Androphy. 2011. 'The COPI vesicle complex binds and moves with survival motor neuron within axons', *Hum Mol Genet*, 20: 1701-11.

Pfeffer, S., L. Burbaum, P. Unverdorben, M. Pech, Y. Chen, R. Zimmermann, R. Beckmann, and F. Forster. 2015. 'Structure of the native Sec61 protein-conducting channel', *Nat Commun*, 6: 8403.

Pfeffer, S. R. 2010. 'How the Golgi works: a cisternal progenitor model', *Proc Natl Acad Sci U S A*, 107: 19614-8.

Pfeffer, S. R., and J. E. Rothman. 1987. 'Biosynthetic protein transport and sorting by the endoplasmic reticulum and Golgi', *Annu Rev Biochem*, 56: 829-52.

Rabu, C., and S. High. 2007. 'Membrane protein chaperones: a new twist in the tail?', *Curr Biol*, 17: R472-4.

Ran, F. A., P. D. Hsu, J. Wright, V. Agarwala, D. A. Scott, and F. Zhang. 2013. 'Genome engineering using the CRISPR-Cas9 system', *Nat Protoc*, 8: 2281-308.

Rapoport, T. A. 2007. 'Protein translocation across the eukaryotic endoplasmic reticulum and bacterial plasma membranes', *Nature*, 450: 663-9.

Reinhard, C., C. Harter, M. Bremser, B. Brugger, K. Sohn, J. B. Helms, and F. Wieland. 1999. 'Receptor-induced polymerization of coatomer', *Proc Natl Acad Sci U S A*, 96: 1224-8.

Reinhard, Constanze, Michael Schweikert, Felix T. Wieland, and Walter Nickel. 2003. 'Functional reconstitution of COPI coat assembly and disassembly using chemically defined components', *Proceedings of the National Academy of Sciences*, 100: 8253-57.

Reiterer, V., S. Maier, H. H. Sitte, A. Kriz, M. A. Ruegg, H. P. Hauri, M. Freissmuth, and H. Farhan. 2008. 'Sec24- and ARFGAP1-dependent trafficking of GABA transporter-1 is a prerequisite for correct axonal targeting', *J Neurosci*, 28: 12453-64.

Robinson, M. S. 2004. 'Adaptable adaptors for coated vesicles', *Trends Cell Biol*, 14: 167-74.

Roth, T. F., and K. R. Porter. 1964. 'Yolk Protein Uptake in the Oocyte of the Mosquito Aedes Aegypti. L', *J Cell Biol*, 20: 313-32.

Rothman, J. E., and F. T. Wieland. 1996. 'Protein sorting by transport vesicles', *Science*, 272: 227-34.

Roux, K. J., D. I. Kim, M. Raida, and B. Burke. 2012. 'A promiscuous biotin ligase fusion protein identifies proximal and interacting proteins in mammalian cells', *J Cell Biol*, 196: 801-10.

Russo, D., F. Della Ragione, R. Rizzo, E. Sugiyama, F. Scalabri, K. Hori, S. Capasso, L. Sticco, S. Fioriniello, R. De Gregorio, I. Granata, M. R. Guarracino, V. Maglione, L. Johannes, G. C. Bellenchi, M. Hoshino, M. Setou, M. D'Esposito, A. Luini, and G. D'Angelo. 2018. 'Glycosphingolipid metabolic reprogramming drives neural differentiation', *EMBO J*, 37.

Sandhoff, K., and K. Harzer. 2013. 'Gangliosides and gangliosidoses: principles of molecular and metabolic pathogenesis', *J Neurosci*, 33: 10195-208.

Schledzewski, K., H. Brinkmann, and R. R. Mendel. 1999. 'Phylogenetic analysis of components of the eukaryotic vesicle transport system reveals a common origin of adaptor protein complexes 1, 2, and 3 and the F subcomplex of the coatomer COPI', *J Mol Evol*, 48: 770-8.

Schuldiner, M., J. Metz, V. Schmid, V. Denic, M. Rakwalska, H. D. Schmitt, B. Schwappach, and J. S. Weissman. 2008. 'The GET complex mediates insertion of tail-anchored proteins into the ER membrane', *Cell*, 134: 634-45.

Serafini, T., G. Stenbeck, A. Brecht, F. Lottspeich, L. Orci, J. E. Rothman, and F. T. Wieland. 1991. 'A coat subunit of Golgi-derived non-clathrin-coated vesicles with homology to the clathrin-coated vesicle coat protein beta-adaptin', *Nature*, 349: 215-20.

Slaymaker, I. M., L. Gao, B. Zetsche, D. A. Scott, W. X. Yan, and F. Zhang. 2016. 'Rationally engineered Cas9 nucleases with improved specificity', *Science*, 351: 84-8.

Spang, Anne. 2009. 'On vesicle formation and tethering in the ER–Golgi shuttle', *Current Opinion in Cell Biology*, 21: 531-36.

Stamnes, M. A., and J. E. Rothman. 1993. 'The binding of AP-1 clathrin adaptor particles to Golgi membranes requires ADP-ribosylation factor, a small GTP-binding protein', *Cell*, 73: 999-1005.

Stanley, P. 2011. 'Golgi glycosylation', *Cold Spring Harb Perspect Biol*, 3.

Stearns, T., M. C. Willingham, D. Botstein, and R. A. Kahn. 1990. 'ADP-ribosylation factor is functionally and physically associated with the Golgi complex', *Proc Natl Acad Sci U S A*, 87: 1238-42.

Stefanovic, S., and R. S. Hegde. 2007. 'Identification of a targeting factor for posttranslational membrane protein insertion into the ER', *Cell*, 128: 1147-59.

Sun, Zhe, Frank Anderl, Kathrin Fröhlich, Liyun Zhao, Stefan Hanke, Britta Brügger, Felix Wieland, and Julien Béthune. 2007. 'Multiple and Stepwise Interactions Between Coatomer and ADP-Ribosylation Factor-1 (Arf1)-GTP', *Traffic*, 8: 582-93.

Tanigawa, G., L. Orci, M. Amherdt, M. Ravazzola, J. B. Helms, and J. E. Rothman. 1993. 'Hydrolysis of bound GTP by ARF protein triggers uncoating of Golgi-derived COP-coated vesicles', *J Cell Biol*, 123: 1365-71.

Thor, F., M. Gautschi, R. Geiger, and A. Helenius. 2009. 'Bulk flow revisited: transport of a soluble protein in the secretory pathway', *Traffic*, 10: 1819-30.

Tippmann, S. C., R. Ivanek, D. Gaidatzis, A. Scholer, L. Hoerner, E. van Nimwegen, P. F. Stadler, M. B. Stadler, and D. Schubeler. 2012. 'Chromatin measurements reveal contributions of synthesis and decay to steady-state mRNA levels', *Mol Syst Biol*, 8: 593.

Tsuchiya, M., S. R. Price, S. C. Tsai, J. Moss, and M. Vaughan. 1991. 'Molecular identification of ADP-ribosylation factor mRNAs and their expression in mammalian cells', *J Biol Chem*, 266: 2772-7.

Ungewickell, E., and D. Branton. 1981. 'Assembly units of clathrin coats', *Nature*, 289: 420-2.

Walter, P., and G. Blobel. 1980. 'Purification of a membrane-associated protein complex required for protein translocation across the endoplasmic reticulum', *Proc Natl Acad Sci U S A*, 77: 7112-6.

Wang, B., J. H. Joo, R. Mount, B. J. W. Teubner, A. Krenzer, A. L. Ward, V. P. Ichhaporia, E. J. Adams, R. Khoriaty, S. T. Peters, S. M. Pruett-Miller, S. S. Zakharenko, D. Ginsburg, and M. Kundu. 2018. 'The COPII cargo adapter SEC24C is essential for neuronal homeostasis', *J Clin Invest*, 128: 3319-32.

Wang, C., C. Xia, W. Bian, L. Liu, W. Lin, Y. G. Chen, S. L. Ang, and N. Jing. 2006. 'Cell aggregation-induced FGF8 elevation is essential for P19 cell neural differentiation', *Mol Biol Cell*, 17: 3075-84.

Watson, P. J., G. Frigerio, B. M. Collins, R. Duden, and D. J. Owen. 2004. 'Gamma-COP appendage domain - structure and function', *Traffic*, 5: 79-88.

Wegmann, D., P. Hess, C. Baier, F. T. Wieland, and C. Reinhard. 2004. 'Novel isotypic gamma/zeta subunits reveal three coatomer complexes in mammals', *Mol Cell Biol*, 24: 1070-80.

Wendeler, M. W., J. P. Paccaud, and H. P. Hauri. 2007. 'Role of Sec24 isoforms in selective export of membrane proteins from the endoplasmic reticulum', *EMBO Rep*, 8: 258-64.

Wieland, F. T., M. L. Gleason, T. A. Serafini, and J. E. Rothman. 1987. 'The rate of bulk flow from the endoplasmic reticulum to the cell surface', *Cell*, 50: 289-300.

Witkos, T. M., W. L. Chan, M. Joensuu, M. Rhiel, E. Pallister, J. Thomas-Oates, A. P. Mould, A. A. Mironov, C. Biot, Y. Guerardel, W. Morelle, D. Ungar, F. T. Wieland, E. Jokitalo, M. Tassabehji, U. Kornak, and M. Lowe. 2019. 'GORAB scaffolds COPI at the trans-Golgi for efficient enzyme recycling and correct protein glycosylation', *Nat Commun*, 10: 127.

Yu, R. K. 1994. 'Development regulation of ganglioside metabolism', *Prog Brain Res*, 101: 31-44.

Zhao, L., J. B. Helms, B. Brugger, C. Harter, B. Martoglio, R. Graf, J. Brunner, and F. T. Wieland. 1997. 'Direct and GTP-dependent interaction of ADP ribosylation factor 1 with coatomer subunit beta', *Proc Natl Acad Sci U S A*, 94: 4418-23.

Zhao, L., J. B. Helms, J. Brunner, and F. T. Wieland. 1999. 'GTP-dependent binding of ADP-ribosylation factor to coatomer in close proximity to the binding site for dilysine retrieval motifs and p23', *J Biol Chem*, 274: 14198-203.

6. Abbreviations

% percentage
°C degree Celsius
bp base pairs
Da dalton
g gram
h hour
k kilo
L litre
m milli
min minute
n nano
s second
U enzyme unit
V Volt
µ micro
µg microgram
µl microlitre
AA amino acid
AP adaptor protein
AP affinity purification
Arf1 ADP-ribosylation factor 1
ATP adenosine triphosphate
BioID method to analyze proximate or interacting proteins in vivo
COPI Coat protein complex I
COPII Coat protein complex II
DAPI 4',6-diamidino-2-phenylindole
α−EMEM Eagle's minimum essential medium alpha modified
DMSO dimethyl sulfoxide
DNA deoxyribonucleic acid
DTT dithiothreitol
EDTA ethylenediaminetetraacetic acid
EM electron microscopy
ER endoplasmic reticulum
ERAD ER-associated degradation
ERGIC ER-Golgi intermediate compartment
GAP GTPase-activating protein
GBF1 Golgi-specific brefeldin-A-resistant factor 1
GEF guanine nucleotide exchange factor
GM130 130 kDa cis-Golgi matrix protein
GO gene ontology
GST glutathione S-transferase
GTP guanosine-5'-triphosphate
Hsp90 heat-shock protein HSP90 beta
IP immunoprecipitation
IPTG isopropyl β-D-1-thiogalactopyranoside
KO knock out

KD knock down
mES mouse embryonic stem cells
mRNA messenger RNA
MS mass spectrometry
NLS nuclear localization sequence
OD optical density
ON over night
P19 embryonic mouse carcinoma cell line derived from embryo derived teratocarcinoma
PAGE polyacrylamide gel electrophoresis
PBS phosphate buffered sialine
PCR polymerase chain reaction
qPCR quantitative PCR
RNA ribonucleic acid
RNAseq RNA sequencing
RNP ribonucleoprotein
rpm rounds per minute
RT room temperature
SDS sodium dodecyl sulfate
SILAC stable isotope labeling by/with amino acids in cell culture
SMN1 survival motor neuron 1
SNARE soluble NSF Attachment Protein receptor
SRP signal recognition particle
TEMED tetramethylethylenediamine
TGN trans-Golgi network
UPR unfolded-protein response
UV ultraviolet
VTC vesicular-tubular clusters

7.   Amino acid code

A   Ala   Alanine
C   Cys   Cysteine
D   Asp   Aspartate
E   Glu   Glutamate
F   Phe   Phenylalanine
G   Gly   Glycine
H   His   Histidine
I   Ile   Isoleucine
K   Lys   Lysine
L   Leu   Leucine
M   Met   Methionine
N   Asn   Asparagine
P   Pro   Proline
Q   Gln   Glutamine
R   Arg   Arginine
S   Ser   Serine
T   Thr   Threonine
V   Val   Valine
Y   Tyr   Tyrosine
W   Trp   Tryptophan

8. Received License

Licensee: Biochemistry Centre Heidelberg University
Order Date: Jan 30, 2019
Order Number: 4518820947623
Publication: Cell
Title: The Mechanisms of Vesicle Budding and Fusion
Type of Use: reuse in a thesis/dissertation
Order Total: 0.00 EUR

Licensee: Biochemistry Centre Heidelberg University
Order Date: Jan 30, 2019
Order Number: 4518830985902
Publication: FEBS Letters
Title: The COPI system: Molecular mechanisms and function
Type of Use: Dissertation/Thesis
Order Total: 0.00 EUR